



universität
wien

DISSERTATION

Titel der Dissertation

Establishment of a Ewing's Sarcoma Mouse Model JAK/STAT Signalling in Ewing's Sarcoma

Verfasserin

Mag.rer.nat. Barbara Sax

angestrebter akademischer Grad

Doktorin der Naturwissenschaften (Dr.rer.nat.)

Wien, 2011

Studienkennzahl lt. Studienblatt: A 091 490

Dissertationsgebiet lt. Studienblatt: Molekulare Biologie

Betreuer: Univ.-Doz. Dr. Heinrich Kovar

Table of contents

ACKNOWLEDGEMENTS	6
ABSTRACT	8
ZUSAMMENFASSUNG	10
1. INTRODUCTION	12
1.1. Ewing’s sarcoma family of tumours-ESFT	12
1.1.1. ESFT - the disease	12
1.1.1.1. Epidemiology	12
1.1.1.2. Diagnosis	13
1.1.1.3. Survival rates and therapy	14
1.1.2. EWS/FLI-1	17
1.1.2.1. EWS/FLI-1 - the aberrant transcription factor	19
1.1.2.2. EWS/FLI-1 target genes	19
1.1.2.3. Biological functions of EWS/FLI-1	22
1.1.2.4. Cooperating mutations	24
1.1.3. Cell of origin	25
1.1.4. Mouse models	26
1.1.5. Limb development	29
1.2. The JAK/STAT pathway	34
1.2.1. JAK/STAT in cancer	38
1.3. Aim of the thesis	40
2. MATERIALS AND METHODS	41
2.1. Working with mice	41
2.1.1. Colony management	41
2.1.1.1. Transgenic mouse strains	41
2.1.1.2. Genotyping mice	42
2.1.1.3. Plug check	44
2.1.2. Xenotransplantation	44
2.1.3. Tissue preparation, paraffin embedding, sectioning	44
2.1.4. Histology	45
2.1.4.1. Haematoxylin and eosin staining (H&E)	45
2.1.4.2. Immunohistochemistry	46
2.1.4.3. <i>In situ</i> hybridisation	47

2.1.5. Skeletal staining	49
2.2. Tissue culture	51
2.2.1. Cell lines	51
2.2.2. Propagation of cell lines	52
2.2.3. Quantitation of cell number.....	52
2.2.4. Freezing/ Thawing of cells.....	52
2.2.5. Cytokine stimulation.....	53
2.2.6. Proliferation assay	53
2.2.7. Flow cytometric analysis.....	54
2.2.8. Isolation of fibroblasts from mouse ear skin	55
2.2.9. Infection of cells with lentivirus.....	55
2.2.10. Isolation of osteoblasts	55
2.2.10.1. Alizarin Red staining	56
2.3. Working with Bacteria.....	57
2.3.1. Bacterial strains and culture	57
2.3.2. Freezing of bacteria	57
2.3.3. Generation of heat shock competent bacteria	58
2.3.4. Transformation of heat shock competent bacteria	58
2.4. Working with DNA.....	60
2.4.1. Plasmid isolation from bacteria.....	60
2.4.1.1. Minipreparation.....	60
2.4.1.2. Midipreparation (Genopure Plasmid Midi Kit, Roche).....	60
2.4.2. Analytical digest	61
2.4.3. Agarose gel electrophoresis	61
2.4.4. Gel extraction (GenElute Gel Extraction Kit, Sigma)	61
2.4.5. DNA Ligation.....	62
2.4.6. Isolation of genomic DNA from cells, tissues or bone	62
2.4.7. PCR to detect deletion of the STOP-cassette of the EF allele	63
2.4.8. PCR to detect expression of EWS/FLI-1 and Cre.....	64
2.4.9. Template preparation for generation of <i>in situ</i> hybridisation probes	64
2.4.10. Dominant-negative STAT mutants	65
2.5. Working with RNA.....	67

2.5.1. RNA isolation	67
2.5.2. RNA agarose gel.....	67
2.5.3. Reverse transcription.....	68
2.5.4. JAK/STAT specific target gene analysis with OligoGEArray	69
2.5.5. Generation of digoxigenin labelled cRNA probes for <i>in situ</i> hybridisation.....	70
2.6. Working with Protein.....	72
2.6.1. Protein extraction.....	72
2.6.1.1. Preparation of protein lysates of mammalian cells and tissues	72
2.6.1.2. Preparation of protein lysates of mammalian cells for EMSA.....	73
2.6.2. Determination of protein concentration (Bradford).....	73
2.6.3. Western blot analysis	74
2.6.3.1. Polyacrylamid (PAA) gel electrophoresis	74
2.6.3.2. Sample preparation	75
2.6.3.3. Protein transfer	75
2.6.3.4. Immunodetection	76
2.6.4. Electrophoretic mobility shift assay (EMSA).....	78
2.6.4.1. Oligo Annealing.....	79
2.6.4.2. Oligo Labelling.....	79
2.6.4.3. Binding Reaction	79
2.6.4.4. Electrophoresis	79
3. RESULTS	82
3.1. Establishment of a conditional EWS/FLI-1 knock-in mouse model ..	82
3.1.1. The search for the appropriate Cre recombinase.....	82
3.1.1.1. A two-hit mouse model for ESFT?.....	84
3.1.1.2. <i>Runx2Cre</i> expression.....	86
3.1.2. Verification of EF knock-in mice	86
3.1.2.1. Analysis of <i>EWS/FLI-1</i> expression from the EF knock-in allele <i>in vitro</i>	87
3.1.2.1. Analysis of <i>EWS/FLI-1</i> expression from the EF knock-in allele <i>in vivo</i>	88
3.1.3. Severe limb defects in Prx1Cre EF mice.....	90
3.2. JAK/STAT signalling in ESFT.....	97
3.2.1. JAK/STAT activity in ESFT cells.....	97
3.2.2. Cytokines activating STAT1/STAT3	101
3.2.3. Dominant negative forms of STAT1/STAT3 in ESFT cell lines.....	106
4. DISCUSSION.....	114

4.1. Establishment of a conditional EWS/FLI-1 knock-in mouse model	114
4.2. JAK/STAT signalling in ESFT.....	122
5. REFERENCES	126
6. ABBREVIATIONS.....	141
CURRICULUM VITAE	147

Acknowledgements

I would like to thank Richard Moriggl for giving me the opportunity to work for my doctoral thesis in his lab. With his help we could establish many collaborations and I learned a lot during the years I spent at the Ludwig Boltzmann Institute for Cancer Research.

I thank Heinrich Kovar for taking over the supervision and for the time we spent in many fruitful discussions.

I am grateful for the cooperations of all my collaborators who enabled me to work for this thesis. Special thanks go to Jan Tuckermann, Enrique Torchia, Suzanne Baker, Christine Hartmann, Manuel Serrano, Malcolm Logan and Michael Kreppel for valuable discussions, sharing reagents and mouse models.

I am glad that my diploma supervisor Egon Ogris and Manuela Baccarini accepted to sacrifice their time to discuss my work in several doctoral committee meetings. They supported me with critical and valuable comments on the progress for this thesis.

I thank my group members, especially Katrin Friedbichler who did not always help out when I needed an extra hand but also became a good friend. Furthermore, I appreciate the practical and emotional support I received from Anu Wanasinghe and Deeba Khan.

Moreover, I thank all other people of the Ludwig Boltzmann Institute for Cancer Research for intra-laboratory help and our secretary Sabine Komnenovic. I also thank Mr. Horvath and Regina Bauer from the Medical University of Vienna because without them the daily routine laboratory work would have not been possible. Additionally, I am thankful for the help and support I received from Veronika Sexl and her group.

I'm deeply indebted to my parents and grandparents who made it possible to do my master study and were always there for me when I needed help. I am much obliged

to my husband who cheered me up when experiments didn't work properly and was always there for me. Last but not least I thank also the rest of my family and all my friends for supporting me during the whole time of my study.

Abstract

The Ewing's sarcoma family of tumours (ESFT) comprises paediatric cancers of bone and soft tissue which presumably originate from mesenchymal progenitor cells (MPC). One hallmark of ESFT is the presence of a chromosomal translocation. In 90% of the cases chromosome 11 fuses with chromosome 22. This translocation generates the EWS/FLI-1 fusion which acts as an aberrant transcription factor de-regulating many genes involved in tumour development. Surgery and/or radiotherapy combined with chemotherapy are the usual forms of treatment for ESFT. But since there is only little progress in the field of chemotherapy the need for an animal model for pre-clinical drug testing is evident.

Thus, the main focus of this thesis was to establish a mouse model that develops sarcomas resembling the phenotype of ESFT. We used a conditional EWS/FLI-1 mouse model, which upon Cre activity (controlled by a tissue specific promotor) expressed EWS/FLI-1 in the targeted cells. Since ESFT arises in bone and surrounding soft tissue we decided to direct expression of EWS/FLI-1 to the mesenchymal lineage by using different Cre lines. Only when using the Prx1Cre, double transgenic mice tolerated EWS/FLI-1 expression. We observed developmental abnormalities with severe skeletal deformations. Bone formation was impaired due to the absence of mature chondrocytes and osteoblasts and hence a lack of calcified bone. The lack of mature bone cells in EWS/FLI-1 expressing Prx1Cre mice supports *in vitro* data showing that EWS/FLI-1 impedes differentiation of murine mesenchymal progenitor cells. Currently, the project is extended to analysis of an inducible Prx1Cre system which circumvents the early lethality of Prx1Cre EF mice. This should provide the basis for tumour formation in these mice and hence the development of an appropriate mouse model for pre-clinical research.

In the second project of my PhD thesis, the role of the Janus Kinase/Signal Transducer and Activator of Transcription (JAK/STAT) signalling pathway in ESFT was investigated. This pathway is known to regulate many functions of a tumour cell such as proliferation, differentiation, survival or tumour surveillance. Although components of this signalling pathway are often de-regulated in human cancers the

role of this network was not investigated so far in detail in ESFT. Thus, we had a careful look on this pathway in ESFT.

We analyzed three different ESFT cell lines for activation of the JAK/STAT pathway and observed activated STAT1 and STAT3 only upon subcutaneous injection into immunocompromised mice, but not in plain monolayer culture. Glycoprotein (gp)130 cytokines were shown to induce activation of STAT1 and STAT3 whereas Interferon (IFN)- γ only led to STAT1 activation. A profound reduction in cell number was observed when cells were stimulated with IFN- γ but proliferation in response to gp130-cytokines was not changed dramatically. Stimulation with gp130 cytokines resulted in up-regulation of STAT1 target genes but STAT3 induced genes did not change their expression significantly.

In summary, components of the JAK/STAT signalling pathway were observed to be active in ESFT cell line xenografts and upon cytokine stimulation. But further analysis is needed to understand the biological function of STAT activation in ESFT and so this project is still ongoing at the Ludwig Boltzmann Institute for Cancer Research.

Zusammenfassung

Die Ewing Sarkom Familie der Tumoren (ESFT) beinhaltet Knochen- und Weichteiltumore, die vermutlich von mesenchymalen Progenitorzellen abstammen. Ein Kennzeichen der ESFT ist die Entstehung einer chromosomalen Translokation. In 90% der Fälle fusioniert das Chromosom 11 mit dem Chromosom 22. Dadurch entsteht das Fusionsprotein EWS/FLI-1, welches als fehlgeleiteter Transkriptionsfaktor agiert und viele Gene beeinflusst, die zur Tumorentstehung beitragen. Chirurgische Maßnahmen und/oder Strahlentherapie in Kombination mit Chemotherapie sind die üblichen Formen der Behandlung für ESFT. Da es aber in den letzten Jahrzehnten im Bereich der Chemotherapie nur kleine Fortschritte gab, ist die Notwendigkeit eines Tiermodells für pre-klinische Studien offenkundig.

Deshalb lag das Hauptaugenmerk dieser Doktorarbeit auf der Entwicklung eines solchen Mausmodells, welches Sarkome entwickelt, die den gleichen Phänotyp wie ESFT zeigen. Wir nutzten ein konditionales EWS/FLI-1 Modell, in welchem durch Steuerung der Aktivität des Cre Enzym das Fusionsprotein in einer bestimmten Zielzelle expremiert wird. Da ESFT in Knochen- und umgebenden Weichteilgewebe entsteht, haben wir uns entschieden die EWS/FLI-1 Expression auf die mesenchymale Abstammungslinie zu begrenzen, welches wir durch das Einsetzen verschiedener Cre Linien erreicht haben. Nur wenn wir die Prx1Cre benutzten, expremierten doppelt transgene Mäuse EWS/FLI-1. Diese Mäuse wiesen Abnormalitäten der Skelettentwicklung auf, am auffälligsten waren die verkürzten Extremitäten. Der Defekt in der Knochenentwicklung war bedingt durch ein Fehlen reifer Chondrozyten und Osteoblasten und damit der Abwesenheit von kalzifiziertem Knochen. Die fehlenden reifen Knochenzellen in EWS/FLI-1 expremierenden Prx1Cre Mäusen unterstützen *in vitro* Daten, die zeigen, dass EWS/FLI-1 die Differenzierung mesenchymaler Progenitorzellen von Mäusen verhindern kann. Momentan wird das Projekt um die Analyse eines induzierbaren Prx1Cre Systems, das die frühe Sterblichkeit umgeht, erweitert. Dies sollte die Grundlage für die Entstehung von Tumoren bieten und folglich die Entwicklung eines adäquaten Mausmodells für die pre-klinische Forschung.

In dem zweiten Projekt meiner Dissertation wurde die Rolle des Janus Kinase/Signal Transducer und Aktivator der Transkription (JAK/STAT) Signalwegs in ESFT untersucht. Dieser Signalweg ist bekannt viele Funktionen einer Tumorzelle zu regulieren wie Zellteilung, Differenzierung, Überleben oder Tumorüberwachung. Obwohl Komponenten dieses Signalweges häufig in humanen Tumoren fehlgeleitet sind, ist die Rolle dieses Netzwerkes in ESFT noch nicht detailliert erforscht worden. Daher untersuchten wir diesen Signalweg in ESFT.

Wir analysierten drei verschiedene ESFT Zelllinien auf die Aktivierung des JAK/STAT Signalweges. Wir konnten aktiviertes STAT1 und STAT3 nachweisen, aber nur wenn die ESFT Zellen subkutan in immunkomprimierte Mäuse injiziert wurden, nicht aber wenn die Zellen in einer Zellkulturschale kultiviert wurden. Glykoprotein (gp)130 Zytokine induzierten die Aktivierung von STAT1 und STAT3, wohingegen Interferon (IFN)- γ nur STAT1 stimulierte. Eine profunde Wachstumsretardation wurde in Zellen beobachtet, die mit IFN- γ inkubiert wurden. Proliferation als Antwort auf gp130 Zytokinstimulation wurde nicht dramatisch verändert. Stimulation mit gp130 Zytokinen resultierte in einer vermehrten Expression von STAT1 Zielgenen, aber STAT3 induzierte Gene änderten ihre Expressionslevel nicht signifikant.

Zusammenfassend kann man sagen, dass Komponenten des JAK/STAT Signalweges aktiv waren in ESFT Xenotransplantaten und durch Zytokinstimulation. Aber weitere Analysen sind nötig um die biologische Funktion der STAT Aktivierung in ESFT zu verstehen und deshalb wird dieses Projekt am Ludwig Boltzmann Institut für Krebsforschung noch weiter verfolgt.

1. Introduction

1.1. Ewing's sarcoma family of tumours-ESFT

1.1.1. ESFT - the disease

Cancer comprises malignant neoplasms in which cells acquire many genetic or epigenetic changes which render them immortal with increased proliferation and survival. Depending on the tissue of origin, there are three major sub-classes: epithelial cells form carcinomas, sarcomas are derived from cells of the mesenchymal tissue and leukaemia or lymphomas are malignancies arising from haematopoietic cells. Carcinomas account for most of the adult cancer cases whereas sarcomas are generally rare. (Alberts *et al.* 1994)

Sarcomas represent less than 5% of adult neoplasms but approximately 15% of paediatric malignancies. This class of tumours includes amongst others synovial sarcoma, chondrosarcoma, osteosarcoma, rhabdomyosarcoma and Ewing's sarcoma. (Mackall *et al.* 2002)

Ewing's sarcoma was first described by James Ewing in 1921 as a diffuse endothelioma of the bone. Since then, Askin tumour, primitive neuroectodermal tumour (PNET) and Ewing's sarcoma were united under the term Ewing's sarcoma family of tumours (ESFT), differing primarily by the degree of tumour cell differentiation. (Khoury 2005) They share a common histogenesis, tumour genetics and based on histo-pathology staining pattern belong to the small blue round cell tumours. (Triche 1987)

1.1.1.1. Epidemiology

ESFT is the second most common bone disease in children and young adolescents after osteosarcoma and comprises 3% of paediatric cancers. It is a rare disease with an incidence of 0,6/million worldwide and peaks in puberty. Boys are slightly more

affected than girls (1,3:1) and the disease is more commonly occurring in the Caucasian than the Asian population. Surprisingly, ESFT is underrepresented in African-Americans and Africans. (Burchill 2003; Ludwig 2008)

1.1.1.2. Diagnosis

ESFT is diagnosed with techniques employing histological, immunohistochemical, cytogenetic and molecular methods.

CD99, a 32 kD transmembrane protein, is highly expressed in ESFT and strong diffuse immunostaining confers a useful marker. Expression of *CD99* is not only restricted to ESFT, T- and B-lymphocytes but also neuroblastoma and rhabdomyosarcoma can have a positive CD99 staining. Therefore, an additional panel of markers is employed to discriminate ESFT from other diseases. Immunostainings specific for muscle (*MyoD*, myogenin), lymphoid (*CD45*, TdT) or neuronal tissue (synaptophysin) can help to obtain proper diagnosis. (Khoury 2005, Ludwig 2008)

Chromosomal translocations are a hallmark of ESFT. The most prominent one connects chromosome 11 to chromosome 22, resulting in the *EWS/FLI-1* fusion protein. The second most common translocation, which is found in 10% of ESFT cases, leads to a fusion of *EWS* to *ERG*. Other translocations fuse *EWS* to different members of the ETS transcription factor family (Table 1). In a rare subtype of ESFT the *EWS* related *TLS/FUS* is fused to *ERG*. (Kovar 2005) Until recently, only ETS family members were found to fuse to members of the EWS family in ESFT. Other combinations were associated with different tumour types and ESFT like neoplasms but an in-frame fusion between *EWS* and *NFATc2* present in four ESFT cases was recently identified. (Szuhai *et al.* 2009)

Several types of in-frame *EWS/FLI-1* chimeric transcripts are possible, but all harbour exon 7 from *EWS* and exon 9 from *FLI-1* (Figure 1). Reverse transcriptase polymerase chain reaction (RT-PCR) with primers specific for these exons can detect all forms of *EWS/FLI-1*. Another method to identify the translocation is fluorescence *in situ* hybridisation (FISH) whereby one labelled probe marks the *EWS* part and the other binds to *FLI-1*. An adaption of this method utilises two probes flanking the *EWS* breakpoint region on chromosome 22 thereby detecting translocations regardless of the fusion partner. (Khoury 2005)

EWS family member	transcription factor (type)	translocation	tumour type
EWS	FLI-1 (ETS)	11;22	ESFT (85%)
EWS	ERG (ETS)	21;22	ESFT (10%)
EWS	ETV1 (ETS)	7;22	ESFT (<1%)
EWS	E1AF (ETS)	17;22	ESFT (<1%)
EWS	FEV (ETS)	2;22	ESFT (<1%)
TLS/FUS	ERG (ETS)	11;22	ESFT (<1%)
EWS	NFATc2	20;22	ESFT (<1%)
EWS	POU5F1	6;22	ESFT like
EWS	SP3 (zinc finger)	2;22	ESFT like
EWS	PATZ1 (zinc finger)	1;22	ESFT like
EWS	ATF1 (leucine zipper)	12;22	melanoma of soft parts, clear cell sarcoma
EWS	WT1 (zinc finger)	11;22	desmoplastic small round cell tumour
EWS	CHOP (leucine zipper)	12;22	myxoid liposarcoma
TLS/FUS	CHOP (leucine zipper)	12;22	myxoid liposarcoma
TLS/FUS	ERG (ETS)	11;22	acute myeloid leukaemia

Table 1: Different fusion types between TET proteins (EWS, TLS/FUS) and members of the ETS transcription factor family (FLI-1, ERG, ETV1, E1AF, FEV) or other fusion partners are present in a variety of tumours. Seven of these fusion types are found in ESFT. adapted from Kovar 2005 and Ordonez *et al.* 2009

1.1.1.3. Survival rates and therapy

Fourty years ago the 5-year survival rate for patients with a localised disease was only 10%. But progress in local therapy as well as systemic chemotherapy raised the survival rates to more than two-thirds. However, the prognosis for the 25% of patients with metastatic ESFT was and still remains poor. (Ludwig 2008)

Management of ESFT consists of systemic chemotherapy and local control. Usually, three phases are employed: neoadjuvant multiagent chemotherapy (vincristine, doxorubicin, cyclophosphamide, ifosfamide, etoposide) to induce rapid cytoreduction; local therapy consisting of surgery and/or radiation therapy and consolidation therapy with chemotherapeutic regimens. (Ludwig 2008)

Even the latest generation of cytotoxic chemotherapy is not capable of improving the survival of patients with metastatic disease. Therefore, the need for targeted therapy is evident for these patients.

The most suitable target in ESFT would be the translocation product itself. Several studies with antagonists or antisense RNA show that *EWS/FLI-1* is indispensable for the growth of ESFT cells. (Kovar *et al.* 1996; Ouchida *et al.* 1995; Toretsky *et al.* 1997) Nevertheless, application in the clinics is much more complicated due to difficulties in delivering nucleic acids. Inclusion of small interfering RNA (siRNA) into nanocapsules could be a solution. It was demonstrated that such nanocapsules are capable of inhibiting tumour growth in a xenograft model with *EWS/FLI-1* expressing NIH3T3 cells. (Toub *et al.* 2006) Additionally, inhibition of tumour growth by *EWS/FLI-1* specific siRNA is also confirmed in xenograft models with ESFT cells. (Hu-Lieskovan *et al.* 2005a; Takigami *et al.* 2011) Further studies will show if this novel therapy is practicable in the clinics.

CD99 might be another useful candidate for targeted therapy because of the high expression in ESFT. Inhibition of CD99 *in vitro* results in growth suppression and a reduced migratory ability. (Kreppel *et al.* 2006) Moreover, an *in vivo* study with an antibody binding to and silencing CD99 demonstrates that tumour growth is suppressed in an ESFT cell xenograft model. (Scotlandi *et al.* 2000) However, there is no direct homologue of CD99 in mice (Kreppel *et al.* 2006) so that the toxicity of this treatment cannot be assessed in mouse models for pre-clinical studies.

The regulatory network responsible for ESFT transformation, growth and metastasis becomes more and more defined whereby novel targets for therapy are emerging. Recently, it was shown that CD99 modulates ESFT tumour differentiation, presumably by regulation of the mitogen activated protein kinase (MAPK) pathway and blockade of this CD99 downstream pathway could be exploited for novel therapeutic approaches. (Rocchi *et al.* 2010) Moreover, phosphatidylinositol 3-kinase (PI3K)/AKT was identified as a core cancer pathway essential for ESFT growth. (Lawlor *et al.* 2002) Further signalling pathways activated in ESFT are Wnt (Wingless, int-1), Hedgehog and mTOR (mammalian target of rapamycin). (Uren *et al.* 2004; Zwerner *et al.* 2008; Zenali *et al.* 2009) These may serve to discover new therapeutic strategies. Recently, it was demonstrated that blocking the Hedgehog pathway with a drug called arsenic trioxide, directly inhibiting GLI1, suppresses growth of ESFT cells and reduces tumour growth in an ESFT xenograft model.

(Beauchamp *et al.* 2011) Moreover, *ALK* was recently identified as a EWS/FLI-1 target in reprogrammed paediatric human mesenchymal stem cells (hMSC) and is also expressed in ESFT cell lines. This receptor tyrosine kinase may serve as a candidate for the novel selective small molecule kinase inhibitors. (Riggi *et al.* 2010)

The most promising strategy for therapy is targeting the insulin-like growth factor-1 receptor (IGF-1R). The existence of an autocrine circuit mediated by IGF-1R and the importance for ESFT survival and pathogenesis was previously shown. (Scotlandi *et al.* 1996; Scotlandi *et al.* 1998) Pre-clinical testing of human monoclonal antibodies against IGF-1R demonstrated broad anti-tumour activity and phase 1 clinical trials seem promising. (Kolb *et al.* 2008; Olmos *et al.* 2010) Currently, there are at least eight IGF-1R blocking antibodies from different pharmaceutical companies that have activity in ESFT, but only some and not all patients are responding. (Subbiah and Anderson 2011) Just these patients suffered from refractory advanced sarcomas that were resistant to all standard chemotherapies but now they have a chance of being cured. (Ludwig 2008) Other means to block IGF signalling are the use of small molecule inhibitors or recombinant proteins that systemically sequester IGF-1. (Hughes 2009)

A new approach using small molecule inhibitors that disrupt the interaction of EWS/FLI-1 with its binding partners may also be applicable for ESFT therapy in the future. A compound found in a surface plasmon resonance screening was demonstrated to block interaction of EWS/FLI-1 with RNA helicase A. Since this co-operation is essential for EWS/FLI-1 activity, the small compound is able to reduce growth of ESFT xenografts. (Erkizan *et al.* 2009)

The therapeutic intervention targeting not the tumour itself but rather the tumour vasculature is not new but seems to be of use for ESFT as well. Antibodies directed against vascular endothelial growth factor receptor-2 (VEGFR-2) were shown to suppress tumour growth, to reduce tumour vessel formation and to inhibit migration of bone marrow cells into the tumour in ESFT xenograft models. (Zhou *et al.* 2007)

1.1.2. EWS/FLI-1

As mentioned above the 11;22 translocation is the most abundant one, resulting in the fusion of *EWS* to *FLI-1*. Different types of in-frame transcripts are also possible within this group (Figure 1). Exon 7 of *EWS* and *FLI-1* exon 9 are present in all of the different transcripts. The most common form (type 1) contains exon 1 - 7 of *EWS* and exon 6 - 9 of *FLI-1* whereas the type 2 fusion links exon 1 - 7 of *EWS* and exon 5 - 9 of *FLI-1*. (Khoury 2005)

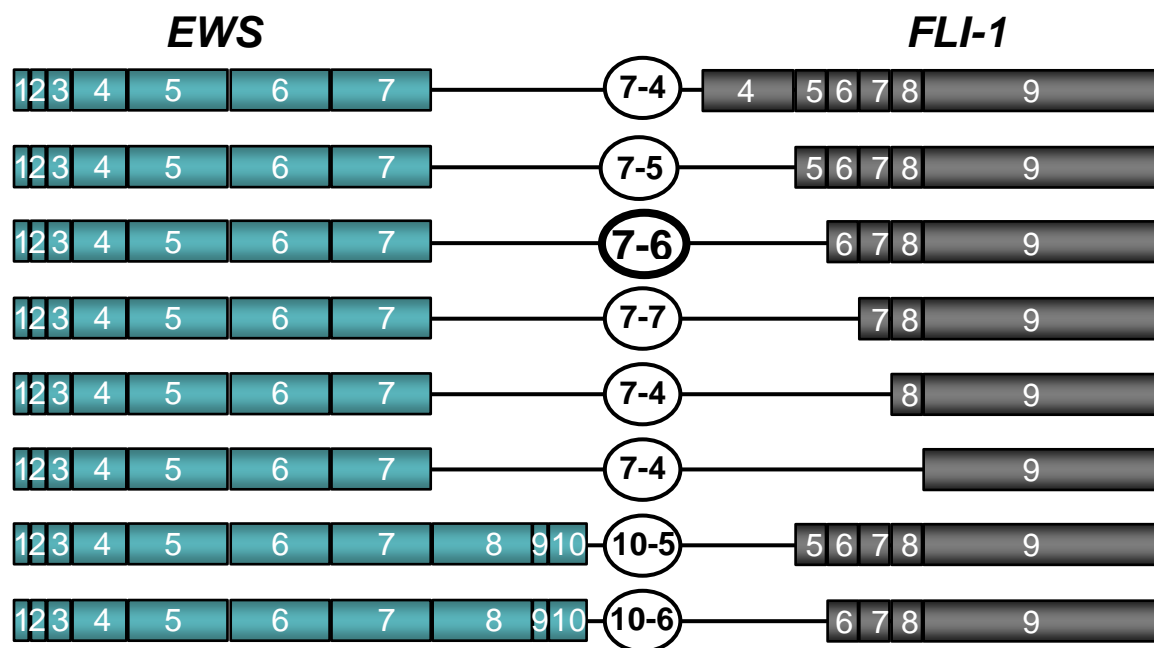


Figure 1: Schematic representation of the most common *EWS/FLI-1* fusion products. All translocations include exon 1 to 7 from *EWS* and exon 9 from *FLI-1*. Two cases have in addition exon 8 to 10 from *EWS*. The contribution of *FLI-1* exons is more versatile and the fusion protein can include exon 4 to 9, 5 to 9, 6 to 9, 7 to 9, 8 to 9 or exon 9 only, which is present in all fusion proteins. The number depicted in bold is the most prevalent translocation, termed type 1 fusion, which includes exon 1 to 7 from *EWS* and exon 6 to 9 from *FLI-1*. adapted from Khoury 2005

For a long time it was believed that patients with a localised disease harbouring a type 1 fusion have a better clinical outcome. The type 1 fusion protein is less potent in transcriptional activation than the type 2 fusion proteins (Lin *et al.* 1999), which would explain the difference in prognostic advantage. However, two recent studies published back to back disprove the assumption that there is a prognostic benefit for patients with a type 1 fusion. (Le Deley *et al.* 2010; van Doorninck *et al.* 2010)

EWS (*Ewing's sarcoma*) is encoded on chromosome 22q12 and constitutes the 5' part of the *EWS/FLI-1* fusion. Together with TLS/FUS and TAF_{II}68, EWS forms the TET family of proteins. Members of this family are characterised by a glutamine rich N-terminus and a putative RNA binding domain at the carboxy terminus (Figure 2). (Arvand and Denny 2001) TET family members are ubiquitously expressed and primarily found in the nucleus. (Andersson *et al.* 2008) More and more insight in the physiological functions of TET family members is gathered. There is evidence that EWS interacts with the basal transcription factor TFIID and RNA polymerase II suggesting a role in RNA transcription and processing. (Bertolotti *et al.* 1998) Moreover, interactions of EWS with various splicing factors are proven, indicating an involvement in RNA splicing. (Knoop *et al.* 2000; Chansky *et al.* 2001) By using *EWS*-deficient mice, two groups recently proposed even more novel functions of EWS. They conclude that EWS might have roles in B-cell development, meiosis, DNA-repair/recombination and cellular senescence of haematopoietic stem cells. (Li *et al.* 2007; Cho *et al.* 2011)

FLI-1 was first identified as a preferential retroviral integration site for the Friend murine leukaemia virus in erythroleukaemias. The ETS family of transcription factors consists of approximately 30 genes, one of them being *FLI-1*. (Arvand and Denny 2001) Members of this family are characterised by the evolutionary conserved ETS domain which binds to the 5'-GGAA/T-3' motif. This winged helix-turn-helix DNA binding domain can be located at variable sites in different family members. In *FLI-1*, the carboxy-terminal part contains the DNA binding domain and the transcriptional activation domain is located near the amino terminus (Figure 2). (Oikawa and Yamada 2003) In adult tissues *FLI-1* is expressed mainly in haematopoietic tissues and plays a regulatory role in erythroid and lymphoid cell function. (Truong and Ben-David 2000) Knock-out studies indicate that *FLI-1* deficiency leads to a defect in haematopoiesis (granulocyte, erythrocyte and NK-cell lineages are affected) and embryonic lethality. (Spyropoulos *et al.* 2000; Masuya *et al.* 2005)

In ESFT the carboxy-terminal part of EWS, containing the RNA binding domain, is replaced by the carboxy terminus of *FLI-1*, harbouring the DNA binding domain. The residual glutamine rich repeats of the EWS amino terminus then function as a transcriptional activator in the *EWS/FLI-1* fusion protein (Figure 2).

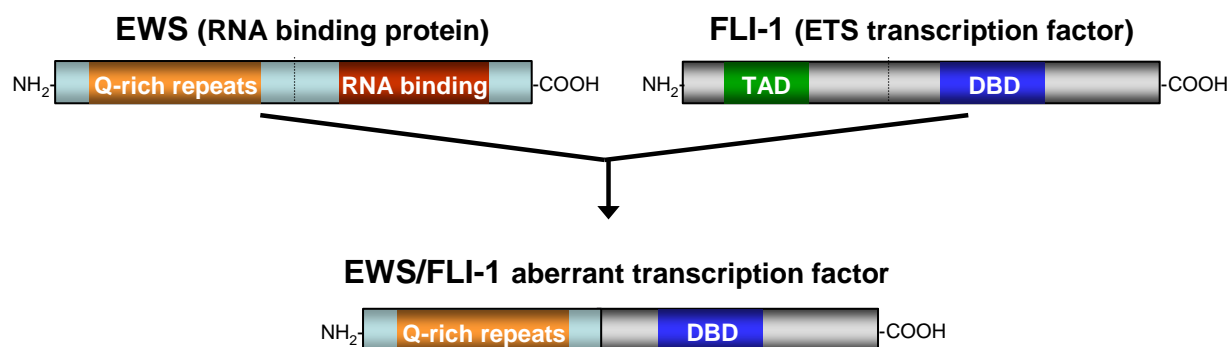


Figure 2: Structure of EWS, FLI-1 and the resulting chimeric transcription factor. EWS contains glutamine-rich repeats in the amino-terminal part and a presumptive RNA binding domain at its carboxy terminus. The TAD of the transcription factor FLI-1 is located near the amino terminus and the carboxyl end of the protein harbours the DBD. In ESFT the 11;22 translocation generates a new protein which consists of the amino-terminal part of EWS with its glutamine-rich repeats and the DBD containing carboxy terminus of FLI-1. TAD = transactivation domain, DBD = DNA binding domain

1.1.2.1. EWS/FLI-1 - the aberrant transcription factor

Since the first experiments almost 20 years ago it became apparent that EWS/FLI-1 is a potent chimeric transcription factor.

Binding to DNA and nuclear localisation are prerequisites for a functional transcription factor. Like germline EWS and FLI-1, the fusion protein is located in the nucleus. The carboxy-terminal part of EWS/FLI-1 contains the ETS domain of FLI-1, conferring DNA binding to the ETS consensus sequence. Early analysis of the DNA binding specificity showed that EWS/FLI-1 retains the ability of FLI-1 to specifically bind to this core element. Deletion of the ETS domain abrogates DNA binding, revealing the importance of this part for the chimeric transcription factor. (May *et al.* 1993b)

1.1.2.2. EWS/FLI-1 target genes

In EWS/FLI-1 the ETS transcriptional domain of FLI-1 is replaced by the amino-terminal part of EWS thereby generating a chimeric transcription factor with novel biochemical and genetic specificity. In a model reporter assay the transcriptional activity of EWS/FLI-1 was proven (May *et al.* 1993b) and since then comparative and functional strategies were used to identify target genes. It was surprising that several gene expression profiling studies uncovered an almost equal number of

genes down-regulated as up-regulated by EWS/FLI-1 (Siligan *et al.* 2005) but experiments in the beginning focused more on the activated targets.

One of the first target genes discovered is *stromelysin 1*. It is a member of the metalloproteinase family that digests extracellular matrix proteins which is linked to tumour invasion and metastasis. (Braun *et al.* 1995) Up-regulation of *manic fringe*, a gene coding for glycosyltransferase important in somatic development, was found in NIH3T3 cells ectopically expressing *EWS/FLI-1*. (May *et al.* 1997) The well-known proto-oncogene *c-myc* is highly expressed in ESFT cells and up-regulated upon inducible expression of *EWS/FLI-1* in neuroblastoma cells. (Dauphinot *et al.* 2001) The promoter activity of a putative tumour suppressor gene (*transforming growth factor beta receptor II (TGF β -RII)*) was shown to be directly suppressed by EWS/FLI-1. (Hahm *et al.* 1999) This list of early studies to identify EWS/FLI-1 target genes is not complete and only a few are named since there is one evident limitation to these findings: all of the above mentioned targets were discovered in heterologous cell systems ectopically expressing *EWS/FLI-1* and not in the original background of ESFT cells.

A better way to determine target genes would be the down-regulation of *EWS/FLI-1* in ESFT cell lines and comparative gene expression profiling. The *IGF binding protein 3 (IGFBP3)*, a major regulator of IGF-1 signalling, was found with this approach. (Prieur *et al.* 2004) Another target discovered with this strategy is *NKX2.2*, a homeobox containing protein with roles in neuronal development. (Smith *et al.* 2006) Immunoprecipitation of chromatin from ESFT cells that is bound by EWS/FLI-1 is a more direct way of identifying EWS/FLI-1 target genes in the authentic cellular background. With this approach 99 putative target genes were identified, one of them being *MK-STYX*, implicated in the regulation of MAPK pathway. (Siligan *et al.* 2005) A further target to be directly regulated by EWS/FLI-1 is *Id2*, a helix-loop-helix protein involved in proliferation processes. (Fukuma *et al.* 2003) *Caveolin-1 (CAV1)*, participating in tumour development and metastasis of a variety of cancers, is another direct target of EWS/FLI-1 that is over-expressed in ESFT cell lines and tumours. (Tirado *et al.* 2006) The orphan nuclear receptor *DAX1* was previously not involved in cancer but it is directly regulated by EWS/FLI-1 and is highly expressed in ESFT tumours. (Garcia-Aragoncillo *et al.* 2008) The Wnt and the Hedgehog pathway were already mentioned to play a role in ESFT. GLI1 is a downstream effector transmitting the Hedgehog signal to the nucleus and was

shown to be directly regulated by EWS/FLI-1. (Beauchamp *et al.* 2009) Moreover, the Wnt signalling pathway is controlled in ESFT by regulation of the Wnt inhibitor *DICKKOPF-1 (DKK-1)* and binding of EWS/FLI-1 to the transcription factor lymphoid enhancer factor 1 (Lef1). (Navarro *et al.* 2010) Among genes down-regulated by EWS/FLI-1 are cell cycle regulators like *p21* and *p57*. (Matsumoto *et al.* 2001; Dauphinot *et al.* 2001)

The hypothesis of ESFT arising from a mesenchymal progenitor cell is more and more substantiated by recent publications (for more detail see 1.1.3.). This offers the opportunity to study EWS/FLI-1 target genes that are required for ESFT initiation in the presumptive cell of origin. Induction of *EZH2*, a member of the polycomb group proteins, is up-regulated in *EWS/FLI-1* expressing human MSCs and is also highly expressed in ESFT patient samples. (Riggi *et al.* 2008) *IGF-1* is induced by EWS/FLI-1 in mouse as well as in human MSCs, depending on the DNA binding integrity of EWS/FLI-1, and may serve as a survival signal in the beginning of tumour development. (Riggi *et al.* 2005; Riggi *et al.* 2008) *ALK*, a receptor tyrosine kinase implicated in transformation and tumorigenesis, is expressed in ESFT cell lines and is also up-regulated in reprogrammed paediatric hMSC expressing *EWS/FLI-1*. Another kinase that shows enhanced expression upon *EWS/FLI-1* induction in reprogrammed paediatric hMSC is *NTRK1*. Its over-expression was shown to activate PI3K/AKT and MAPK signalling pathways. The embryonic stem cell genes *OCT4* and *SOX2* are responsible for maintaining an undifferentiated state. Induction of these genes by EWS/FLI-1 creates an environment allowing paediatric hMSC to form of a cell population with cancer stem cell characteristics. Both genes are indirectly regulated by EWS/FLI-1 via reversal of miRNA145 repression and *SOX2* is probably additionally regulated in a direct way. (Riggi *et al.* 2010)

For some of the mentioned target genes it was shown that down-regulation of EWS/FLI-1 activated genes (*NKX2.2*, *CAV1*, *DAX1*, *GLI1*, *EZH2*) and restoration of normal levels of EWS/FLI-1 repressed genes (*TGF- β RII*) results in diminished tumorigenic potential of ESFT cells. (Smith *et al.* 2006; Tirado *et al.* 2006; Garcia-Aragoncillo *et al.* 2008; Riggi *et al.* 2008; Hahm *et al.* 1999) But until now, no single target gene was found that fully recapitulates the phenotype of a EWS/FLI-1 transformed cell. (Arvand and Denny 2001)

Altogether, one can say that EWS/FLI-1 participates in ESFT pathogenesis by controlling the major characteristics of tumorigenesis: activation of genes involved in cell proliferation and survival (*c-myc*, *NKX2.2*, *GLI1*, *DAX1*...) and repression of genes regulating growth inhibition and apoptosis (*p21*, *p57*, *TGF- β RII*...). More recently, EWS/FLI-1 is also implicated in up-regulation of genes involved in cell differentiation (*SOX2*, *EZH2*) and vascularisation (*VEGF*). (Riggi *et al.* 2010; Richter *et al.* 2009; Nagano *et al.* 2010)

It is important to mention that EWS/FLI-1 influences the cells behaviour not only by target gene regulation but also through regulation of RNA-maturation and protein-protein interactions. However, the two latter processes are not studied well enough in ESFT. (Lin *et al.* 2011)

1.1.2.3. Biological functions of EWS/FLI-1

Since it was not clear for a long time from which cell of origin ESFT arises, most of the experiments were carried out in heterologous cell systems. Through the use of a variety of different cells, it became early apparent that the biological function of EWS/FLI-1 is dependent on the cellular context.

As already mentioned, the fusion protein is absolutely essential for ESFT cells to survive. Down-regulation of *EWS/FLI-1* by means of antisense oligonucleotides or siRNA results in growth inhibition and a reduction of tumorigenicity *in vitro* as well as *in vivo*. (Toretzky *et al.* 1997; Takigami *et al.* 2011) Therefore, it became clear that EWS/FLI-1 as an aberrant transcription factor drives proliferation and is responsible for the transformed phenotype of ESFT cells.

Introduction of EWS/FLI-1 into NIH3T3 cells uncovered that the fusion protein is a potent transforming agent whereas FLI-1 alone is not. The transforming ability is strictly dependent on the presence of both the EWS domain and the carboxy-terminal DNA binding domain. (May *et al.* 1993a) The fusion protein is a more potent transcriptional activator than the amino-terminal region of FLI-1 alone. This might explain the discrepancy that FLI-1 is non-transforming whereas EWS/FLI-1 efficiently transforms NIH3T3 cells. (May *et al.* 1993b)

The cellular background of NIH3T3 cells seems to be permissive for stable *EWS/FLI-1* expression whereas the cellular context of primary mouse embryonic fibroblasts (MEFs) is not. Expression of *EWS/FLI-1* in MEFs induces apoptosis and growth arrest.

(Deneen and Denny 2001) Experiments with primary human fibroblasts demonstrate the same growth inhibitory effect of EWS/FLI-1 in this cell system. (Lessnick *et al.* 2002)

Since more and more evidence uncovers a multi-potent mesenchymal progenitor as the ESFT cell of origin (see 1.1.3.), recent experiments make use of this cell type. Two reports published in the same year uncovered the tumourigenic potential of EWS/FLI-1 in such primary bone derived murine cells. (Castillero-Trejo *et al.* 2005; Riggi *et al.* 2005) In a subsequent publication, human MSCs were shown to tolerate *EWS/FLI-1* expression without growth inhibition. (Riggi *et al.* 2008) The gene expression profile of hMSCs expressing *EWS/FLI-1* is similar to that of ESFT but in paediatric hMSCs *EWS/FLI-1* induces a molecular profile that more accurately recapitulates that of ESFT. (Riggi *et al.* 2010) Moreover, *EWS/FLI-1* was shown to induce genetic reprogramming of paediatric hMSCs by modulating miRNA145 and SOX2 expression. (Riggi *et al.* 2010)

There is also evidence that *EWS/FLI-1* can block differentiation. A murine cell line with mesenchymal characteristics is blocked in differentiation after *EWS/FLI-1* induction and murine marrow stromal cells deficient in *p19^{ARF}* lose their differentiation plasticity upon *EWS/FLI-1* expression. (Eliazar *et al.* 2003; Li *et al.* 2010; Torchia *et al.* 2003) In contrast, human *EWS/FLI-1* expressing MSCs retain their differentiation potential. (Riggi *et al.* 2008) Despite the discrepancy between the species, ESFT cells itself are not able to differentiate into mesenchymal lineages but suppression of the fusion product recovers their differentiation potential. (Tirode *et al.* 2007)

Another feature of *EWS/FLI-1* is the induction of trans-differentiation with concomitant up-regulation of ESFT markers like *c-myc* and *CD99*. (Rorie *et al.* 2004; Hu-Lieskovan *et al.* 2005b)

Altogether, these studies demonstrate that *EWS/FLI-1* contributes to the ESFT morphology by attenuating the differentiation programme of its precursor cell leading to a less differentiated and more proliferative state. This assumption is also underscored by functional annotation of *EWS/FLI-1* regulated genes showing that *EWS/FLI-1* activated genes mainly regulate proliferation whereas repressed genes are involved in differentiation processes. (Kauer *et al.* 2009)

1.1.2.4. Cooperating mutations

The *p53* tumour suppressor gene is one of the most frequently altered genes in human malignancies. However, in childhood cancers like ESFT *p53* mutations seem to play only a minor role. Different reports on the *p53* status of ESFT patients demonstrate that mutations occur, but to a limited extent (5 to 14%). (de Alava *et al.* 2000; Komuro *et al.* 1993; Kovar *et al.* 1993; Park *et al.* 2001) In contrast, the frequency of *p53* mutations in ESFT cell lines is dramatically increased, indicating a growth advantage *in vitro*. (Hamelin *et al.* 1994; Komuro *et al.* 1993; Kovar *et al.* 1993) Moreover, patients with a *p53* mutation have a reduced overall survival. Therefore, *p53* alterations appear to define only a small subset of ESFT patients with a markedly poor outcome. (de Alava *et al.* 2000)

Besides mutations in the *p53* pathway, alterations of RB (retinoblastoma) pathway components play also a role in malignant transformation. $p16^{\text{INK4A}}$ is a member of the RB cell cycle regulatory pathway and is encoded by the *INK4A/ARF* locus, from which also $p14^{\text{ARF}}$ (in mouse: $p19^{\text{ARF}}$) is expressed. This locus is often deleted in a variety of different cancers. The prevalence of *INK4A/ARF* alterations in ESFT varies from 13 to 30%. (Huang *et al.* 2005; Kovar *et al.* 1997; Lopez-Guerrero *et al.* 2001) As seen with *p53* alterations, loss of the *INK4A/ARF* locus is enriched in cell lines as a consequence of a selection process *in vitro*. (Kovar *et al.* 1997) Prognosis for patients with alterations in the *INK4A/ARF* locus is worse than for patients without this aberration. (Lopez-Guerrero *et al.* 2001) Loss of the *INK4A/ARF* locus is therefore the second most common molecular alteration observed in ESFT so far. Moreover, experiments with MEFs and primary human fibroblasts confirm the importance of *INK4A/ARF* in the transformation process of ESFT. *EWS/FLI-1* leads to a reduced proliferation in MEFs but arrest effects are attenuated when *EWS/FLI-1* is expressed in *INK4A/ARF* deficient cells. These cells are able to form tumours in immunocompromised mice but *p53* deficient *EWS/FLI-1* expressing MEFs cannot. In primary human fibroblasts *EWS/FLI-1* is only tolerated when the $p16^{\text{INK4A}}$ -Rb pathway is disrupted, whereas alterations in the *p53* pathway alone do not have a similar effect. Hence, loss of the *INK4A/ARF* locus creates an environment permissive for *EWS/FLI-1* expression, at least in immortal fibroblasts. (Deneen and Denny 2001)

1.1.3. Cell of origin

Since the discovery of ESFT, the question of the cellular origin was eminent. James Ewing himself described the disease as a diffuse endothelioma of the bone with unknown origin. (Ewing 1972) Later on, a neural crest origin was discussed, as ESFT cells have the potential to differentiate into the neuronal lineage. (Cavazzana *et al.* 1987) Additionally, neuronal markers like neuron-specific enolase, Leu-7 and the Y1 receptor for neuropeptide Y were found on the ESFT cell surface. (Kawaguchi *et al.* 1987; van Valen *et al.* 1992) But later analysis revealed that EWS/FLI-1 itself induces a certain degree of neuronal features (Hu-Lieskovan *et al.* 2005b; Riggi *et al.* 2008; Teitell *et al.* 1999) which led to a re-thinking in the quest for the ESFT cell of origin.

The current hypothesis assumes that ESFT originates from a primitive multi-potent cell that can give rise to bone and soft tissue. MSCs would perfectly fit these requirements. Usually they are prepared from bone marrow, plated on plastic and the adherent cells are the presumptive MSCs. When cultured under appropriate conditions, these cells can differentiate along the osteogenic, adipogenic or chondrogenic lineage. It is noteworthy that these preparations are heterogeneous, composed of not one single cell type but rather a mixture of cells. (Lin *et al.* 2011) Authors give these cells different names: from mesenchymal stem cells, marrow stromal cells, primary bone derived cells to mesenchymal progenitor cells. Hereafter, the term mesenchymal progenitor cell (MPC) will be used to refer to this kind of cell mixture.

Recent publications highlight the similarity of gene expression profiles of human MPCs and *EWS/FLI-1* silenced ESFT cells. (Tirode *et al.* 2007; Kauer *et al.* 2009) Moreover, silencing of *EWS/FLI-1* in ESFT cell lines recovers part of their differentiation potential and ESFT cells are then able to differentiate along the osteoblastic and adipogenic lineage, whereas wild type ESFT cells cannot. (Tirode *et al.* 2007) This is only partly true because within the ESFT cells a CD133-positive population exists that retains its differentiation plasticity. This CD133-positive population displays cancer stem cell (CSC) characteristics (= ESFT CSC) and is thought to arise from MPCs. (Suva *et al.* 2009) ESFT CSCs have the capacity to self-renew, express genes involved in stem cell maintenance and nuclear reprogramming and have the potential to initiate and sustain tumour growth, thereby fulfilling the criteria of a CSC. (Suva *et al.* 2009)

Experiments with human MPCs identified their permissiveness for *EWS/FLI-1* expression and that MPCs expressing *EWS/FLI-1* induce a gene expression profile reminiscent of that of ESFT. As opposed to mouse MPCs, human MPCs keep their differentiation potential after *EWS/FLI-1* induction. (Riggi *et al.* 2008) Two years later the same group discovered that human paediatric MPCs expressing *EWS/FLI-1* resemble the gene expression profile of ESFT more closely than their adult counterpart. (Riggi *et al.* 2010) This was not surprising, since ESFT arises at a young age and only rarely in adults, from which usually the bone marrow is obtained to isolate MPCs. The highest similarity with ESFT gene expression profiles observed so far can be achieved with reprogrammed *EWS/FLI-1* expressing paediatric MPCs, which then resemble some features of ESFT CSC. (Riggi *et al.* 2010)

In summary, these results suggest that ESFT cells might arise from MPCs which are transformed by *EWS/FLI-1* (CD133-positive, ESFT CSC characteristics) and retain their differentiation plasticity. (Riggi *et al.* 2010) ESFT CSCs can also generate a CD133-negative population which represents 92 - 96% of ESFT cells. (Suva *et al.* 2009) These cells, which build up the tumour bulk, lost their differentiation ability and cannot give rise to cells of the mesenchymal lineages. (Tirode *et al.* 2007)

1.1.4. Mouse models

In recent years, some good candidates for targeted therapy were discovered (see 1.1.1.3.) but their way into the clinics is demanding and cost intense. Another dilemma is that an appropriate mouse model for pre-clinical drug testing is lacking. So far, functionality of target modulation is tested in xenograft models where cell lines that have been cultivated over a long time, which may select for acquired mutations of tumour suppressor genes, form tumours in orthotopic sites, but this does not adequately recapitulate the biology of ESFT.

Concerning translocation-associated sarcomas in general, there are currently three animal models that mimic the human disease. Conditional expression of *TLS/FUS-CHOP* results in myxoid liposarcoma, alveolar rhabdomyosarcoma is formed in mice harbouring the *Pax3-Fkhr* fusion and synovial sarcoma is initiated by *SYT-SSX2* in this mouse model. (Haldar *et al.* 2007; Keller *et al.* 2004; Perez-Losada *et al.* 2000) The first report about a mouse that expresses a fusion protein present in ESFT was published in 2005. This group uses a new conditional gene fusion model (invertor

knock-in) that mimics a chromosomal translocation. An *ERG* cassette, flanked by *loxP* sites, is knocked into the endogenous *EWS* locus in inverted orientation. Upon Cre activity, the cassette is flipped and the EWS/ERG chimeric protein is expressed (Figure 5A). The benefit of this strategy is that the fusion protein is under control of the endogenous *EWS* promoter, like in the human disease. The authors assess the tumour initiating potential of EWS/ERG in committed lymphoid cells. Therefore, they use the Rag1Cre to conditionally express *EWS/ERG* in B- and T-cells. Expression of the fusion protein is tolerated in this cellular background and clonal T-cell neoplasia arises in the invertebrate knock-in mice. Thus, EWS/ERG is able to initiate tumours in the lymphoid system. (Codrington *et al.* 2005)

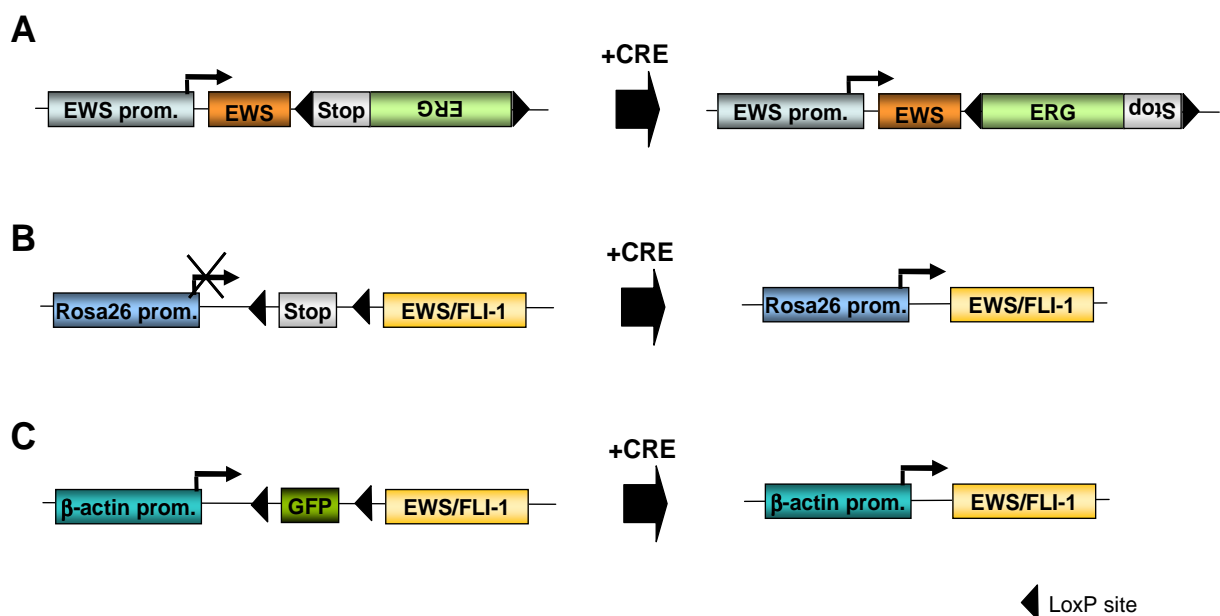


Figure 3: Conditional mouse models for expression of fusion proteins present in ESFT. A The inverter knock-in strategy: an *ERG* cassette is introduced into the endogenous *EWS* locus in inverted orientation. Only upon Cre activity the *ERG* cassette is flipped and *EWS/ERG* can be expressed. B A floxed *STOP*-cassette in front of *EWS/FLI-1* prevents transcription. Only upon Cre activity and concomitant excision of the *STOP*-cassette *EWS/FLI-1* is expressed. This construct is knocked-in into the ubiquitously expressed *Rosa26* locus. C This *EWS/FLI-1* transgenic construct was designed with a β -actin promoter and a floxed *GFP*-cassette in front of *EWS/FLI-1*. Expression of *GFP* prevents transcription of the subsequent fusion gene. Only upon Cre activity and concomitant excision of the *GFP*-cassette *EWS/FLI-1* is expressed.

Two years later another strategy for the generation of a conditional EWS/FLI-1 mouse model was reported. This group used a construct with a *loxP* flanked *STOP*-cassette in front of the *EWS/FLI-1* type 1 fusion, knocked into the *Rosa26* locus.

Upon Cre activity the *STOP*-cassette is excised and *EWS/FLI-1* is expressed in the target cells (Figure 3B). Since ESFT is believed to arise in MPCs, which are located in the bone marrow compartment, a Cre recombinase under control of an interferon regulated promoter is employed. (Torchia *et al.* 2007) Upon stimulation of the interferon pathway, *Mx1Cre* is expressed in haematopoietic cells or the liver and to a lesser extent also in other tissues. (Kuhn *et al.* 2005) The conditional expression of *EWS/FLI-1* induces rapid development of a myeloproliferative disease with expansion of immature erythroid progenitor cells, densely infiltrating the liver, spleen or bone marrow. This confirms the oncogenic potential of *EWS/FLI-1* *in vivo*, but no sarcoma formation could be observed with this model. (Torchia *et al.* 2007)

Both publications mentioned above report mouse models with tumours in the haematopoietic system but do not mimic the human situation where ESFT arise in bone and soft tissue. (Codrington *et al.* 2005; Torchia *et al.* 2007) As discussed in 1.1.3., it is currently hypothesised that ESFT originates from a primitive mesenchymal cell, in which *EWS/FLI-1* has to be expressed in a proper mouse model. The selection of the right cellular background to express *EWS/FLI-1* is the most tricky and essential part in designing a mouse model that develops sarcomas resembling ESFT. And this could also answer in part the question of the cellular origin.

During the work for this PhD thesis the generation of a transgenic mouse which expresses *EWS/FLI-1* in the primitive mesenchymal cells of the developing limb bud was published. (Lin *et al.* 2008) They used a similar strategy as Torchia *et al.* 2007 but instead of the *STOP*-cassette, a *loxP* flanked *GFP*-cassette was introduced in front of the *EWS/FLI-1* type 1 fusion (Figure 3B). Upon Cre activity, the *GFP*-cassette is excised and *EWS/FLI-1* is expressed in the target cells. This group uses the *Prx1Cre*, which is expressed early in the limb bud mesenchyme. (Logan *et al.* 2002) Double transgenic mice show developmental defects like limb shortening and immature bone but do not display tumours. However, conditional deletion of *p53* with *Prx1Cre* results in the formation of predominantly osteosarcomas with a median tumour latency of 50 weeks. In this setting *EWS/FLI-1* accelerates tumour formation and shifts the tumour spectrum to a more poorly differentiated sarcoma phenotype. (Lin *et al.* 2008)

1.1.5. Limb development

To better understand the biology of ESFT origin, it is necessary to know how bone development occurs under normal circumstances. Skeletal elements are already formed in the embryo by either intramembranous ossification, where mesenchymal cells differentiate directly into osteoblasts, or endochondral ossification. Most parts of the skeleton are formed by the latter process, where a cartilage template is replaced by bone. Endochondral ossification starts with mesenchymal condensations at the place of the future bone. Mesenchymal progenitors, which originate from the neural crest, somites and lateral plates, differentiate first into chondrocytes and form the cartilage template. Later, differentiated osteoblasts invade from the perichondrium, the area surrounding the cartilage element, into the chondrocyte zones and form bone.

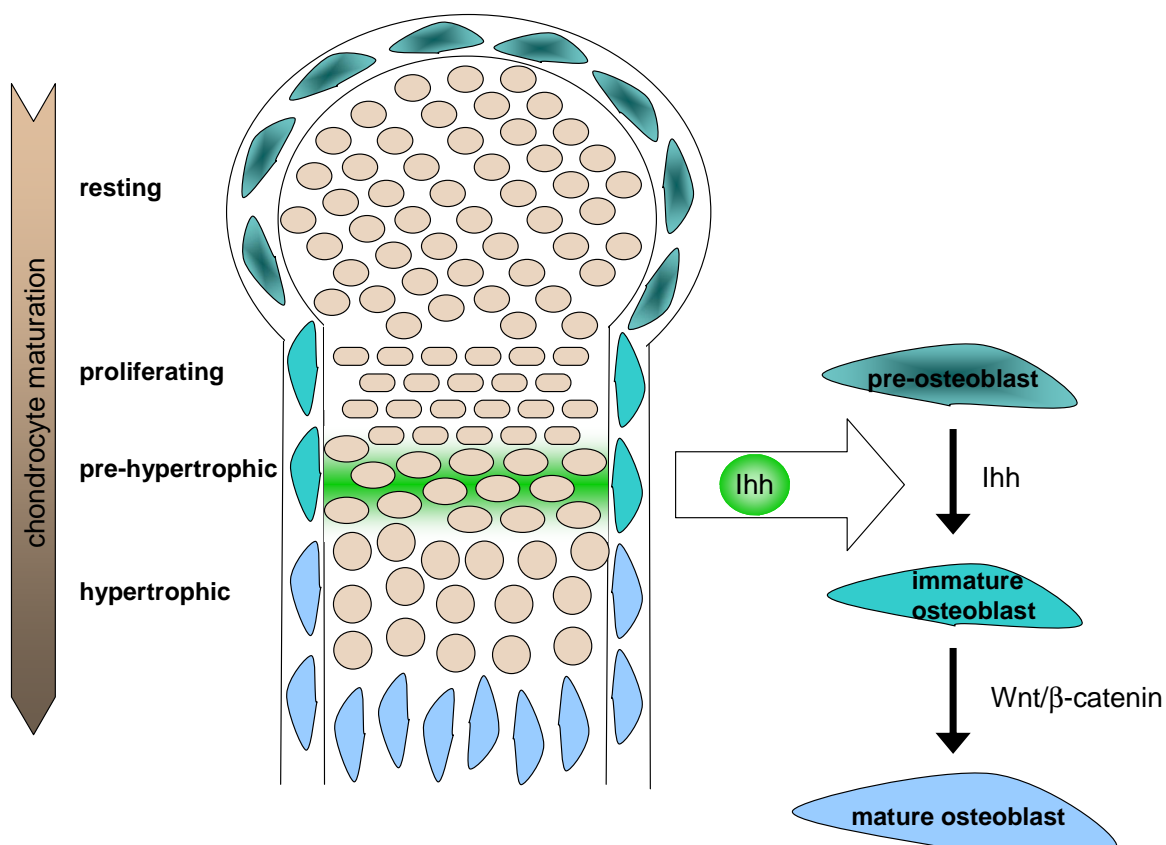


Figure 4: Endochondral bone formation. A cartilage template, divided into distinct zones of chondrocyte maturation stages, is replaced by the bone forming osteoblasts that invade from the perichondrium, the area surrounding the chondrocyte cells. Differentiation of chondrocytes is tightly coupled to osteoblast maturation. Secretion of Indian Hedgehog (Ihh) from pre-hypertrophic chondrocytes induces differentiation of osteoblasts. Moreover, Wnt/ β -catenin signalling is required for the final maturation step of osteoblasts. Ihh = Indian Hedgehog, Osx = Osterix, Opn = Osteopontin. adapted from Day and Yang 2008

Endochondral bone formation is tightly linked to chondrocyte differentiation. The cartilage element consists of distinct zones of chondrocytes stages along the longitudinal axis (Figure 4). In the resting zone, chondrocytes divide slowly and are small and round. In the process of maturation, chondrocytes leave this zone, increase their proliferation rate and have an elongated shape. Then, the cells stop dividing, start to differentiate in pre-hypertrophic, later hypertrophic chondrocytes and finally die by apoptosis. Signalling molecules secreted by these differentiated chondrocytes are required for subsequent osteoblast differentiation. (Day and Yang 2008; Hartmann 2007)

Two key signalling pathways are indispensable for proper skeletal development, namely Hedgehog and Wnt signalling. Hedgehog and Wnt proteins are secreted ligands that bind to their respective receptors and transduce the signal to the nucleus (Figure 5). Hedgehog molecules bind to Patched1 (Ptch1) thus releasing Smoothed (Smo) from its inhibition. Smo can then transmit the signal into the nucleus where target genes like *Ptch1* and *Gli1* are transcribed. In the process of endochondral bone formation, Indian Hedgehog (Ihh) is released by pre-hypertrophic chondrocytes and regulates the differentiation of osteoblasts (Figure 4). (Day and Yang 2008) Moreover, Ihh blocks chondrocyte hypertrophy by up-regulating parathyroid hormone related peptide (PTHrP), generating a feedback loop that controls chondrocyte maturation. (Lai and Mitchell 2005)

In absence of a Wnt signal, glycogen synthase kinase-3 (Gsk-3) phosphorylates β -catenin and marks it for proteasomal degradation. GSK-3 acts in the “destruction complex” including adenomatous polyposis coli (APC) and Axin. Upon binding of Wnts to their co-receptors Frizzled (Fz) and lipoprotein receptor-related protein (LRP) 5/6, Dishevelled (Dsh) is activated causing disassembly of the “destruction complex”. β -catenin is stabilised, accumulates and translocates to the nuclear compartment. Together with T-cell factor (Tcf) / lymphoid enhancer factor (Lef) transcription factors β -catenin activates gene expression. Wnt/ β -catenin signalling controls the differentiation of progenitor cells into either osteoblasts or chondrocytes and also plays a role downstream of Ihh in promoting maturation of osteoblasts (Figure 4 and 6). (Day and Yang 2008)

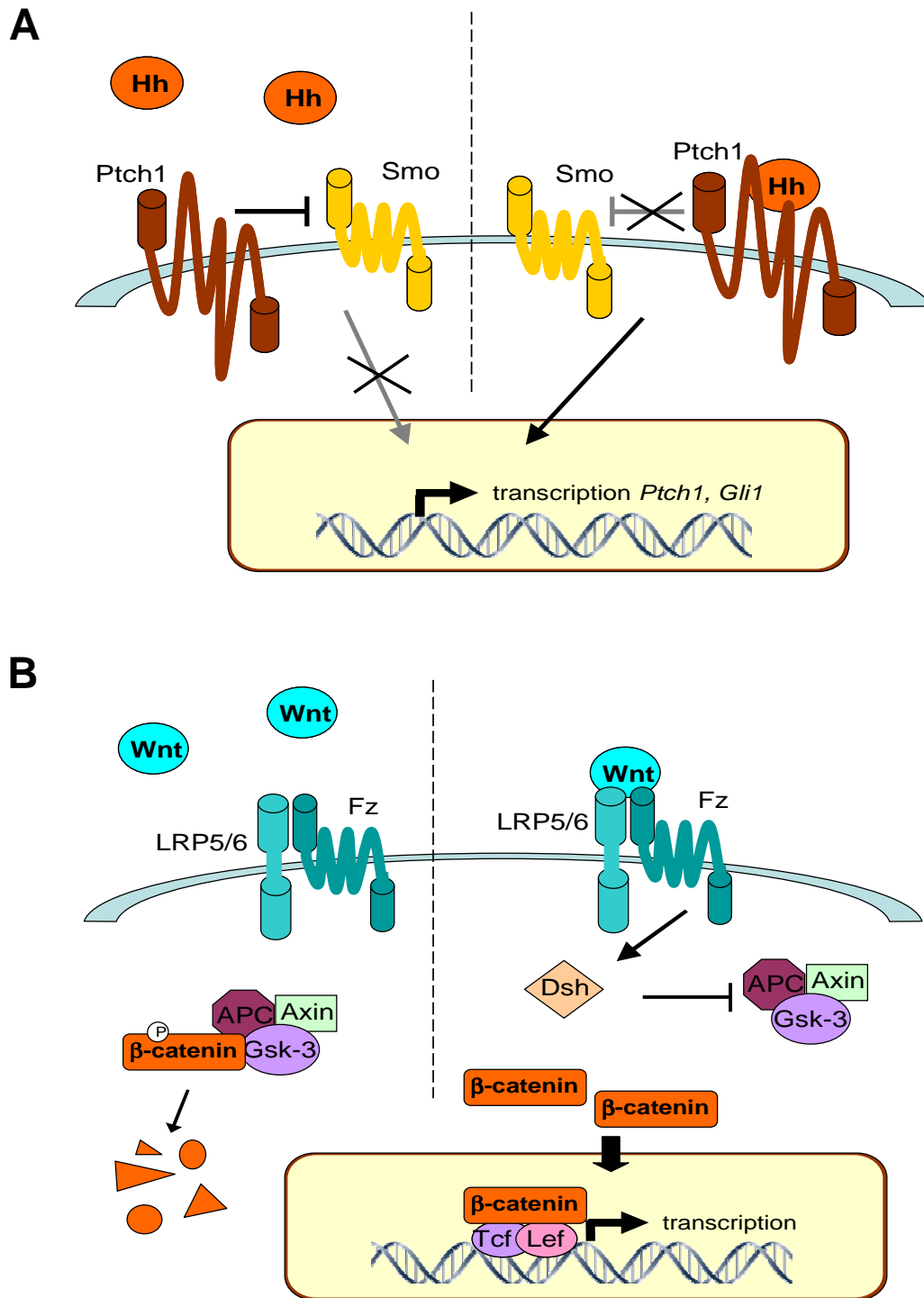


Figure 5: Hedgehog and Wnt signalling pathways. **A** In the absence of Hh molecules binding to its receptor Ptch1, Smo is repressed. Upon ligand binding, Ptch1 relieves its repression and Smo can transmit the signal to the nucleus, where target genes like *Gli1* and *Ptch1* are transcribed. **B** In the absence of Wnt molecules binding to its receptors Fz and LRP5/6, β -catenin is phosphorylated by Gsk-3, in a complex with Axin and APC, and degraded. Wnt binding to the receptors activates Dsh which inhibits the “destruction complex”. β -catenin is stabilised and together with Tcf/Lef induces gene transcription. Ptch1 = Patched1, Smo = Smoothed, Hh = Hedgehog, Fz = Frizzled, LRP5/6 = lipoprotein receptor-related protein 5/6, Gsk-3 = glycogen synthase kinase-3, APC = adenomatous

polyposis coli, Dsh = Dishevelled Tcf = T-cell factor, Lef = lymphoid enhancer factor. adapted from Day and Yang 2008

During the process of chondrocyte and osteoblast differentiation, specific genes are up-regulated that can be used as markers to distinguish distinct stages (Figure 6). Mesenchymal condensations up-regulate *Sox9* which is necessary for differentiation into chondrocytes. (Hartmann 2007) On the other hand *Runx2* accounts for osteoblast differentiation. β -catenin is required for osteoblast lineage differentiation and inhibits chondrogenesis, which is associated with the repression of *Sox9*. (Hill *et al.* 2005) Along the osteoblast lineage *Osterix* (*Osx*) is expressed in immature osteoblast whereas *Osteocalcin* (*Osc*) and *Collagen1* (*Col1*) are markers for mature osteoblasts. *Collagen2* (*Col2*) is expressed in proliferating and pre-hypertrophic chondrocytes, *Ihh* only in pre-hypertrophic chondrocytes and *Collagen10* (*Col10*) is exclusively present in hypertrophic chondrocytes. (Day and Yang 2008; Hill *et al.* 2005; Lai and Mitchell 2005)

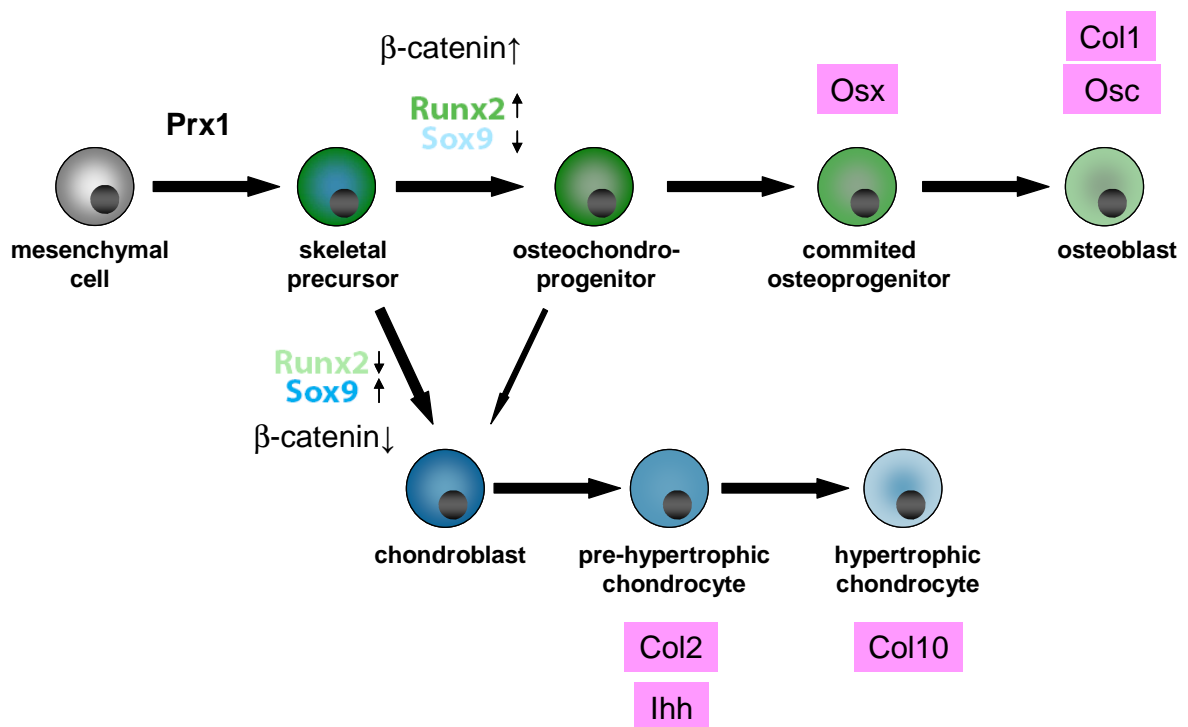


Figure 6: Markers for different stages of osteoblast and chondrocytes. Mesenchymal cell fate is dependent on *Runx2*, β -catenin and *Sox9* levels. High *Runx2* and β -catenin levels initiate the osteoblast differentiation programme whereas high *Sox9* levels are responsible for commitment to the chondrocyte lineage. Markers depicted in pink are used for *in situ* hybridisation to distinguish distinct maturation stages of osteoblasts and chondrocytes. *Osx* = Osterix, *Osc* = Osteocalcin, *Col1* =

Collagen1, Col2 = Collagen2, Ihh = Indian Hedgehog, Col10 = Collagen10; adapted and modified from <http://www.imp.ac.at/research/christine-hartmann/research>

1.2. The JAK/STAT pathway

Cytokines are signalling molecules that play a critical role in the normal development and function of the immune system. They are responsible for the intercellular communication and transmit signals via the Janus kinase (JAK) / Signal transducer and activator of transcription (STAT) pathway. Cytokine receptors lack intrinsic kinase activity and instead depend on JAK to pass on the signal to the nucleus. (Ortmann *et al.* 1999)

The JAK family is a rather small family of tyrosine kinases with four mammalian members - JAK1, JAK2, JAK3 and TYK2. In contrast to the other family members that are quite ubiquitously expressed, JAK3 has a more restricted expression. JAKs are quite large proteins with more than 1100 amino acids. The amino-terminal part facilitates binding to the appropriate cytokine receptor whereas the carboxyl-terminus contains the kinase domain. (Ortmann *et al.* 1999)

STATs are latent cytosolic transcription factors that upon phosphorylation translocate to the nucleus and activate target gene transcription. In mammals seven members are identified: STAT1, STAT2, STAT3, STAT4, STAT5A, STAT5B and STAT6. (Yu and Jove 2004) The amino-terminal part of the protein is necessary for receptor docking, co-factor binding and oligomerisation (Figure 7). The coiled coil domain mediates binding to regulatory proteins and other transcription factors. The DNA binding domain confers direct contact to STAT consensus sequences. Two types of DNA motifs are essential: IFN stimulated response element (ISRE) AGTT(N₃)TTTCC to which STAT1, STAT2 and interferon regulated factor (IRF) 9 bind; γ -activated sequence (GAS) TT(N₄₋₆)AA that is recognised by STAT1, STAT3, STAT4, STAT5A, STAT5B and STAT6. (Ortmann *et al.* 1999) The src homology 2 (SH2) domain enables reciprocal binding to the phosphorylated tyrosine of the STAT dimerisation partner. Dimerisation and subsequent nuclear translocation are required for binding to DNA. At the most carboxy-terminal part resides the transactivation domain responsible for regulating gene transcription and the tyrosine phosphorylation site. Tyrosine phosphorylation is a prerequisite for dimerisation and nuclear translocation. (Yu and Jove 2004) Moreover, STAT1, STAT3, STAT4 (except the splice isoforms), STAT5A, STAT5B and STAT6 contain additional phosphorylation sites at serine and threonine residues that were

reported to enhance transcriptional activity in some STATs. (Friedbichler *et al.* 2011) Unlike tyrosine phosphorylation, the functional significance of the phosphorylated serine residue is controversial but recent evidence points to a so far underrated role for cancer cell transformation or proper immune cell function. (Friedbichler *et al.* 2010; Pilz *et al.* 2009)

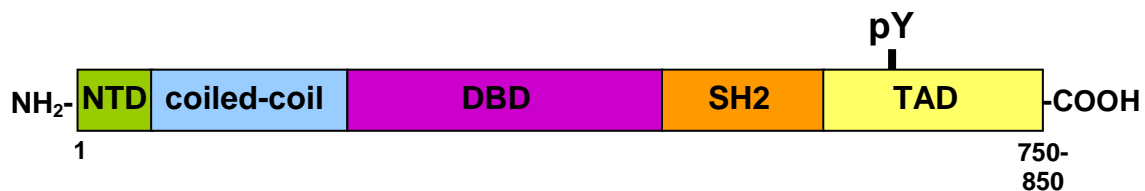


Figure 7: Schematic representation of the general STAT structure. All STAT members have a quite similar domain organisation with a length of the whole protein varying from approximately 750 amino acids (most of the STATs, except the β isoform of STAT1 and STAT3) to 850 amino acids (STAT2 and STAT6). The most amino-terminal part confers receptor docking, co-factor binding and oligomerisation. Binding to regulatory proteins and other transcription factors is enabled by the coiled coil domain. With the DBD STAT proteins specifically bind to the respective consensus sequences. The SH2 domain is necessary for dimerisation by facilitating binding to the phosphorylated tyrosine of the STAT dimerisation partner. Gene regulation is mediated by the carboxy-terminal part that contains the TAD and the tyrosine phosphorylation site. This domain is lacking in the β isoforms of STAT1 and STAT3. NTD = N-terminal domain, DBD = DNA binding domain, SH2 = src homology 2, TAD = transactivation domain, pY = tyrosine phosphorylation site

In general, the process of signal transduction via the JAK/STAT pathway starts with ligand binding to the corresponding receptor (Figure 8). The individual receptor chains dimerise and bring the associated JAKs in close proximity which reciprocally phosphorylate each other. Subsequently, the cytoplasmic tails of the receptors are phosphorylated which serve as docking platforms for STAT proteins. (Aaronson and Horvath 2002) Not so long ago, it was believed that un-phosphorylated STAT proteins are present in the cytosol as monomers but researchers discovered that they exist as a STAT dimer which binds to the phosphorylated receptor. (Sehgal *et al.* 2008) The critical tyrosine residues are phosphorylated and the STAT dimer translocates to the nucleus and activates target gene transcription. (Aaronson and Horvath 2002)

This “old-fashioned” linear view on JAK/STAT signal transmission is complemented with more and more new data leading to following conclusions: Not all of the phosphorylated STATs are located in the nucleus and possible cytoplasmic functions

could be modulation of the duration of signal transmission or cross-talk with other pathways. Un-phosphorylated STATs constantly shuttle between the nuclear and cytoplasmic compartment, so nuclear import is not dependent on tyrosine phosphorylation. (Sehgal *et al.* 2008) Moreover, un-phosphorylated STATs are transcriptionally active but with a set of target genes different from those activated during cytokine signalling. (Cheon *et al.* 2011)

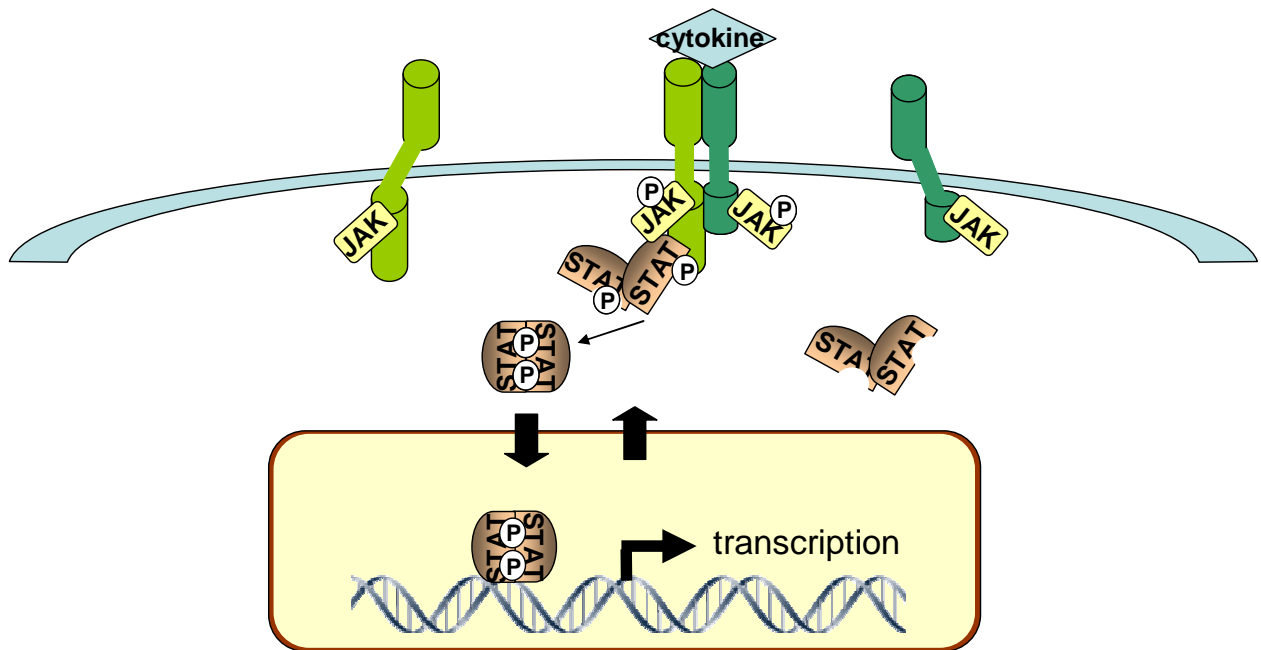


Figure 8: Simplified schematic representation of signalling via the JAK/STAT pathway. Cytokine receptors are transmembrane proteins that lack an intrinsic kinase domain but have instead JAK kinases attached. Upon ligand binding, individual receptor chains are brought together so that the associated JAK kinases phosphorylate each other and the receptors. STAT proteins then bind to the phosphorylated region of the receptors and are phosphorylated by the JAK kinases. Subsequently, STAT dimers travel to the nucleus, bind to DNA consensus sequences and regulate gene transcription.

In terms of regulation of this signal transduction pathway there are different means of shutting down signal transmission.

Protein tyrosine phosphatases like SHP1, SHP2 and PTP1B act at the level of the receptor kinase complex or directly on STAT dimers. (Klampfer 2006)

In contrast to regulating phosphorylation, there are also proteins that directly bind to JAKs and inhibit their activity. Suppressor of cytokine signalling (SOCS) members are SH2 domain proteins that are induced rapidly upon cytokine stimulation and serve as classical negative feedback inhibitors. (Klampfer 2006)

Moreover, protein inhibitors of activated STAT (PIAS) bind directly to activated STAT dimers and inhibit gene activation. (Aaronson and Horvath 2002; Klampfer 2006)

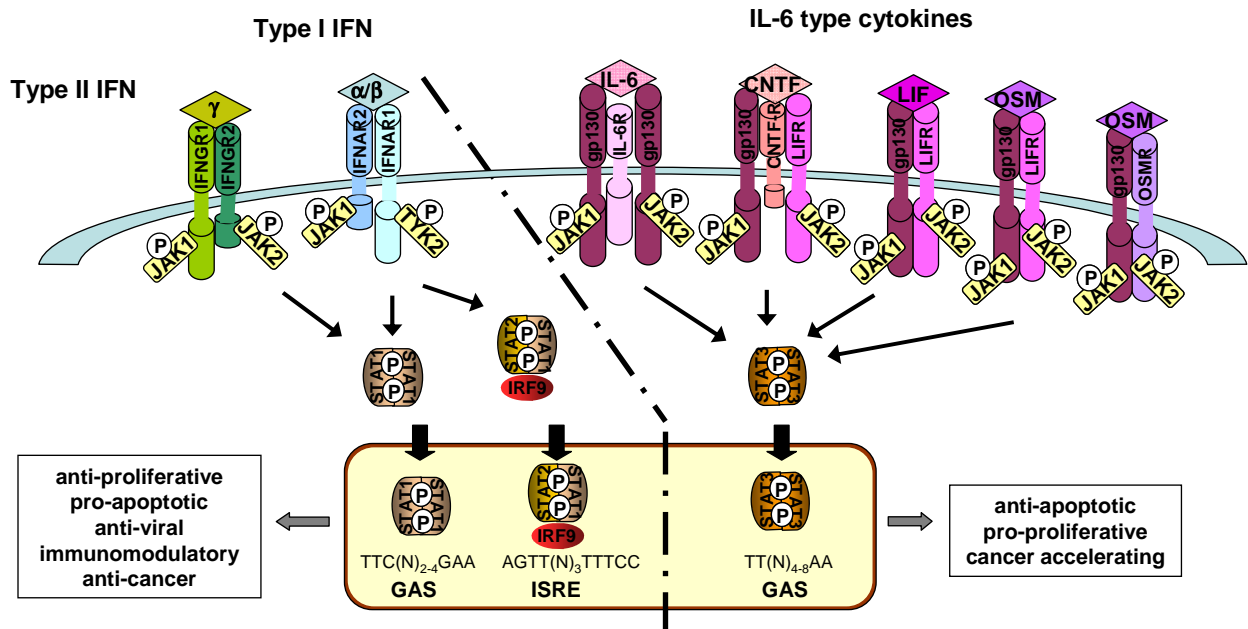


Figure 9: Simplified overview of STAT1 and STAT3 activating cytokine signalling pathways. On the left side the receptors and cytokines that mainly activate STAT1 are depicted and the right side shows mainly STAT3 activating ligand/receptor combinations. IFN- γ employs to IFNGR1 and IFNGR2 and only STAT1 homo-dimers, which bind GAS sequences, are formed. Via IFNAR1 and IFNAR2, type I IFNs (IFN- α and IFN- β) lead to activation of STAT1 homo-dimers as well as a complex consisting of STAT1, STAT2 and IRF9 that specifically binds to ISRE elements. STAT1 proteins are known to have following properties: anti-proliferative, pro-apoptotic, anti-viral, immunomodulatory and hence anti-cancer. Gp130 is a component of all IL-6 type cytokine receptor complexes together with an individual receptor chain. IL-6 binds two gp130 molecules and the specific IL-6R. LIFR is present in receptor complexes that bind CNTF, LIF and OSM. CNTF engages, together with gp130 and LIFR, the CNTFR chain. OSMR is exclusively present in the complex binding OSM. All these combinations activate mainly STAT3 and act therefore anti-apoptotic, pro-proliferative and hence cancer accelerating. IFN = interferon, IFNGR = interferon- γ receptor, IFNAR = interferon- α receptor, gp130 = glycoprotein 130, IL-6 = interleukin-6, CNTF = ciliary neurotrophic factor, LIF = leukaemia inhibitory factor, OSM = oncostatin M, IL-6R = IL-6 receptor α , CNTFR = CNTF receptor α chain, LIFR = LIF receptor, OSMR = OSM receptor, ISRE = IFN stimulated response element, GAS = γ -activated sequence

Interferons (IFN) are cytokines that have the property to act in an anti-viral, anti-proliferative and immunomodulatory manner. There are two main classes of IFNs, namely type I, which comprise IFN- α and IFN- β , and type II IFN including only IFN- γ .

Type I IFNs are distinct from the majority of STAT activating cytokines. Activation of JAK1 and TYK2 associated with type I IFN receptors leads to phosphorylation of STAT1 and STAT2 (Figure 9). These two STAT proteins constitute a trimeric complex together with IRF9, called interferon-stimulated gene factor 3 (ISGF3), which binds to ISRE elements and activates anti-viral target genes. (Platanias 2005) Activation of STAT3 is also induced by IFN- α but its function is not so well studied. A possible role for IFN- α activated STAT3 might be negative regulation of the inflammatory response which is obtained by STAT1 sequestration. (Ho and Ivashkiv 2006) IFN- γ signalling requires JAK1 and JAK2, activating only STAT1 proteins. STAT1 homo-dimers recognise GAS elements and activate an anti-tumour immune response. (Platanias 2005)

Moreover, other signalling pathways, like the mitogen-activated protein kinase (MAPK) or PI3K/AKT pathway, are also activated by IFNs. They interact with the JAK/STAT mediated signalling either on the level of gene transcription or by regulating serine phosphorylation of STAT1. (Platanias 2005)

The interleukin (IL)-6 type cytokines activate mainly STAT3 (STAT1 phosphorylation is more transiently) and regulate differentiation, survival, proliferation and are also major players in immune responses. One receptor chain, glycoprotein (gp) 130, is included in all receptor complexes employed by the different family members (Figure 9). IL-6 type cytokines include ciliary neurotrophic factor (CNTF), leukaemia inhibitory factor (LIF) and oncostatin M (OSM). IL-6 and CNTF bind to a complex of gp130 molecules or gp130 and LIF receptor (LIFR) and the non-signalling IL-6 receptor α (IL-6R) or CNTF receptor α chain (CNTFR), respectively. In contrast, LIF and OSM bind to complexes consisting of one gp130 molecule and one LIFR or OSMR chain. (Heinrich *et al.* 2003) Gp130 can bind to JAK1, JAK2 and TYK2 and thereby activates STAT3. (Ortmann *et al.* 1999)

1.2.1. JAK/STAT in cancer

STATs regulate several processes that control proliferation, cell survival, angiogenesis and immune responses. Since de-regulation of these processes can lead to neoplastic transformation, perturbation of JAK/STAT signalling is predestined to be involved in tumourigenesis. (Klampfer 2006; Yu and Jove 2004)

There are no mutations in *STAT* genes found in tumours but many mutations affect tyrosine kinases. In fact, all four JAK kinases have been discovered to be mutated in human cancer. (Ghoreschi *et al.* 2009) Additionally, over-production of cytokines or their receptors, hyperactive tyrosine kinases or silencing of negative regulators (SOCS or PIAS) renders *STAT* proteins constitutively active. (Bromberg 2002; Klampfer 2006)

Hyperactivation of *STAT1* is only rarely found in some tumour types. Which is not surprising with *STAT1* being a potent inhibitor of growth (induction of *p21*, *p27*; repression of *c-myc*, *cyclins*) and promoter of apoptosis (up-regulation of *caspase-8* expression). (Fulda *et al.* 2002; Regis *et al.* 2008) With these tumour suppressor properties, constitutive active *STAT1* is rather an indicator of good prognosis for e.g. breast cancer patients than driving tumourigenesis. (Klampfer 2006)

Constitutive active *STAT3* is sufficient to transform fibroblasts *in vitro*, demonstrating the oncogenic properties of *STAT3*. (Bromberg 2002) *STAT3* drives cell proliferation (up-regulation of *cyclin D1*, *c-Myc*), inhibits apoptosis (induction of *Bcl* family members), promotes angiogenesis (*VEGF* up-regulation) and suppresses anti-tumour immune responses, processes that are involved in tumourigenesis. (Regis *et al.* 2008) Indeed, constitutive activation of *STAT3* is often discovered in lymphomas or solid tumours. (Yu and Jove 2004)

STAT5 activation is frequently found in various leukaemias promoting proliferation and inhibiting apoptosis. One way to constitutively activate *STAT5* is the presence of the well-known Bcr-Abl tyrosine kinase, resulting from a chromosomal translocation (Philadelphia chromosome) in chronic myelogenous leukaemia (CML). (Klampfer 2006) There are many other mechanisms how tumour cells render *STAT5* active and they are well described in the literature but only discussed shortly here since *STAT5* was not relevant for the PhD thesis.

1.3. Aim of the thesis

Chromosomal translocations are a hallmark of ESFT and present the driving force in ESFT pathogenesis. The most prominent one rearranges chromosome 11 with chromosome 22, resulting in the *EWS/FLI-1* fusion gene. Depending on the cellular context, *EWS/FLI-1* is able to transform cells or leads to apoptosis or growth arrest. The question for the cell of origin is still under debate but more and more evidence points to a mesenchymal origin.

ESFT is usually treated by chemotherapy in combination with surgery and/or radiotherapy. But since there is only little progress in the field of chemotherapy, the need for a mouse model is evident. Several attempts were already undertaken to generate a mouse model for ESFT but at the beginning of this study no mouse expressing *EWS/FLI-1* was available that recapitulates the human phenotype.

Thus, our goal was to establish a mouse model that expresses *EWS/FLI-1* in the relevant cellular background and that later on develops a sarcoma similar to ESFT. We used a conditional *EWS/FLI-1* mouse model, which upon Cre activity (controlled by a tissue specific promoter) expressed *EWS/FLI-1* in the targeted cells. Since ESFT arises in bone and surrounding soft tissue we decided to direct expression of *EWS/FLI-1* to the mesenchymal lineage.

Cytokines, either produced in the tumour microenvironment or released by tumour cells, are important regulators of signalling networks controlling many functions necessary for a tumour cell such as proliferation, differentiation, survival or tumour surveillance. Among others, the JAK/STAT signalling pathway regulates these functions. Although components of this pathway are often de-regulated in human cancers, not much is known about its function in ESFT. Only a few publications demonstrate that *JAK1* is up-regulated and *STAT3* was reported to be activated to variable degrees in ESFT patient samples.

The aim of the second study of this thesis was to better understand the role of the JAK/STAT pathway in ESFT. Therefore, we carefully analysed different ESFT cell lines for activation of the JAK/STAT pathway.

2. Materials and Methods

2.1. Working with mice

2.1.1. Colony management

Mice were kept under standard conditions at the Decentralised Biomedical Facility from the Medical University of Vienna on a 12 hours light-dark cycle. All animal experiments were approved by the Austrian ministry for science and research (license number: BMWF-66009/0139-C/GT/2007).

Between 18-21 days after birth pups were weaned, marked with ear tags and a small piece of tail was collected for genotyping.

2.1.1.1. Transgenic mouse strains

Mice harbouring a Cre-inducible EWS/FLI-1 knocked into the ubiquitous Rosa26 locus (Rosa26loxP-STOPloxP-HA-EWS/FLI-1 allele, homozygous mice were hereafter referred to as EF) were kindly provided by Dr. Suzanne Baker (St. Jude Children's Research Hospital, Memphis, Tennessee, USA) via Material Transfer Agreement (MTA). (Torchia *et al.* 2007)

To express EWS/FLI-1 in a restricted manner in the osteoblast lineage, mice harbouring the EF allele were crossed to Runx2Cre mice (courtesy of Dr. Jan Tuckermann, Fritz Lipmann Institute, Jena, Germany). (Rauch *et al.* 2010) Two Runx2 isoforms exist that are expressed from promoters P1 and P2. (Stock and Otto 2005) P1 is assumed to be highly regulated and expresses the bone specific variant of Runx2. (Stock and Otto 2005) Therefore, the P1 promoter is employed in the construct for generation of Runx2Cre transgenic mice. This strain was generated with a BAC (bacterial artificial chromosome) approach, thus there were different transgenic lines available (777, 784, 1634). (Rauch *et al.* 2010) Runx2Cre EF mice were also bred to mice deficient in $p16^{INK4A}$ and $p19^{ARF}$, thereafter referred to as INK4A/ARF (kindly provided by Dr. Manuel Serrano, Spanish National Cancer

Research Centre, Madrid, Spain) (Serrano *et al.* 1996), since deletion of INK4A/ARF is present in 20% of ESFT. (Lopez-Guerrero *et al.* 2001) Moreover, expression of *EWS/FLI-1* in the limb bud mesenchyme was achieved by crossing EF to Prx1Cre mice (kindly provided by Dr. Malcolm Logan, National Institute for Medical Research, Mill Hill, United Kingdom via MTA). (Logan *et al.* 2002) Additionally, Mx1Cre was crossed into EF mice to proof proper expression of *EWS/FLI-1* from the EF allele as published originally by Dr. Suzanne Bakers group. (Torchia *et al.* 2007)

2.1.1.2. Genotyping mice

Tail biopsies were digested with 0,5 mg/ml Proteinase K (Sigma), diluted in tail digestion buffer at 56 °C overnight. Thereafter, 1 µl was used for genotyping PCR and the products were visualised on an agarose gel.

Tail digestion buffer

- 50 mM KCl
- 10 mM Tris pH 8,3
- 2 mM MgCl₂
- 0,1 mg/ml gelatine
- 0,45% NP-40
- 0,45% Tween-20

PCR reaction mix

- 0,2 µl Taq polymerase (5 U/µl, 5Prime)
- 3 µl PCR buffer (10 x, 5Prime)
- 0,5 µl dNTP mix (10 mM, Fermentas)
- 1 µl primer mix
- 3 µl 10% DMSO (only required for EF PCR)
- ad 30µl ddH₂O

Sequences of Primers, the expected products and the corresponding genotype are given in the tables below.

Runx2Cre

name	sequence	concentration	product [Bp]		genotype	
cbfa_30	5' GGAGCTGCCGAGTCAATAAC 3'	2,5 pmol	780	600	wt	Cre+
cbfa_24	5' CCAGGAAGACTGCAAGAAGG 3'	10 pmol				
cbfa_25	5' TGGCTTGCAGGTACAGGAG 3'	10 pmol				

EF

name	sequence	concentration	product [Bp]		genotype	
RosaWT-R	5'ACACACCAGGTTAGCCTTTAAG 3'	15 pmol	240	366	wt	EF
RosaWT-F	5'GAGTTGTTATCAGTAAGGGAGC 3'	15 pmol				
RosaKI-R	5'GATCCACTAGTTCTAGAGCGGC 3'	15 pmol				

Prx1Cre and Mx1Cre

name	sequence	concentration	product [Bp]	genotype
Cre1	5'CGGTTCGATGCAACGAGTGATGAGG 3'	10 pmol	700	Cre+
Cre2	5'CCAGAGACGGAAATCCATCGCTCG 3'	10 pmol		

INK4A/ARF

name	sequence	concentration	product [Bp]	genotype
P16F	5'CCCAGGTGAGCATAGTTGGT 3'	10 pmol	300	wt
P16R	5'GGAAGTGGAGAGGCTGCAAAAC 3'	10 pmol		
Neo_F	5'CTATCAGGACATAGCGTTGG 3'	10 pmol	700	knock-out
UTR_R	5'AGTGAGAGTTTGGGGACAGAG 3'	10 pmol		

PCR conditions:

94°C	2 minutes		initial denaturation
94°C	20 seconds	40x	denaturation
55°C	20 seconds		annealing
72°C	90 seconds		elongation
72°C	2 minutes		final elongation
22°C	∞		storage

The INK4A/ARF PCR required an annealing temperature of 60°C.

2.1.1.3. Plug check

For embryo experiments vaginal plugs of females in breeding cages were checked daily. If a plug was found the female was separated and noon at that day was counted as E (embryonic day) 0,5. Embryos were then harvested at indicated time points.

2.1.2. Xenotransplantation

Severe combined immunodeficiency (SCID) mice (Charles River, c.b.17/1crHanHsd) have a reduced immune system (B- and T-cell deficiency) and are therefore suitable for transplantation of human cells. Since they are highly susceptible to infections they were kept in filter top cages with a separate air supply to prevent entry of pathogens.

Tumourigenicity was determined after subcutaneous injection of 4×10^6 cells. Tumour growth was assessed 3 times a week by measuring tumour size. For ethical reasons, mice were sacrificed when the mean tumour volume ($(a^2 \times b) \times 2$) exceeded $1,5 \text{ mm}^3$. Tumours were either fixed in 4% formaldehyde in PBS for at least 48 hours at room temperature and processed as described in 2.1.3. or snap frozen in liquid nitrogen for RNA and protein extraction.

PBS (Phosphate buffered saline)

2,7 mM KCl

1,4 mM KH_2PO_4

137 mM NaCl

4,3 mM Na_2HPO_4

pH 7,4

2.1.3. Tissue preparation, paraffin embedding, sectioning

Mice were sacrificed by cervical dislocation or by euthanising with diethyl ether, organs were excised with sterile scissors and cut into 5 mm x 5 mm pieces to ensure proper fixation. Bones were cut out and freed from surrounding muscle

tissue. Organs were then snap frozen in liquid nitrogen or fixed in 4% formaldehyde/PBS for at least 48 hours at room temperature, washed twice with PBS and stored at 4°C. Bones were additionally decalcified in 0,5 M EDTA for 2 - 4 weeks before further usage. Embryos were fixed in 4% paraformaldehyde (PFA)/PBS overnight at 4°C, washed twice with PBS, dehydrated manually with an ascending ethanol series (25%, 50%, 75%, 100%) and stored in 100% ethanol at -20°C.

Dehydration, if not done manually, and paraffinisation were done automatically as followed: Organs were dehydrated with an ascending ethanol series (50%, 2 x 70%, 2 x 80%, 3 x 96%), washed twice with xylene at 40°C and incubated in paraffin at 60°C with 3 changes. Then, organs were embedded in paraffin filled metal moulds and allowed to solidify. Blocks were stored at room temperature until needed.

Blocks were sectioned with a microtome into 2 µm or 5 µm thick slices. The sections were transferred carefully to a 55°C water bath to get rid of wrinkles and were picked up with Superfrost microscopic slides. Sections were dried overnight and stored at room temperature or 4°C for several weeks.

2.1.4. Histology

2.1.4.1. Haematoxylin and eosin staining (H&E)

Sections were deparaffinised by incubation in xylene substitute (Shandon) for 15 minutes (twice) and re-hydrated with a descending ethanol series (2 x 100%, 75%, 50%, 25%) for 5 minutes each. Slides were incubated 5 minutes in dH₂O and stained with Mayer's haematoxylin solution (1:1 dilution in dH₂O, Merck) for 10 minutes. Subsequently, sections were incubated in tap water for 5 - 10 minutes followed by dipping twice in 3% HCl/70% ethanol. Slides were rinsed with tap water for 7 minutes and de-hydrated using an ascending ethanol series (25%, 50%, 75%). The tissue was counterstained with eosin staining solution for 2,5 minutes and incubated twice in 100% ethanol for 2 minutes. After a final 2 minutes incubation in xylene substitute, tissue sections were mounted with Eukitt mounting medium (Lactan) and analysed with a Zeiss Axio Imager.Z1 microscope.

Eosin staining solution

0,1% Eosin Y

70% ethanol

0,25% acetic acid

2.1.4.2. Immunohistochemistry

Sections were deparaffinised by incubation in xylene substitute (Shandon) for 15 minutes (twice) and re-hydrated with a descending ethanol series (2 x 100%, 75%, 50%, 25%) for 5 minutes each. Slides were incubated 5 minutes in dH₂O.

Antigen retrieval was achieved by heating in a microwave oven. Slides were brought to boil (800 W, 2 minutes) in 10 mM citrate buffer pH 6,0 (Dako) and then maintained at a sub-boiling temperature (210 W) for 10 minutes. Afterwards, the slides were allowed to cool down and washed three times with PBS. After every following step, slides were washed three times with PBS.

Endogenous peroxidase can cause non-specific background staining when a horse radish peroxidase (HRP) coupled secondary antibody is used. Therefore, slides were incubated for 15 minutes in H₂O₂ block (3% H₂O₂ in PBS) to quench endogenous peroxidase activity and the tissue was encircled with Dako Pen (Dako). To eliminate background caused by endogenous avidin or biotin, an additional blocking step was employed. Slides were incubated for 10 minutes with Avidin Block (Avidin/Biotin Blocking Kit, Vector-Labs) and subsequently 10 minutes with Biotin Block, followed by incubation with Superblock (ID-Labs) for not more than 7 minutes. Since the secondary antibody used later is polyvalent and therefore also recognises endogenous mouse immunoglobulins, another blocking step was utilised. Mouse Block (2 drops in 2,5 ml PBS, M.O.M. Vector Labs) was left on slides for one hour and then slides were incubated with the primary antibody diluted in 1% BSA/PBS at 4°C.

The next day, slides were incubated with Anti Polyvalent Biotinylated Antibody (ID-Labs) for 10 minutes and with Streptavidin-HRP (ID-Labs) for 10 minutes. Subsequently, signals were detected with the AEC Staining Kit (4 ml dH₂O + 2 drops Acetate buffer, 1 drop AEC Chromogen, 1 drop H₂O₂; Sigma). Staining intensity was controlled under the microscope and when assessed as appropriate, the reaction was stopped with dH₂O. To differentiate the nucleus from the cytoplasm, staining with haematoxylin for 2 - 5 minutes was applied. Slides were rinsed in tap water,

mounted with Aquatex (Lactan) and analysed with a Zeiss Axio Imager.Z1 microscope.

antibody	recognises	dilution	features
pSTAT1	STAT1 p-Tyr701	1:100	rabbit polyclonal (9171, Cell Signaling)
pSTAT3	STAT3 p-Tyr705	1:50	rabbit polyclonal (9131, Cell Signaling)

2.1.4.3. In situ hybridisation

All solutions were prepared or diluted with DEPC treated water.

Slides were de-waxed twice 15 minutes in xylene substitute (Shandon) and re-hydrated to PBS with a descending ethanol series (2 x 100%, 75%, 50%, 25%) for 5 minutes each.

After fixation with 4% PFA/PBS for 10 minutes the slides were washed three times with PBS-T. Antigen retrieval was achieved with incubation in 1 µg/ml Proteinase K/PBS for 10 minutes. Subsequent washing with PBS-T was followed by fixation with 4% PFA/PBS for 10 minutes and another three washing steps. After acetylation for 15 minutes with 0,25% acetic anhydride in 0,1 M triethanolamine and three washing steps with PBS-T slides were air-dried for 30 minutes.

For one slide 100 µl hybridisation solution was incubated for 3 minutes at 85°C, mixed with 1 µl labelled probe (see 2.5.5) and applied to the slide. To protect the solution from evaporation, slides were covered with coverslips avoiding air bubbles. Hybridisation was done in a 65°C water bath for at least 16 hours.

All washes were carried out in a water bath and solutions were pre-warmed. Coverslips were removed by rinsing in 5 x SSC and slides were incubated for 30 minutes at 65°C in 1 x SSC/50% formamide. Following a 10 minute wash in TNE at 37°C for 10 minutes, RNA was digested with 20 µg/ml RNase A in TNE at 37°C for 30 minutes. After another TNE wash at 37°C for 10 minutes, slides were incubated once in 2 x SSC and twice in 0,2 x SSC for 20 minutes each at 65°C.

Two washes in MAB-T for 5 minutes at room temperature were followed by blocking in 20% HISS/MAB-T for one hour at room temperature. Anti-digoxigenin-alkaline phosphatase antibody (1:2000, Roche) was diluted in 2% HISS/MAB-T and slides were incubated overnight at 4°C in a humidified box.

The next day slides were washed 4 times in MAB-T, once in NTMT for 10 minutes and BM purple AP substrate (Roche) was added. Incubation was done for up to 3 days until a colour reaction could be seen.

To stop the reaction, slides were rinsed in NTMT and washed twice in PBS for 5 minutes. Then the tissue was post-fixed in 4% PFA/PBS for 10 to 20 minutes. Slides were rinsed twice in PBS and then in ddH₂O. Finally, pre-warmed (65°C) glycerol mounting medium (Dako) was applied and slides were analysed with a Zeiss Axio Imager.Z1 microscope.

ddH₂O-DEPC

DEPC (1 ml/l) was added to ddH₂O, mixed well, incubated overnight at room temperature and autoclaved.

PBS

10 x PBS was diluted to 1 x concentration with ddH₂O-DEPC.

PBS-T

1 x PBS + 0,1% Tween-20

Hybridisation Solution

10 mM Tris pH 7,5

500 mM NaCl

1 mM EDTA

0,25% SDS

10% Dextran sulphate

1 x Denhardt's

200 µg/ml yeast tRNA (Gibco)

50% formamide

filtered and stored at -20°C

50 x Denhardt's

1% Ficoll 400

1% Polyvinylpyrrolidone

1% BSA

filtered and stored at -20° C

20 x SSC

3 M NaCl

0,3 M sodium citrate

5 x TNE

50 mM Tris pH 7,5

2,5 M NaCl

5 mM EDTA

2 x MAB

200 mM Maleic Acid

300 mM NaCl

adjusted to pH 7,5 with 10 M NaOH

MAB-T

1 x MAB + 0,1% Tween-20

HISS

Sheep serum (Sigma) was heat inactivated at 56° C for 30 minutes and stored at -20° C.

NTMT

100 mM NaCl

100 mM Tris pH 9,5

50 mM MgCl₂

0,1% Tween-20

2.1.5. Skeletal staining

Embryos were skinned, eviscerated and incubated in 96% ethanol for at least 24 hours at room temperature (embryos could be stored for several weeks at this stage). E 16.5 or younger embryos were additionally fixed in 4% PFA/PBS at 4° C

overnight and then incubated in 96% ethanol. All further steps were carried out at room temperature. Fat was removed by incubating in acetone and the following day embryos were stained with Alcian Blue/Alizarin Red. After 24 hours skeletons were dehydrated in a descending alcohol series (96%, 70%, 50%, 25%) for 30 minutes each and then digested with 1% potassium hydroxide (KOH) until surrounding tissue was cleared and the bones could be nicely seen. To store the skeletons a KOH:glycerol series was applied (3:1, 1:1, 1:3) and finally transferred into pure glycerol.

Alcian Blue/Alizarin Red

60% ethanol

5% acetic acid

5% Alcian Blue stock

5% Alizarin Red stock

Alcian Blue stock

0,3% Alcian Blue in 70% ethanol

Alizarin Red stock

0,1% Alizarin Red in 96% ethanol

2.2. Tissue culture

2.2.1. Cell lines

SK-N-MC

ESFT cell line established by Dr. June Biedler (Memorial Sloan-Kettering Cancer Centre, New York, USA) from a metastatic site of a neuroepithelioma from a 14-year-old Caucasian female. (Biedler *et al.* 1973)

karyotype: pseudo-diploid (<http://www.dsmz.de>)

INK4A/ARF locus: no genetic alteration but Rb absent (Kovar *et al.* 1997)

p53: truncated (Kovar *et al.* 1997)

EWS/FLI-1 fusion: type1 (Kovar *et al.* 2001)

EWS expression: present (Kovar *et al.* 2001)

STA-ET-7.2

ESFT cell line established at the Children's Cancer Research Institute, Vienna, Austria from a pleural effusion of a 4-year-old female patient (the primary tumour was located in the chest wall). (Kovar *et al.* 1997)

karyotype: near-triploid (Kovar *et al.* 2001)

INK4A/ARF locus: no mutation but lack of protein expression (Kovar *et al.* 1997)

p53: mutated (Kovar *et al.* 1997)

EWS/FLI-1 fusion: type2 (Kovar *et al.* 2001)

EWS expression: absent (Kovar *et al.* 2001)

TC-71

Cell line established by Dr. Timothy Triche (Department of Pathology, University of Southern California, Los Angeles, USA) from a local Ewing's sarcoma relapse of the humerus. (Whang-Peng *et al.* 1984)

karyotype: hyper-triploid (<http://www.dsmz.de>)

INK4A/ARF locus: lack of expression (Zhang *et al.* 2004)

p53: mutated (Zhang *et al.* 2004)

EWS/FLI-1 fusion: type1 (<http://www.dsmz.de>)

EWS expression: present

All cell lines were provided by Dr. Heinrich Kovars group (Children's Cancer Research Institute, Vienna, Austria) and were cultivated in RPMI (PAA) supplemented with 10% fetal calf serum (FCS, PAA) and 1% Penicillin-Streptomycin (PAA).

2.2.2. Propagation of cell lines

Cells were cultivated in an incubator at 37°C in an atmosphere with 5% CO₂.

It was important to split the cells every two to three days according to their doubling time so that the cells never became over-confluent.

Medium was removed and cells were washed with PBS. Then Trypsin (PAA) or Accutase (PAA) was added. After 10 minutes of incubation the cells were detached from the petri dish. Next, new medium was added, cells were resuspended and the cell number was determined (see 2.2.3.). Then the cells were diluted as required and were plated on new dishes.

Additionally, dishes for STA-ET-7.2 and TC-71 were coated with fibronectin. One milligram fibronectin (Chemicon) was diluted in 30 ml PBS and dishes were incubated for 45 minutes at room temperature. Fibronectin solution was collected and could be re-used several times. Either the dishes were used directly or stored at 4°C. When cells were harvested with Accutase, fibronectin coated dishes could be re-used several times.

2.2.3. Quantitation of cell number

For the determination of cell number, 20 µl of the cell suspension was counted in a Neubauer-chamber. The number of counts in a square multiplied with 10⁴ indicated the number of cells/ml.

2.2.4. Freezing/ Thawing of cells

Cells were trypsinised and pelleted by centrifugation for 5 minutes at 1200 rpm. The pellet was resuspended in pre-cooled 90% FCS/10% DMSO and incubated on ice

for 20 minutes. Afterwards the cells were stored overnight in a freezing container (VWR) at -80°C and were then transferred to liquid nitrogen.

To thaw cells, the frozen tube was incubated in a 37°C warm water bath until the cell suspension was liquid. Immediately afterwards, the cell suspension was diluted in 5 ml pre-warmed medium and centrifuged. Finally, the cell pellet was resuspended in the desired volume of the appropriate medium.

2.2.5. Cytokine stimulation

For protein extracts, cells were stimulated 30 minutes at 37°C with the required cytokine before they were harvested.

Alternatively, for target gene expression analysis cells were stimulated for 4 hours with the appropriate cytokine at 37°C and RNA was isolated.

To measure proliferation in response to a cytokine, cells were stimulated with this cytokine one day after seeding and then medium containing the cytokine was changed every second day.

Following cytokines were usually used at indicated concentrations, if not stated otherwise: 10 ng/ml ciliary neurotrophic factor (CNTF, Peprotech), 10 ng/ml interferon alpha ($\text{IFN-}\alpha$, Roche), 1 ng/ml interferon gamma ($\text{IFN-}\gamma$, Boehringer Ingelheim), 100 ng/ml interleukin 6 (IL-6, Immunotools), 1 ng/ml leukaemia inhibitory factor (LIF, Chemicon), 10 ng/ml oncostatin M (OSM, Immunotools).

2.2.6. Proliferation assay

To follow proliferation of cell lines over a defined time span, a proliferation assay employing the ability of crystal violet to stain viable cells was applied.

Cells were fixed in the culture dish for 30 minutes with 10% formalin at room temperature and washed with PBS. Either they were used directly or stored at 4°C in PBS until further needed.

Then, cells were stained 30 minutes with 0,1% Crystal Violet (Sigma) and subsequently washed with dH_2O until the washing water was clear. The dye was extracted with 10% acetic acid, diluted 1:4 with dH_2O and measured in a 96well-plate at 570 nm. The values for the optical density were then compared to control and experimental groups.

2.2.7. Flow cytometric analysis

Cells were harvested with Accutase and cell number was determined. For one antibody staining 0,5 - 1×10^6 cells were resuspended in 100 μ l 5% FCS/PBS. The first antibody (see list below) was added in the indicated concentration and cells were incubated for 30 minutes at 4°C in the dark. After washing with PBS, anti-mouse IgG FITC conjugate (Sigma) was diluted 1:100 in 100 μ l 5% FCS/PBS and cells were incubated with the secondary antibody for 30 minutes at 4°C in the dark. After a final wash with PBS, cells were resuspended in 500 μ l 5% FCS/PBS and analysed on a FACScan.

antibody	amount needed for 1×10^6 cells	features
CNTFR α	5 μ l	mouse monoclonal, 0,2 μ g/ μ l (AN-B2, Santa Cruz sc-9993)
gp130	10 μ l	mouse monoclonal (BR-3, Diaclone)
IL-6R	10 μ l	mouse monoclonal (BR-6, Diaclone)
LIFR	10 μ l	mouse monoclonal (10B12, 1 μ g/ μ l)
OSMR β	5 μ l	mouse monoclonal, 0,2 μ g/ μ l (AN-A2, Santa Cruz sc-9992)

The LIFR antibody was a courtesy of Dr. Gerhard Müller-Newen, University Hospital Aachen, Germany.

For flow cytometric analysis of mouse tissue, cells were dissociated by passing the tissue through a 70 μ m cell strainer (BD Biosciences). Red blood cells were lysed by incubating the homogenised tissue for 5 minutes at room temperature in ACK lysis buffer. Cells were resuspended in PBS and 50 μ l were used for each antibody staining. Antibodies (directly linked to a chromogen) were diluted 1:100 in PBS and 50 μ l were added to the cell suspension. After incubation for 30 minutes at 4°C in the dark, cells were washed with PBS and analysed on a FACSCanto.

ACK lysis buffer

155 mM NH₄Cl

10 mM KHCO₃

0,1 mM EDTA pH 8,0

adjusted to pH 7,3 with HCl

antibody	conjugate	features
cKit	PE-Cy5 conjugate	mouse monoclonal, 0,2 µg/µl (BD Bioscience)
CD43	Phycoerythrin (PE)	rat monoclonal, 0,2 µg/µl (BD Bioscience)
CD71	Fluorescein-5-isothiocyanat (FITC)	mouse monoclonal (BD Bioscience)

2.2.8. Isolation of fibroblasts from mouse ear skin

Mice were sacrificed, ears were sterilised with ethanol and only the part without hairs was excised. Each ear was washed in PBS and then minced with a scalpel in 600 µl DMEM with 4 µg/µl Collagenase D (Roche) and 4 µg/µl Dispase II (Sigma) in a well of a 12 well-plate. Ear pieces were incubated in a 37°C incubator. The next day 1,5 ml DMEM + 10% FCS was added and the cells were singularised with a 70 µm cell strainer. Cells from one ear were plated into one well of a 6 well-plate. The following day medium was changed and cells were grown until subconfluency. Then they were re-plated and used for experiments.

2.2.9. Infection of cells with lentivirus

Fibroblasts isolated from mouse ear skin were infected with lentiviral vectors (pRRL-GFP and pRRL-CreIRESGFP; courtesy of Dr. Christopher Baum, Hannover Medical School, Germany).

Old medium was removed from cells in a 12 well-plate and 10 µl virus (pRRL-GFP and pRRL-CreIRESGFP; transduction efficiency: $6,3 \times 10^7$ /ml) was added together with 400 µl DMEM and 4 µg/µl protamine sulphate. The cells were centrifuged in the plate at 2000 rpm for 1 hour at room temperature. After 6 hours at 37°C in the incubator 600 µl fresh medium was added. The next day medium was changed and cells were analysed for GFP expression 48 hours after infection.

2.2.10. Isolation of osteoblasts

Newborn mice (up to 6 days old) were sacrificed by cervical dislocation in a sterile hood and dipped into ethanol. Then the skin on top of the head was removed. Calvariae were cut out with a transsection from the back of the skull over the eyes

on both sides up to the nose and were lifted, avoiding taking the brain along. Residual skin was removed and calvariae from one pup were put into one tube with 1 ml PBS + 1% Penicillin-Streptomycin (PAA) and kept on ice.

PBS was replaced by 1 ml digestion solution (MEMalpha (PAA) + 1% Penicillin-Streptomycin + 0,2% Collagenase A (Roche) and 0,2% Dispase II (Sigma)) and incubated at 37°C on a heating block shaking with 600 rpm for 10 minutes. The liquid phase (fraction 1) was discarded and digestion was repeated with 1 ml digestion solution. Fractions 2 - 5 were collected in a big tube and stored on ice in-between. Cells were then collected by centrifugation at 1500 rpm for 5 minutes and cells from one pup were plated in a well of a 6 well-plate with 2 ml growth medium (MEMalpha +10% FCS + 1% Penicillin-Streptomycin).

Cells were grown until subconfluency and re-plated at a density of 10 000 cells/cm². At confluency the cells were induced with 100 µg/ml ascorbic acid (Sigma) and 5 mM β-glycerophosphate (Sigma) in growth medium. Medium was changed twice a week for a total of 14 days and then analysed. Mineralisation of cells was controlled with Alizarin Red staining.

2.2.10.1. Alizarin Red staining

Cells were fixed for 10 minutes in 4% formalin/PBS and then stained with Alizarin Red S (Sigma, 2% in dH₂O, pH 4,1) for 5 minutes. After rinsing with dH₂O, nuclei were stained with haematoxylin for 5 minutes. Dehydration with an ascending ethanol series (50%, 70%, 96%) and subsequent rinsing in xylene was followed by mounting with Eukitt (Sigma).

2.3. Working with Bacteria

2.3.1. Bacterial strains and culture

E.coli strains *XL1-blue* or *DH5 α* were used for propagation of plasmids.

XL1-blue (Stratagene):

recA1 endA1 gyrA96 thi-1 hsdR17 supE44 relA1 lac [F' proAB lacIqZ Δ M15 Tn10 (Tetr)].

DH5 α (Invitrogen):

F- ϕ 80lacZ Δ M15 Δ (lacZYA-argF)U169 recA1 endA1 hsdR17(rk-, mk+) phoA supE44 thi-1 gyrA96 relA1 λ -

Bacteria were grown in liquid culture or on agar plates at 37°C.

LB-medium

1% Bacto-tryptone

0,5% Bacto-yeast extract

85 mM NaCl

LB-agar plates

1% Bacto-tryptone

0,5% Bacto-yeast extract

85 mM NaCl

1,5% Bacto agar

100 μ g/ml ampicillin or 30 μ g/ml kanamycin (antibiotics were only added when agar cooled down)

2.3.2. Freezing of bacteria

To store transformed bacteria, 100 μ l glycerol and 900 μ l liquid culture were mixed and frozen at -80°C.

2.3.3. Generation of heat shock competent bacteria

A single colony from a LB plate with non-competent bacteria was inoculated in 2,5 ml LB medium and grown overnight at 37°C. The culture was then diluted 1:100 in 250 ml LB + 20 mM MgSO₄ and grown until OD₅₉₅ = 0,4 - 0,6. Cells were pelleted by centrifugation at 5000 rpm for 5 minutes at 4°C. The pellet was resuspended in 10 ml TFBI and incubated for 5 minutes on ice. After centrifugation at 5000 rpm for 5 minutes at 4°C cells were resuspended in 10 ml TFBII and incubated on ice for 15 - 60 minutes. 100 µl aliquots were then frozen on dry-ice with ethanol and stored at -80°C.

TFBI

- 30 mM potassium acetate
- 100 mM RbCl
- 10 mM CaCl₂
- 50 mM MnCl₂
- 15% glycerol
- adjusted to pH 5,8 with acetic acid and filtered

TFBII

- 10 mM MOPS (3-Morpholinopropanesulfonic acid)
- 75 mM CaCl₂
- 10 mM RbCl
- 15% glycerol
- adjusted to pH 6,5 with KOH and filtered

2.3.4. Transformation of heat shock competent bacteria

To transform the competent bacteria, an aliquot was thawed on ice and then incubated with up to 1 µg plasmid DNA (5 - 10 ng for retransformation or 10 µl of ligation reaction) on ice for 15 minutes. The transformation mixture was then transferred to a heating block at 42°C for 1 minute and after this it was put back on ice for another minute. One ml of LB broth was added and the suspension was left on a shaker at 37°C for 1 hour. After the incubation, an aliquot (200 µl) of the

transformed bacteria was spread onto LB agar plates, containing the appropriate antibiotics. Then the plate was incubated overnight at 37°C and stored at 4°C.

2.4. Working with DNA

2.4.1. Plasmid isolation from bacteria

2.4.1.1. Minipreparation

Bacterial cells from an overnight culture were harvested by centrifugation at 5000 rpm for 7 minutes. The pellet was resuspended in 250 µl Suspension Buffer (Roche), 250 µl Lysis Buffer (Roche) was added and the tube was mixed by inverting. After incubation for 4 minutes at room temperature, 450 µl Neutralisation Buffer (Roche) was added. The suspension was gently mixed by inverting and centrifuged at 14000 rpm for 15 minutes at 4°C. The supernatant was mixed with 600 µl isopropanol and centrifuged again at 14000 rpm for 30 minutes at 4°C. The pellet was washed with 500 µl 70% ethanol. After centrifugation at 14000 rpm for 15 minutes at 4°C, the pellet was air-dried and resuspended in ddH₂O.

2.4.1.2. Midipreparation (Genopure Plasmid Midi Kit, Roche)

One millilitre of an overnight culture was diluted in 30 ml LB-Amp and incubated at 37°C with vigorous shaking over night. The cells were harvested by centrifugation at 5000 rpm for 15 minutes at 4°C. The pellet was resuspended in 4 ml Suspension Buffer + RNase, 4 ml Lysis Buffer were added and the tube was inverted 6 - 8 times. After incubation for 2 - 3 minutes at room temperature, 4 ml chilled Neutralisation Buffer was added. The suspension was gently mixed by inverting 6 - 8 times and incubated on ice for 5 minutes. After clearing the lysate by filtration it was applied to a column, which was previously equilibrated with 2,5 ml Equilibration Buffer. When the solution passed the column, the column was washed twice with 5 ml Wash Buffer. The DNA was then eluted with 5 ml pre-warmed (50°C) Elution Buffer. Next, 3,6 ml isopropanol was added and the tube was centrifuged at 12000 rpm for 30 minutes at 4°C. The pellet was washed with 3 ml chilled 70% ethanol and centrifuged at 12000 rpm for 10 minutes at 4°C. The pellet was air-dried and resuspended in 100 µl ddH₂O.

The DNA concentration was calculated by measuring the absorption at 260 nm. When OD₂₆₀ =1 the solution contained 50 µg/ml double stranded DNA.

$OD_{260} \times \text{dilution} \times 50 \mu\text{g/ml} = \text{concentration in } \mu\text{g/ml}$

2.4.2. Analytical digest

All restriction endonucleases used were obtained from Fermentas.

DNA (up to 1 μg) was mixed with 10 U enzyme and 1 x buffer in a total volume of 20 μl and incubated at 37°C. After 2 hours digestion the fragments were separated on an agarose gel.

2.4.3. Agarose gel electrophoresis

Agarose (0,5 - 1,5 g) was dissolved in 100 ml 1 x TAE (0,5 - 1,5% w/v) and heated in a microwave oven. After cooling down to about 60°C, 5 μl ethidium bromide (10 mg/ml, Sigma) was added to an end concentration of 0,5 $\mu\text{g/ml}$ and the gel was poured in the appropriate apparatus with combs. After the gel was solidified, it was transferred into the electrophoresis-apparatus filled with 1 x TAE. When the probes, mixed with loading buffer, and 5 μl 100 Bp or 1 kB marker (Gene Ruler DNA ladders, Fermentas) were loaded, the gel was run at 100 V until separation was satisfying.

50 x TAE

2 M Tris

50 mM EDTA pH 8

5,7% acetic acid

6 x loading buffer

0,25% bromphenolblue

0,25% xylene cyanol

30% glycerol

2.4.4. Gel extraction (GenElute Gel Extraction Kit, Sigma)

To purify PCR products or DNA fragments after restriction digest, the samples were loaded on an agarose gel and excised with a clean scalpel. The piece was put in a

1,5 ml tube together with 3 gel volumes of Gel Solubilisation Solution and incubated at 50°C for 10 minutes under continuous shaking. The gel slice should be completely dissolved and the colour of the solution should be yellow. In the meantime the GenElute Binding Column G was prepared by loading 500 µl of the Column Preparation Solution, centrifugation for 1 minute at maximum speed and discarding the flow-through. One gel volume of isopropanol was added and 700 µl of the solution were applied to the column. If the total volume exceeded 700 µl, aliquots were successively loaded onto the column. After centrifugation for 1 minute at full speed, the flow-through was discarded. When all the liquid was loaded, the column was washed with 750 µl Wash Solution and centrifuged 1 minute at maximum speed. The flow-through was discarded and the column was centrifuged for another minute at maximum speed to remove excess ethanol. The column was then transferred to a new tube and DNA was eluted with 50 µl ddH₂O by incubating 1 minute at room temperature and subsequent centrifugation for 1 minute at maximum speed.

2.4.5. DNA Ligation

The ratio between insert and vector should be 5:1 and they must have the same or compatible end sites.

Insert and plasmid were mixed with 1 x Ligation Buffer and 1 U T4 DNA Ligase (Fermentas) in a total volume of 20 µl. The ligation reaction was incubated in a 16°C water bath overnight and subsequently used for transformation of bacteria (see 2.3.4.) or stored at 4°C.

2.4.6. Isolation of genomic DNA from cells, tissues or bone

Organs were cut into small pieces and bones were crushed with mortar and pestle while constantly cooled with liquid nitrogen. Samples were then transferred to a microcentrifuge tube with 800 µl DNA extraction buffer.

For cells, the DNA extraction buffer was added to the culture dish. The plate was then incubated for at least one hour at 37°C and the viscous solution was transferred to a microcentrifuge tube with a cut-off blue pipette tip.

Elimination of proteins was achieved by digestion with 0,5 mg/ml Proteinase K overnight at 56 °C with vigorous shaking. Proteins were precipitated by adding 0,3 volumes 6 M NaCl, vortexing for 5 minutes and centrifugation at 13000 rpm for 5 minutes at 4 °C. The supernatant was transferred to a new tube and mixed with 1 volume of Phenol:Chloroform:Isoamylalcohol (25:24:1, Invitrogen). The sample was centrifuged for 5 minutes at 13000 rpm and the aqueous upper phase was transferred to a new tube. DNA was precipitated with 0,7 volumes isopropanol followed by mixing and centrifugation at 13000 rpm for 15 minutes at 4 °C. The pellet was washed once with 500 µl 70% ethanol to remove excess salt, air-dried for 10 minutes and resuspended in ddH₂O.

DNA extraction buffer

- 50 mM Tris pH 8,0
- 100 mM EDTA pH 8,0
- 100 mM NaCl
- 1% SDS

2.4.7. PCR to detect deletion of the STOP-cassette of the EF allele

To detect deletion of the STOP-cassette of the Rosa26loxP-STOPlloxP-HA-EWS/FLI-1 (EF) allele a PCR strategy was established. The forward primer was located in the endogenous Rosa26 locus (RosaWT_F) and the reverse primers were located shortly after the first loxP site (RosaKI_R) and within *EWS/FLI-1* (EF_R1). A product of the forward (RosaWT_F) and the EF_R1 primer could only be observed when the STOP-cassette was cut out by the Cre-recombinase. Otherwise, the distance between the two primers would be too long for the DNA polymerase to amplify this sequence. Genomic DNA was used as a template and PCR reaction mix and PCR conditions (50 °C annealing temperature) were already described above (see 2.1.1.2.)

name	sequence	concentration	product [Bp]		genotype	
RosaKI_R	5'GATCCACTAGTTCTAGAGCGGC 3'	10 pmol	366	800	KI	ΔSTOP
RosaWT_F	5'GAGTTGTTATCAGTAAGGGAGC 3'	10 pmol				
EF_R1	5'GGTATCATAAGCACCAAGTG 3'	10 pmol				

2.4.8. PCR to detect expression of EWS/FLI-1 and Cre

Expression of EWS/FLI-1 or Cre on the mRNA level was analysed with conventional block PCR. mHPRT was used as a control for the reverse transcription reaction. cDNA (see 2.5.3.) was mixed with PCR reaction mix and amplified with standard PCR conditions (see 2.1.1.2.). The presence or absence of products was analysed on an agarose gel.

name	sequence	concentration	product [Bp]
EF_F2	5'CAGAGTAGCTATGGTCAAC 3'	10 pmol	370
EF_R3	5'GTGATACAGCTGGCGTTG 3'	10 pmol	
Cre1	5'CGGTCGATGCAACGAGTGATGAGG 3'	10 pmol	700
Cre2	5'CCAGAGACGGAAATCCATCGCTCG 3'	10 pmol	
mHPRTa	5'CAAATCAAAAGTCTGGGGACGC 3'	10 pmol	350
mHPRTas	5'GCTTGCTGGTGAAAAGGACCTC 3'	10 pmol	

2.4.9. Template preparation for generation of *in situ* hybridisation probes

Ten micrograms of the plasmid containing the sequence for the gene to be analysed were cut with the corresponding restriction enzyme in a volume of 100 µl for 2 hours at 37°C (2.4.2.). Completeness of digestion was checked by loading 2 µl of the samples on a 1% agarose gel. The linearised plasmid was then extracted by adding 1/10 volume of 3 M sodium acetate and 1 volume of Phenol:Chloroform:Isoamylalcohol (25:24:1). After short vortexing, the sample was centrifuged for 5 minutes at 13000 rpm. The aqueous upper phase was transferred to a new tube and DNA was precipitated with 2,5 volumes absolute ethanol

followed by mixing and centrifugation at 13000 rpm for 15 minutes at 4°C. The pellet was washed once with 500 µl 70% ethanol to remove excess salt, air-dried for 10 minutes and resuspended in 10 µl nuclease-free H₂O (final concentration: 1 µg/µl).

List of plasmids used for *in situ* hybridisation (all kindly provided by Dr. Christine Hartmann, IMP, Vienna, Austria):

gene	vector	restriction enzyme for antisense probe	polymerase for antisense probe	size [Bp]
Col1a1	pBSKS	BamHI	T3	500
Col2a1	Litmus28	EcoRI	T7	405
Col10a1	pBSKS	Clal	T3	650
IHH	pBSKS	XbaI	T7	1800
Osc	pBSKS	BamHI	T3	320
Osx	pGEM T-easy	SpeI	T7	670
Runx2	pGEM T-easy	NcoI	SP6	550

2.4.10. Dominant-negative STAT mutants

STAT1 Y701F was kindly provided by Dr. Thomas Decker, Max F. Perutz Laboratories, Vienna, Austria and STAT3 Y705F and STAT3 Δ683 were provided by Dr. Richard Moriggl, Ludwig Boltzmann Institute for Cancer Research, Vienna, Austria. The mutated constructs were located in pMSCV, a vector based on the murine stem cell virus. The gene of interest is followed by an internal ribosomal entry site (IRES) and the green fluorescent protein (GFP), facilitating sorting of infected cells.

STAT1 Δ677 was established based on STAT3 Δ683, the dominant-negative form of STAT3 lacking the last 90 amino acids harbouring the transactivation domain. S1_F and S1Δ_R were designed in a way that STAT1 was truncated at amino acid 677, the end of the SH2 domain. Both primers harboured a unique restriction site (BamHI and SacII) with which the PCR product was ligated into pMSCV.

PCR reaction mix

1 µl pMSCV STAT1 Y701F (diluted 1:100 from Midi-prep)
 0,4 µl High Fidelity PCR Enzyme Mix (5 U/µl, Fermentas)
 5 µl High Fidelity PCR buffer (10 x, Fermentas)
 0,5µl dNTP mix (10 mM, Fermentas)
 0,5 µl primer S1_F
 0,5 µl primer S1Δ_R
 ad 50 µl ddH₂O

PCR conditions:

95°C	4 minutes		<u>initial denaturation</u>
95°C	40 seconds	40x	denaturation
50°C	1 minute		annealing
68°C	90 seconds		<u>elongation</u>
68°C	7 minutes		final elongation
22°C	∞		storage

name	sequence	concentration	product [kB]
S1_F	5'GACGTAGTCATGCATGCATCATAGG ATCCACCATGTCTCAGTGGTACG 3'	10 pmol	2,1
S1Δ_R	5'TACGATCCC GCGGTCAGGCATGGTC TTTGTCAATATTTG3'	10 pmol	

2.5. Working with RNA

2.5.1. RNA isolation

For cultured cells, 1 ml Trizol (Gibco) was added per 10 cm², incubated for 5 minutes at room temperature and then transferred to an RNase-free tube. Tissue samples (approximately 5 x 5 x 5 mm) were directly homogenised in 5 ml Trizol with a tissue homogeniser and incubated for 5 minutes at room temperature. Skeletal elements were crushed with mortar and pestle while constantly cooled with liquid nitrogen. The “bone powder” was then mixed with 5 ml Trizol and incubated for 5 minutes at room temperature.

All following measurements correspond to the volumes needed per 1 ml initial Trizol. Chloroform (200 µl) was added to the homogenate, vortexed for 15 seconds and the mixture was incubated for 2 minutes at room temperature. After centrifugation at 10000 rpm for 15 minutes at 4°C, the upper aqueous phase was transferred to a new tube. Addition of 500 µl isopropanol and vortexing was followed by 10 minutes incubation at room temperature. The RNA was pelleted by centrifugation at 10000 rpm for 10 minutes at 4°C and washed with 1 ml 70% ethanol. After centrifugation at 7500 rpm for 5 minutes at 4°C, the pellet was air dried for 15 minutes and resuspended in 50 µl ddH₂O-DEPC. RNA was stored at -20°C for short times and at -80°C for long-term storage.

2.5.2. RNA agarose gel

Agarose (0,8 g) was dissolved in 100 ml 1 x MOPS and heated in a microwave oven. After cooling down to about 60°C, 5 µl ethidium bromide (10 mg/ml) was added and the gel was poured in the appropriate tray containing combs. After the gel was solidified it was put in the electrophoresis-apparatus filled with running buffer. The probes were mixed with 2 x RNA loading buffer and boiled for 5 minutes at 95°C. The gel was run at 90 V until the blue front containing bromphenolblue reached the end of the gel.

2 x RNA loading buffer

- 1 x MOPS
- 6,8% formaldehyde
- 50% formamide
- 15% glycerol
- 66 mM EDTA
- 0,2% bromphenolblue in H₂O

50 x MOPS

- 1 M MOPS
- 250 mM sodiumacetate
- 50 mM EDTA

Running buffer

- 1 x MOPS

2.5.3. Reverse transcription

To ensure amplification of RNA only, DNA was digested with RNase-free DNase. RNA (0,5 - 1 µg) was incubated with 10 U DNaseI (Roche) in a total volume of 10 µl for 30 minutes at 37°C. The reaction was then stopped by incubating at 75°C for 10 minutes and RNA was ready to use for cDNA synthesis or was stored at -80°C.

Reverse transcription was carried out using the RevertAid H Minus First Strand cDNA Synthesis Kit (Fermentas) according to the manufacturer's protocol. Briefly, template RNA was incubated with 1 µl random hexamer primer in a total volume of 12 µl for 5 minutes at 70°C and chilled on ice. After addition of 4 µl 5 x reaction buffer, 0,5 µl RiboLock RNase Inhibitor and 2 µl 10 mM dNTP Mix, the mixture was incubated for 10 minutes at room temperature. RevertAid H Minus M-MuLV Reverse Transcriptase (1 µl) was added and the tube was incubated for 10 minutes at room temperature, followed by 60 minutes at 42°C. The reaction was terminated by heating at 70°C for 10 minutes. Resulting cDNA was directly used for PCR or stored at -20°C.

2.5.4. JAK/STAT specific target gene analysis with OligoGEArray (SuperArray)

High quality RNA was isolated with the RNeasy Mini kit (Quiagen) according to manufacturer's protocol. Cells were trypsinised and pelleted by centrifugation at 1200 rpm for 5 minutes. The cell pellet was then disrupted by addition of Buffer 600 μ l RLT (for 5×10^6 - 1×10^7 cells). The lysate was applied to a QIAshredder and centrifuged for 2 minutes at 13000 rpm to homogenise the sample. The flow-through was mixed with 600 μ l 70% ethanol, applied to the column and centrifuged for 15 seconds at 10000 rpm. If the volume exceeded 700 μ l, aliquots were successively loaded onto the column. The flow-through was discarded and 700 μ l Buffer RW1 were applied to the column. After centrifugation for 15 seconds at 10000 rpm, the column was transferred to a new collection tube and 500 μ l Buffer RPE were added. Centrifugation for 15 seconds at 10000 rpm was followed by another wash with 500 μ l Buffer RPE. The column was transferred to a new collection tube and centrifuged again for 1 minute at 13000 rpm to get rid of residual ethanol. Finally, the column was transferred in a new microcentrifuge tube and RNA was eluted by addition of 30 μ l ddH₂O-DEPC and centrifugation for 1 minute at 10000 rpm.

cDNA synthesis

Total RNA (3 μ g) was mixed with component G1 in a final volume of 10 μ l and incubated for 10 minutes at 70°C. RNase-free H₂O (4 μ l), 4 μ l 5x cDNA Synthesis Buffer (G3), 1 μ l RNase inhibitor (RI) and 1 μ l cDNA Synthesis Enzyme Mix (G2) were added and incubated at 42°C for 50 minutes. Following incubation at 75°C for 5 minutes, the sample was allowed to cool down to 37°C.

cRNA synthesis and purification

Amplification Master Mix (16 μ l 2,5 x RNA Polymerase Buffer (G24), 2 μ l 10mM Biotinylated-UTP, 2 μ l RNA Polymerase Enzyme (G25) in a total volume of 20 μ l) was added to the cDNA synthesis reaction and incubated for 1 hour at 37°C.

RNase-free H₂O (50 μ l) was added to the cRNA synthesis reaction and the sample was mixed with 315 μ l Lysis & Binding Buffer (G6). Absolute ethanol (315 μ l) was added, mixed and the sample was loaded onto the column provided. After centrifugation at 8700 rpm for 30 seconds, the column was washed with 600 μ l Washing Buffer (G17). The flow-through was discarded and the column was washed

with 200 µl Washing Buffer (G17). Centrifugation at 10000 rpm for 1 minute was followed by another centrifugation step for 2 minutes at 10000 rpm. cRNA was eluted by addition of 50 µl RNase-Free 10 mM Tris Buffer pH 8,0 (G26), incubation for 2 minutes and centrifugation at 8700 rpm for 1 minute. cRNA was measured by UV spectrometry and 4 µg were used for hybridisation.

Hybridisation

The array membrane was put into hybridisation tube, pre-wet with 5 ml dH₂O for 5 minutes and incubated with 2 ml pre-warmed (60°C) GEHyb Hybridisation Solution for 1 hour at 60°C with slow agitation. cRNA (4 µg) was mixed with 0,75 ml GEHyb Hybridisation Solution and added to the pre-hybridised membrane. Hybridisation was done overnight at 60°C. Then, the membrane was washed with 5 ml Wash Solution 1 (2 x SSC, 1% SDS) at 60°C for 15 minutes. Another washing step with 5 ml Wash Solution 2 (0,1 x SSC, 0,5% SDS) at 60°C for exactly 15 minutes was applied. Wash Solution was discarded and the membrane was allowed to cool to room temperature inside the hybridisation tube.

Chemiluminescent detection

GEAblocking Solution Q (2 ml) was added to the membrane and the tube was incubated with continuous agitation for 40 minutes at room temperature. Next, AP-SA Buffer (alkaline phosphatase-conjugated streptavidin diluted 1:8000 in 1 x BufferF) was added and the tube was incubated for exactly 10 minutes with gentle agitation. The membrane was washed four times with 4 ml 1 x BufferF for 5 minutes and rinsed twice with 3 ml Buffer G. CDP-Star chemiluminescent substrate (1 ml) was added to the membrane and the tube was incubated for 5 minutes. The membrane was then wrapped in saran foil and exposed to ECL films (Pierce) for various time periods.

2.5.5. Generation of digoxigenin labelled cRNA probes for *in situ* hybridisation

One microgram of the linearised plasmid (2.4.10.) was transcribed *in vitro* with the RNA DIG labelling kit (Roche) according to the manufacturer's protocol. All solutions were prepared or diluted with DEPC treated water. DNA was mixed with 1 x Transcription Buffer, 1 x DIG RNA Labeling Mix, 0,5 µl RNase Inhibitor, 1,5 µl RNA

polymerase in a total volume of 20 μ l. After transcription at 37°C for 2 hours, 1 μ l of the reaction was checked on a 1% agarose gel and residual DNA was digested with 1 μ l DNase (Roche). The labelled RNA probe was purified by adding 1 μ l glycogen (Roche), 10 μ l 4 M LiCl 100 μ l TE pH 8, 300 μ l absolute ethanol (-20°C) and incubating at -20°C for 1 hour or overnight. Following 15 minutes centrifugation at 13500 rpm at 4°C, the pellet was washed once with 500 μ l 70% ethanol. The labelled RNA probe was air-dried for 5 to 10 minutes, resuspended in 100 μ l ddH₂O-DEPC and stored at -20°C.

2.6. Working with Protein

2.6.1. Protein extraction

2.6.1.1. Preparation of protein lysates of mammalian cells and tissues

Small pieces of tissue samples were directly homogenised in a minimal amount of IP-buffer with a tissue homogeniser. Skeletal elements were crushed with mortar and pestle while constantly cooled with liquid nitrogen. The “bone powder” was then mixed with a minimal amount of IP-buffer and incubated at 4°C on a rotating shaker for at least 1 hour.

Growth medium was removed from adherent cells and they were washed twice with PBS. The cells were scraped off and the liquid including the cell debris was transferred to a 1,5 ml tube. Cells were centrifuged at 1200 rpm for 5 minutes and the appropriate amount of IP-buffer was added (approximately 100 µl IP-buffer for 10⁶ cells). To enhance cell disruption, the tube was incubated at 4°C on a rotating shaker for at least 1 hour.

Subsequently, cellular debris was removed by centrifugation at 13000 rpm for 30 minutes at 4°C. The supernatant was transferred to a new tube and protein concentration was determined. Protein samples were stored at -20°C or for longer periods at -80°C.

IP-buffer base

25 mM Hepes pH 7,5

150 mM NaCl

10 mM EDTA

0,1% Tween-20

0,5% NP-40

10 mM β-glycerophosphate

IP buffer (IP buffer base + freshly added inhibitors)

1 mM Na₃VO₄

1 mM NaF

10 µg/ml Leupeptin
10 µg/ml Aprotinin
1 mM PMSF
1 x complete (25 x stock: 1 Protease Inhibitor Cocktail Tablet in 2 ml H₂O;
Roche)

2.6.1.2. Preparation of protein lysates of mammalian cells for EMSA

Culture dishes of adherent cells were rinsed twice with ice-cold PBS, cells were scraped off and pelleted by centrifugation for 5 minutes at 1200 rpm. Pellets were mixed with two times the volume of the pellet with whole cell extract buffer, vortexed, frozen in liquid nitrogen and thawed on ice. Freeze-thaw cycles were repeated 4 times. Extracts were centrifuged at 13000 rpm for 20 minutes at 4°C and the supernatant was transferred to a new tube. Protein concentration was determined and samples were directly subjected to EMSA or stored at -80°C.

whole cell extract buffer

20 mM Hepes pH 7,9
20% Glycerol
50 mM KCl
1 mM EDTA
1 mM DTT
400 mM NaCl
5 µg/ml Leupeptin
0,2 U/ml Aprotinin
1 mM PMSF
5 mM Na₃VO₄
10 mM NaF
5 mM β-glycerophosphate
stored at -20°C

2.6.2. Determination of protein concentration (Bradford)

Protein concentration was quantified with Bradford reagent (Bio-Rad Protein Assay). Different concentrations of BSA (1 µg, 5 µg, 10 µg and 15 µg) were used as a

standard. One microlitre of the lysate or the standard were mixed with 1 ml Bradford reagent (diluted 1:5 with dH₂O) in a cuvette and incubated for 7 minutes at room temperature. The absorption at 595 nm was measured in a spectrophotometer and the protein concentration of the lysates was calculated using the values of the standard as a reference.

2.6.3. Western blot analysis

2.6.3.1. Polyacrylamid (PAA) gel electrophoresis

For Western blotting the Mini-PROTEAN 3 system from Bio-Rad was used. The glass plates were cleaned with water and ethanol and the gel unit was assembled. First, the components for the separating gel were mixed and poured between the glass plates, leaving 2,5 cm space for the stacking gel to be added later. After pouring, the gel was overlaid with isopropanol and left to solidify. When the separating gel was polymerised, isopropanol was removed, the remaining space was filled with the stacking gel and the comb was inserted, avoiding to generate air bubbles. The polymerised gel was then inserted into the running unit and submerged with 1 x running buffer. Now the comb was removed carefully and the slots were rinsed with running buffer to remove unpolymerised acrylamide.

separating gel:	8%	10%	12%
Acrylamide/Bis (30%)	2,7 ml	3,3 ml	4,3 ml
1,5 M Tris pH 8,8	2,5 ml	2,5 ml	2,5 ml
ddH ₂ O	4,6 ml	4 ml	3 ml
10% SDS	100 µl	100 µl	100 µl
10% APS	100 µl	100 µl	100 µl
TEMED	6 µl	6 µl	6 µl

stacking gel:

Acrylamide/Bis (30%)	0,5 ml
1 M Tris pH 6,8	0,38 ml
10% SDS	30 μ l
ddH ₂ O	2,1 ml
10% APS	30 μ l
TEMED	3 μ l

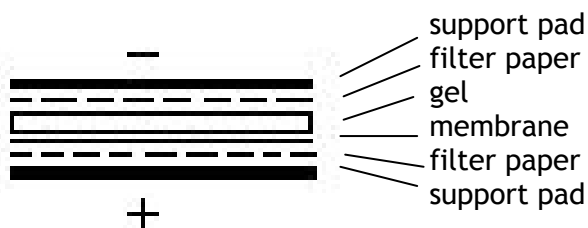
2.6.3.2. Sample preparation

Before the proteins were loaded onto the gel, the samples were boiled for 5 minutes mixed with 4 x sample buffer. PageRuler Prestained Protein Ladder (Fermentas) was also loaded on the gel (5 μ l).

Gels were run at 30 mA per gel. When the proteins reached the separating gel the current was elevated to 50 mA per gel.

2.6.3.3. Protein transfer

After separation of the proteins on a SDS-PAA gel, they were transferred onto a nitrocellulose membrane for immunodetection. Therefore the stacking gel was removed, the filterpaper (Whatman Chromatography Paper) and the nitrocellulose membrane (GE Healthcare) were cut to the size of the gel and the sandwich was assembled in the following order: support pad soaked in transfer buffer, one sheet of filterpaper (soaked in transfer buffer), gel, nitrocellulose membrane (wetted in transfer buffer), one sheet of filterpaper (again soaked in transfer buffer) and a support pad (also soaked in transfer buffer).



It was necessary to pay attention avoiding air bubbles in all steps of the assembly. The sandwich was put into the transfer buffer filled transfer unit with the gel on the side of the minus pole. After blotting at 4°C with a constant voltage of 100 V for 1,5 hours the sandwich was disassembled and the membrane was washed with dH₂O. Transfer efficiency was controlled with a PonceauS staining whereby the membrane was stained for 5 minutes with PonceauS staining solution. To remove excess dye, the membrane was de-stained with dH₂O until bands were visible.

2.6.3.4. Immunodetection

The Western blot membrane was blocked with blocking solution at room temperature for one hour under gentle shaking in a plastic tray. After blocking, the membrane was incubated at 4°C with the primary antibody (diluted as listed below). The next day the primary antibody was removed and the membrane was washed three times for 5 minutes with washing buffer. Then the membrane was incubated with the secondary mouse or rabbit antibody (horse raddish peroxidase linked, GE Healthcare) diluted 1:5000 in antibody-solution for 1 hour at room temperature. Next it was washed three times for 10 minutes in washing buffer.

Finally, the proteins were detected with SuperSignal West Pico Chemiluminescent Substrate (Pierce). Equal amounts of Luminol/Enhancer and Stable Peroxide Buffer were mixed, poured on the membrane and incubated for 1 minute, ensuring an even distribution of the reagents. After the ECL solution was removed, the membrane was wrapped in saran foil and exposed to ECL films (Pierce) for various time periods.

After a protein was detected, the membrane could be blocked again half an hour and incubated with other primary and secondary antibodies to detect a different protein or the membrane was stripped for 30 minutes at 50°C with stripping solution. Afterwards the membrane was extensively washed with washing buffer, blocked for one hour and incubated with the required antibody.

4 x sample buffer

240 mM Tris pH 6,8
40 mM DTT
8% SDS
0,01% bromphenol blue
40% glycerol
2,5 mM Na₃VO₄
stored at -20 °C

10 x Running buffer

250 mM Tris
2 M glycine
1% SDS

Transfer buffer

25 mM Tris
192 mM glycine
20% methanol

PonceauS staining solution

0,1% PonceauS (Sigma)
5% acetic acid

10 x Washing buffer (TBS-T)

250 mM Tris pH 8
1,5 M NaCl
0,5% Tween-20

Blocking buffer

5% BSA in washing buffer

Antibody solution

1% BSA in washing buffer

Stripping solution

2% SDS

62,5 mM Tris pH 6,8

1,4% β -mercaptoethanol

antibody	recognises	dilution	features	kD
β -Actin	N-terminus of β -Actin	1:10000	mouse monoclonal, (A 5316, Sigma)	42
STAT1	N-terminus of STAT1	1:1000	mouse monoclonal (610115, BD)	84/91
pSTAT1	STAT1 p-Tyr701	1:1000	rabbit polyclonal (9171, Cell Signaling)	84/91
STAT3	N-terminus of STAT3	1:1000	mouse monoclonal (610190, BD)	92
pSTAT3	STAT3 p-Tyr705	1:1000	rabbit polyclonal (9131, Cell Signaling)	92
HA	HA-tag	1:1000	mouse monoclonal 16B12 (Covance)	
Cre	Cre	1:5000	rabbit polyclonal	38
FLI-1	C-terminus of hFLI-1	1:3	mouse monoclonal (Hybridoma Fli 7.3)	70
HSC-70	C-terminus of hHSC-70	1:10000	mouse monoclonal (sc-7298, Santa Cruz)	70

Fli 7.3 hybridoma supernatant was a kind gift of Dr. Heinrich Kovars group (Children's Research Institute, Vienna, Austria). The Cre antibody was kindly provided by Dr. Gitta Erdmann (German Cancer Research Centre, Heidelberg, Germany).

2.6.4. Electrophoretic mobility shift assay (EMSA)

EMSA (or band shift assay) is a widely used technique to analyse the binding ability of proteins (mostly transcription factors) to defined DNA elements. Binding of the native protein to the labelled oligonucleotide results in a shift of the electrophoretic mobility of the designated DNA element. This can be seen as a band on a non-reducing PAA-gel. Moreover, to proof that the identified band really contains the protein of interest, a supershift can be performed. An antibody specific to the favoured protein is added to the DNA-protein mixture. When the identified band changes its migratory ability (either migrates slower or is absent at all) the antibody recognised the DNA-protein complex and the protein is therefore proven as the right one, binding to the DNA element of interest.

2.6.4.1. Oligo Annealing

Oligos were purchased from VBC-biotech and resuspended in the indicated volume needed for 250 pmol/ μ l. Exact DNA concentration was measured with a photometer and oligos were diluted to a final concentration of 100 pmol/ μ l.

Both oligos were mixed in an equimolar ratio together with 1 x annealing buffer (10 x = 0.625 x PCR BufferII (Roche); 9,4 mM MgCl₂) in a total volume of 100 μ l. The mixture was then incubated in a 95°C heating block for 10 minutes and slowly cooled down to room temperature. The annealed oligo was then incubated on ice for 10 minutes, diluted to 2,5 μ M and stored at -80°C.

2.6.4.2. Oligo Labelling

Five picomol double stranded annealed oligo were radioactively labelled in a reaction with 5 μ l γ -³²P-ATP (Amersham; 370 MBq/ml) and 10 U polynucleotide kinase (Roche) in a total volume of 20 μ l at 37°C for 1 hour.

The radiolabelled oligo was then separated from free ATP through purification on size exclusion columns (Micro Bio-Spin Chromatography Columns; Bio-Rad). The lower cap from the column was removed and several drops were drained on paper. The column was then put into an empty collection tube and centrifuged at 2500 rpm for 1 minute to get rid of excess liquid.

The labelling mix was stretched with 30 μ l ddH₂O and applied onto middle of the column matrix. After centrifugation at 2500 rpm for 1 minute the flow-through was collected and stored at -80°C.

2.6.4.3. Binding Reaction

In a 20 μ l reaction, 10 - 20 μ g protein sample, 2 μ l BSA solution, 2 μ l Poly dI-dC (1 μ g/ μ l; Roche), 4 μ l 5 x binding buffer and 0,5 to 1 μ l hot probe were mixed and incubated for 5 to 30 minutes at room temperature before loading. For supershifts, protein samples were pre-incubated for at least 5 minutes on ice with antibody.

2.6.4.4. Electrophoresis

Complexes were separated on a non-denaturing 4% PAA-gel containing 0,25 x TBE and run in 0,25 x TBE at 200 V for about 3 hours. Orange G was used as a mobility dye. As soon as the Orange G reached the lower part of the gel it was transferred

onto filter paper, dried on a vacuum gel dryer at 80°C for two hours and exposed to x-ray films (Kodak Biomax MR) at -80°C for at least one day.

BSA solution

10 mg/ml BSA
20 mM KPO₄
50 mM NaCl
0,1 mM EDTA
5% glycerol

5 x Binding buffer

50 mM Tris
5 mM DTT
1 mM PMSF
0,5 mM EDTA
25% glycerol
250 mM NaCl
0,5% NP-40

Orange G

0,5% Orange G (Sigma)
25% Ficoll T₄₀₀
100 mM EDTA

10 x TBE

0,89 M Tris
0,89 M boric acid
20 mM EDTA

Oligos

M67 CATTTC³CGTAAATC
GATTTACGGGAAATG

β-casein AGATTTCTAGGAATTCAAATC
GATTTGAATTCCTAGAAATCT

antibody	recognises	dilution	features
M-22X	STAT1, C-terminus	1:20	rabbit polyclonal (sc-592, Santa Cruz)
C-20X	STAT3, C-terminus	1:20	rabbit polyclonal (sc-482, Santa Cruz)

3. Results

3.1. Establishment of a conditional EWS/FLI-1 knock-in mouse model

3.1.1. The search for the appropriate Cre recombinase

A lot of effort was already made to generate a mouse model for ESFT but no report about a mouse recapitulating the human phenotype existed when we started this project. As mentioned in the introduction, the cellular context for *EWS/FLI-1* expression is important but lack of knowledge about the tissue of origin makes it difficult to target expression of the fusion protein to the right cellular environment in a mouse model.

Since ESFT arises in bone and surrounding soft tissue we first decided to direct expression of *EWS/FLI-1* to a skeletal precursor that can differentiate into osteoblasts, the bone forming cells (Figure 6). For this purpose we made use of the Cre-inducible *EWS/FLI-1* knock-in mouse (hereafter referred to as EF) (Torchia *et al.* 2007) and crossed it to mice harbouring the *Cre recombinase* under the control of the *Runx2* promoter, a transcription factor necessary for differentiation of mesenchymal cells into the osteoblastic lineage. (Komori 2000) There are three different lines of the *Runx2Cre* transgenic mice available (Rauch *et al.* 2010) but we concentrated our analysis on two *Runx2Cre* transgenic lines in the beginning: 1634 *Runx2Cre*, with Cre activity in bone, cartilage and heart, and 784 *Runx2Cre*, where Cre is active in bone and cartilage (Dr. Jan Tuckermann, personal communication and Rauch *et al.* 2010). Resulting *Runx2Cre* EF mice were viable and fertile but showed no overt phenotype at young age. Mice were carefully controlled over a period of 18 month but no tumour formation or any other phenotype could be observed (n = 10 for each *Runx2Cre* line). Analysis of these mice for the deletion activity of the Cre recombinase revealed that there was excision of the *STOP*-cassette in bone, bone marrow, testis and isolated osteoblasts

(n = 8 for each Runx2Cre line) (Figure 10A). However, the efficiency was probably not very strong since deletion of the *STOP*-cassette could not be detected by Southern blotting (data not shown). Only a PCR strategy, which is a more sensitive method, revealed that excision of the *STOP*-cassette took place. Surprisingly, we were not able to detect *EWS/FLI-1* RNA in tissues of Runx2Cre EF mice (n = 8 for each Runx2Cre line) (Figure 10B). Both lines, 784 and 1634, had the same results in respect to phenotype, deletion of the *STOP*-cassette and *EWS/FLI-1* expression, so only one representative example is shown in the following figures.

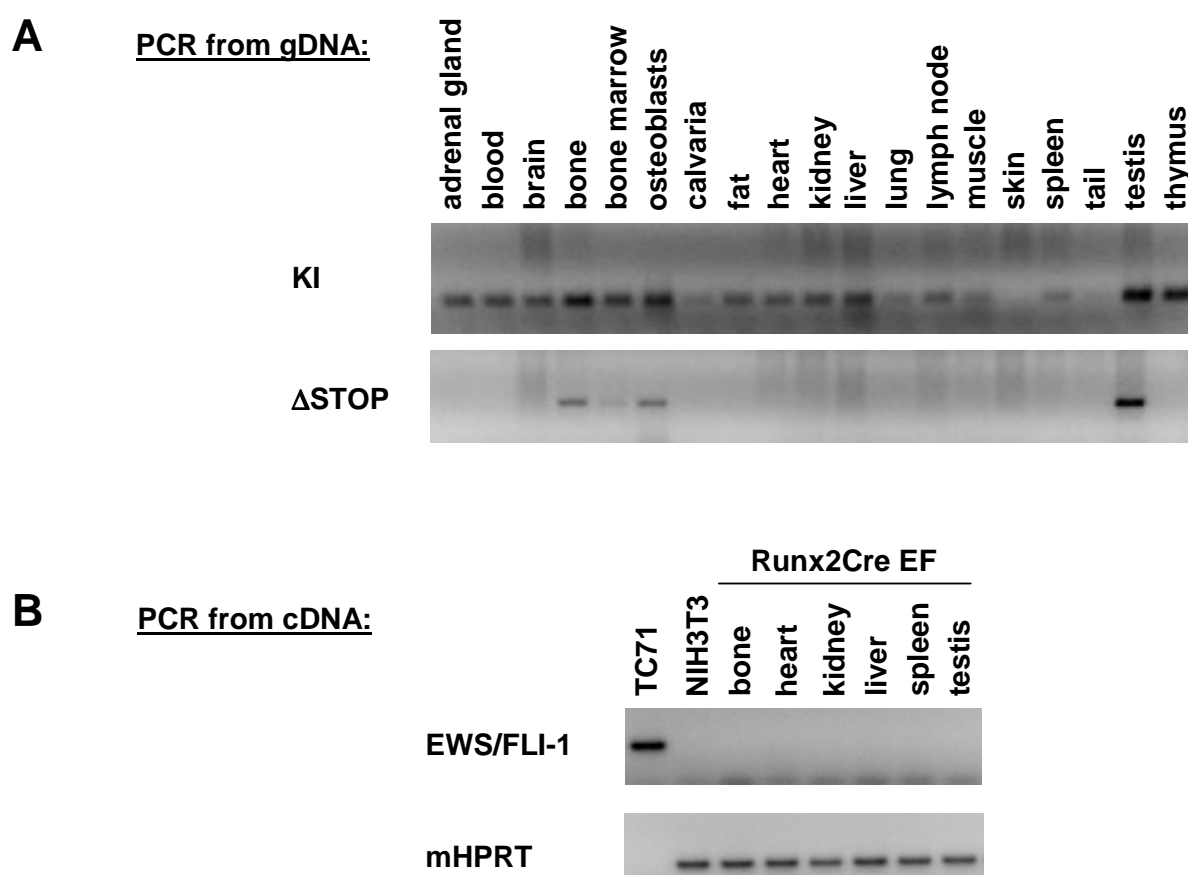


Figure 10: Molecular analysis of Runx2Cre EF mice. **A** Genomic DNA (gDNA), isolated from several different tissues and isolated osteoblasts of 784 Runx2Cre EF mice, was analysed for deletion of *STOP*-cassette (Δ STOP) with a PCR strategy (see 2.4.7.). Existence of the knocked in EF allele (KI) was used as a control to ensure presence of gDNA in the sample. *STOP*-cassette deletion was detected in bone, bone marrow, isolated osteoblasts and testis. **B** *EWS/FLI-1* RNA was detected with specific primers from reverse transcribed cDNA, but could not be observed in tissues of 784 Runx2Cre EF mice. mHPRT was used to ensure proper cDNA transcription. The human TC71 cell line had no mHPRT band since the primers were specific for the mouse homologue and did not recognise the human counterpart. NIH3T3: mouse cell line used as a negative control for *EWS/FLI-1* expression; TC71: ESFT cell line used as a positive control for *EWS/FLI-1* expression.

In the course of this study, we analysed a third transgenic line of the Runx2Cre mice (777). Apart from bone, Cre activity in the 777 Runx2Cre line could also be detected in the haematopoietic system (Dr. Jan Tuckermann, personal communication). Crossing this 777 Runx2Cre line to EF mice did not result in viable double positive offspring (12 litters), rather 777 Runx2Cre EF embryos died before E 13.5 (n = 13, from two litters).

3.1.1.1. A two-hit mouse model for ESFT?

It is already known from *in vitro* studies that EWS/FLI-1 can lead to apoptosis and growth arrest in mouse as well as in human primary fibroblasts but can be rescued by deletion of the *INK4A/ARF* locus or disruption of the p53 pathway. (Deneen and Denny 2001; Lessnick *et al.* 2002) Moreover, alterations of the *INK4A/ARF* locus are the most common second hit in ESFT, occurring in approximately one quarter of patients. (Huang *et al.* 2005; Kovar *et al.* 1997; Lopez-Guerrero *et al.* 2001) Therefore, we decided to cross Runx2Cre EF mice onto the $p16^{INK4A}/p19^{ARF}$ (hereafter named *INK4A/ARF*^{-/-}) knock-out background. Careful analysis of these Runx2Cre EF *INK4A/ARF*^{-/-} mice did not result in enhanced *EWS/FLI-1* expression, similar as seen in Runx2Cre EF mice (n = 7 for each Runx2Cre line). Deletion of the *STOP*-cassette was detected in bone and testis (Figure 11A), but no significant *EWS/FLI-1* RNA could be observed in these tissues (Figure 11B). Moreover, *INK4A/ARF*^{-/-} mice are prone to tumour formation (e.g. fibrosarcoma, liposarcoma, lymphomas) (Serrano *et al.* 1996) and expression of an oncogene like *EWS/FLI-1* should aggravate tumour phenotypes and shift the tumour spectrum towards ESFT. Of 14 Runx2Cre EF *INK4A/ARF*^{-/-} mice analysed, the median latency of tumour development was 23 weeks (compared to 29 weeks in the original publication), with primarily malignancies arising from haematopoietic cells but also tumours in muscle and fat were observed. However, we failed to reproducibly detect the fusion protein in the tumours (Figure 11B), so the slight discrepancy might have been due to mouse housing conditions or different monitoring status. Certainly, the earlier tumour onset was not linked to *EWS/FLI-1* expression.

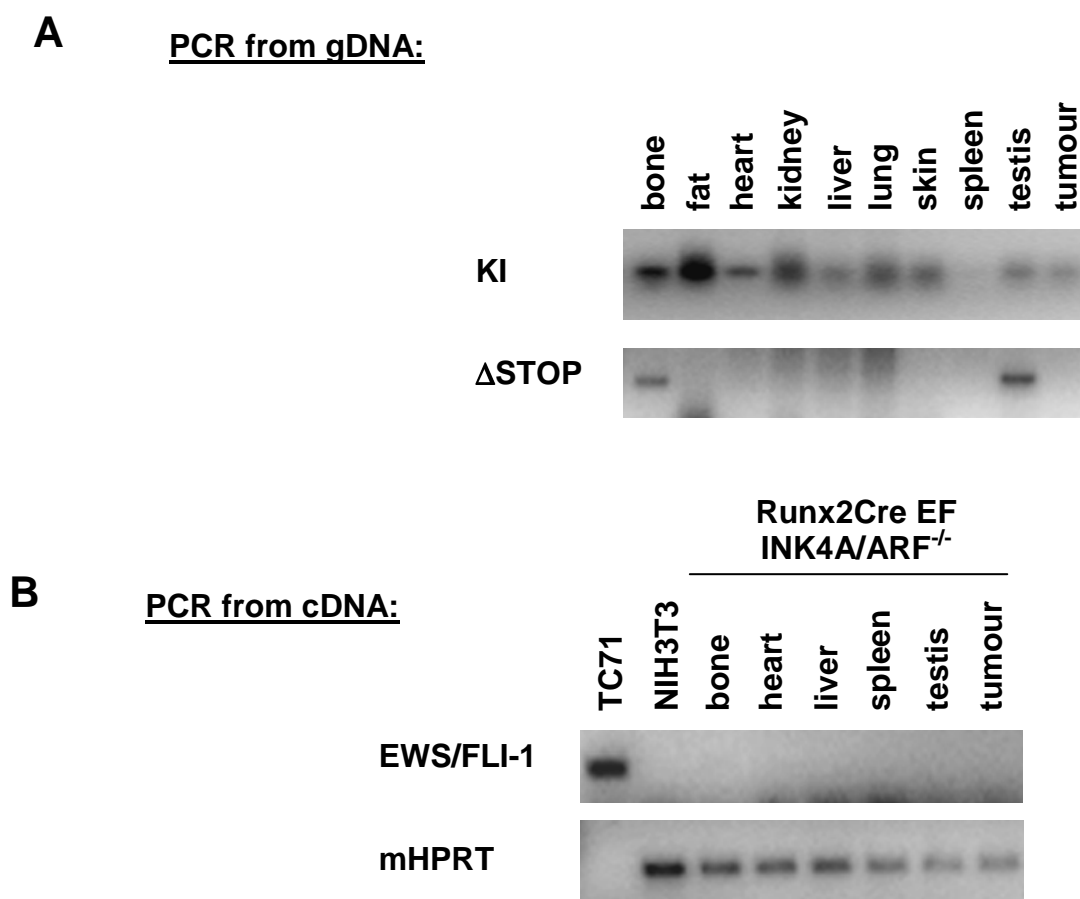


Figure 11: Molecular analysis of Runx2Cre EF INK4A/ARF^{-/-} mice. The representative example (784 Runx2Cre EF INK4A/ARF^{-/-}) shown in this figure had a tumour in the leg near the bone at 15 weeks of age. **A** Genomic DNA (gDNA), isolated from several different tissues of 784 Runx2Cre EF INK4A/ARF^{-/-} mice, was analysed for deletion of *STOP*-cassette (Δ STOP) with a PCR strategy (see 2.4.7.). Existence of the knocked in EF allele (KI) was used as a control to ensure presence of gDNA in the sample. *STOP*-cassette deletion was only detected in bone and testis but not in the tumour sample. **B** *EWS/FLI-1* RNA was detected with specific primers from reverse transcribed cDNA but could not be observed in tissues of 784 Runx2Cre EF INK4A/ARF^{-/-} mice. mHPRT was used to ensure proper cDNA transcription. The human TC71 cell line had no HPRT band since the primers were specific for the mouse homologue and did not recognise the human counterpart. NIH3T3: mouse cell line used as a negative control for *EWS/FLI-1* expression; TC71: ESFT cell line used as a positive control for *EWS/FLI-1* expression.

3.1.1.2. *Runx2Cre* expression

Since only low levels of *STOP*-cassette deletion could be detected and no *EWS/FLI-1* RNA was seen, we asked whether the *Cre recombinase* is expressed correctly in *Runx2Cre* EF mice. Thus, we analysed cDNA from wild type, *Runx2Cre*, *Runx2Cre* EF and *Runx2Cre* EF *INK4A/ARF*^{-/-} mice for the presence of a *Cre* transcript (n = 3 for each *Runx2Cre* line). *Cre* expression could only be verified in *Runx2Cre* mice, lacking the *EF* allele (Figure 12). But mice harbouring *Runx2Cre* and the *EF* allele, whether deficient in the *INK4A/ARF* locus or not, did not express the *Cre recombinase*.

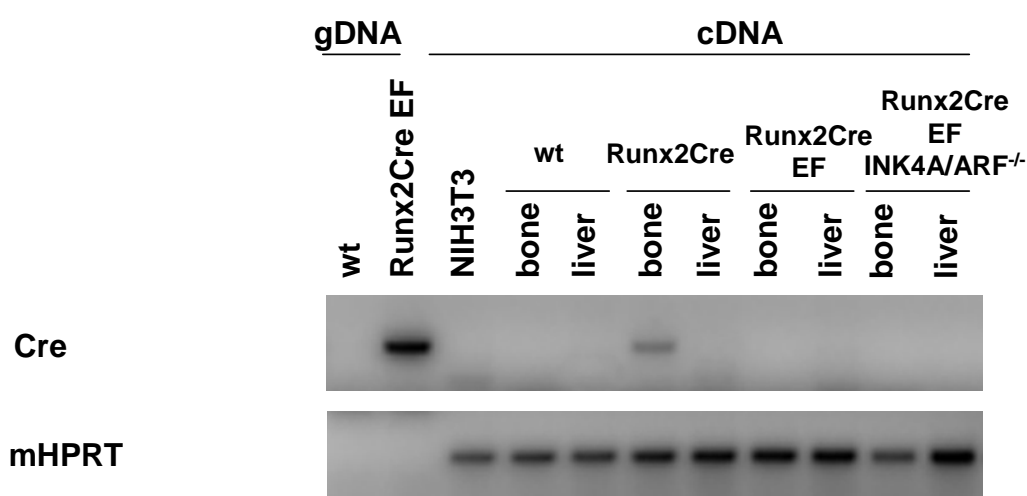


Figure 12: Analysis of *Cre* expression in *Runx2Cre* mice. *Cre* RNA was detected from reverse transcribed cDNA with primers specific for the *Cre recombinase*. gDNA from wild type (wt) and 784 *Runx2Cre* EF mice were used as negative and positive controls for presence of *Cre* DNA. Presence of *Cre* transcript could only be verified in 784 *Runx2Cre* mice but not in 784 *Runx2Cre* EF and 784 *Runx2Cre* EF *INK4A/ARF*^{-/-} mice. mHPRT was used to ensure proper cDNA transcription. The primers specific for mHPRT were designed in two different exons so that only mRNA but not the genomic allele was recognised. Therefore, there was no HPRT band visible in gDNA samples. NIH3T3: mouse cell line used as a negative control for *Cre* expression.

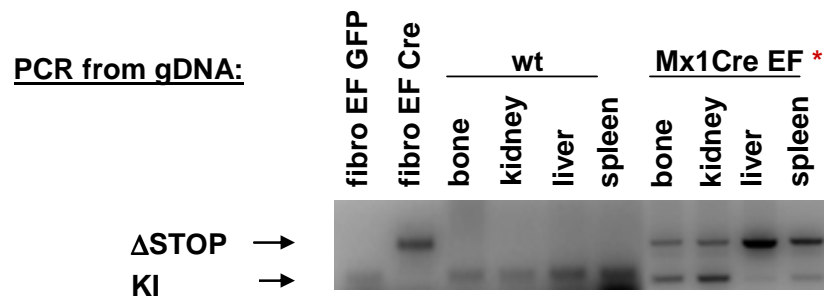
3.1.2. Verification of EF knock-in mice

EWS/FLI-1 could not be expressed in *Runx2Cre* EF mice due to absent *Cre* expression. To ensure that the EF knock-in locus generally allows expression of the transgene in our mouse background, we analysed in more detail this locus *in vitro* as well as *in vivo*.

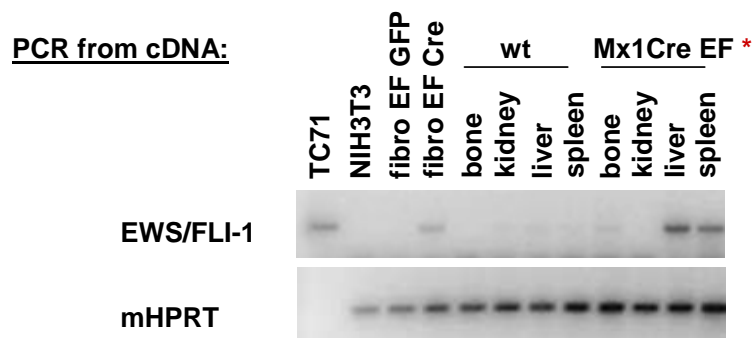
3.1.2.1. Analysis of *EWS/FLI-1* expression from the EF knock-in allele *in vitro*

To analyse the accessibility of the EF knock-in locus *in vitro*, we first isolated fibroblasts from an EF mouse and transduced them with a lentivirus containing GFP or the Cre recombinase. The *STOP*-cassette was efficiently excised in fibroblasts expressing the *Cre recombinase* and no deletion was observed in fibroblasts transduced with a GFP construct (Figure 13A). Moreover, *EWS/FLI-1* RNA and protein were present in Cre transduced fibroblasts (Figure 13B-C).

A



B



C

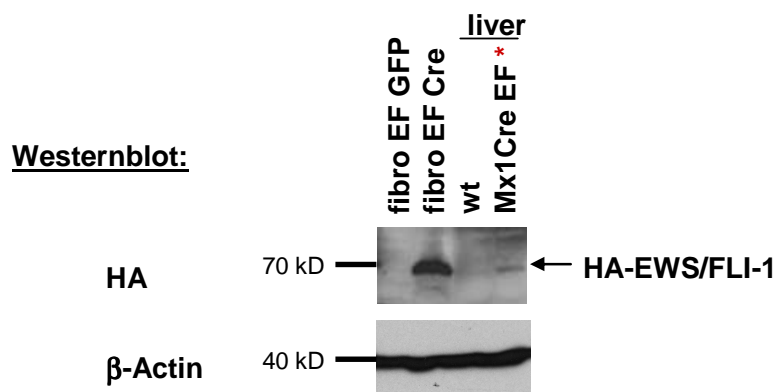


Figure 13: Analysis of *EWS/FLI-1* expression from the EF knock-in allele. **A** Deletion of *STOP*-cassette (Δ STOP) was detected with a PCR strategy in fibroblasts isolated from EF mice (lentivirally transduced with a construct containing GFP or the Cre recombinase) and tissues of wild type or Mx1Cre EF mice, 4 days after polyinosinic and polycytidylic acid (PolyIC) injection (=Mx1Cre EF^{*}). *STOP*-cassette deletion was demonstrated in isolated fibroblasts expressing the *Cre recombinase* and in tissues of Mx1Cre EF^{*} mice. Existence of the knocked in EF allele (KI) was used as a control to ensure presence of gDNA in the sample. **B** *EWS/FLI-1* RNA was detected from reverse transcribed cDNA with primers specific for *EWS/FLI-1* and was present in fibroblasts isolated from EF mice expressing *Cre* and in liver and spleen of Mx1Cre EF^{*} mice. mHPRT was used to ensure proper cDNA transcription. The human TC71 cell line had no HPRT band since the primers were specific for the mouse homologue and did not recognise the human counterpart. TC71: ESFT cell line used as a positive control for *EWS/FLI-1* expression; NIH3T3: mouse cell line used as a negative control for *EWS/FLI-1* expression. **C** Presence of *EWS/FLI-1* protein in fibroblasts isolated from EF mice expressing *Cre* and in liver of Mx1Cre EF^{*} mice was verified with Western blot analysis using an antibody specific for the HA-tag. β -Actin was used as a loading control.

3.1.2.1. Analysis of *EWS/FLI-1* expression from the EF knock-in allele *in vivo*

We also assessed functionality of the EF knock-in locus *in vivo*. Thus, we crossed EF mice to the polyinosinic and polycytidylic acid (PolyIC) inducible Mx1Cre mice. Resulting Mx1Cre EF mice were peritoneally injected with PolyIC (= Mx1Cre EF^{*}) and analysed at indicated time points. Deletion of the *STOP*-cassette, *EWS/FLI-1* RNA and protein could be detected already 4 days after Cre induction, most prominent in liver and spleen (n = 4) (Figure 13). To further test the biological functionality of *EWS/FLI-1* expression in these mice, we wanted to recapitulate the phenotype of Mx1Cre EF^{*} mice published by Torchia *et al.* 2007. We carefully analysed Mx1Cre EF^{*} mice until 17 days after PolyIC injection, the approximate time when signs of disease emerged (scrubby fur, hunchback, swelled belly). Histological analysis revealed that Mx1Cre EF^{*} mice (n = 6) had massive infiltrations in spleen and liver (Figure 14A) and therefore a strong increase in spleen/bodyweight and liver/bodyweight ratio (Figure 14B).

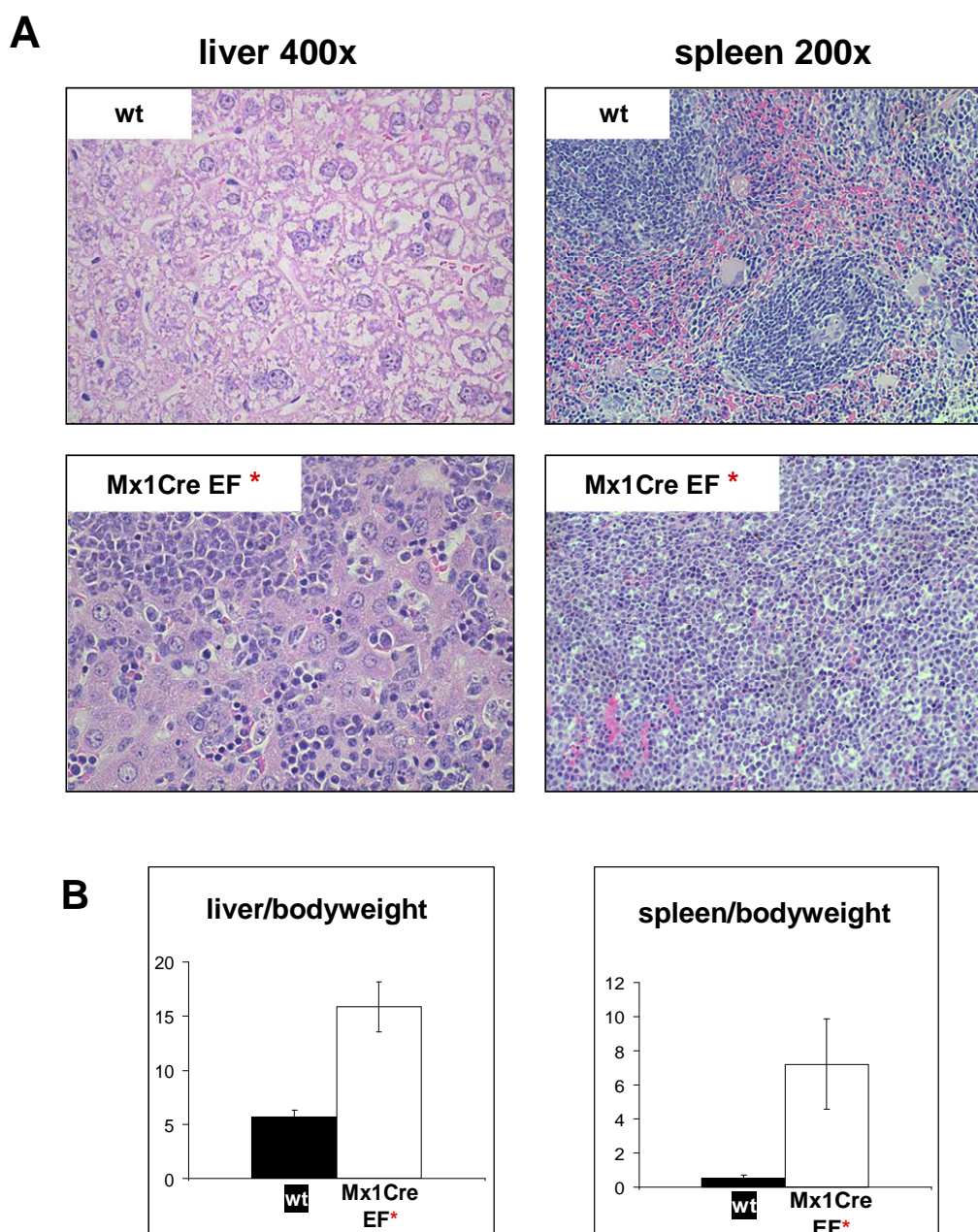


Figure 14: Histological analysis of Mx1Cre EF* mice. A Haematoxylin and eosin staining on sectioned livers or spleens of wild type (wt) or Mx1Cre EF mice, 17 days after PolyIC injection (=Mx1Cre EF*) revealed disorganisation of spleen structure and massive infiltration in the liver of Mx1Cre EF* mice. B Ratios of spleen or liver to bodyweight were massively increased in Mx1Cre EF mice* compared to wild type mice (n = 6).

The original finding reported a myeloproliferative neoplasm with expansion of a CD43/CD71/CD117 positive population, representing a severe increase in erythroblasts. (Torchia *et al.* 2007) We detected the same population in Mx1Cre EF* mice (n = 2) with antibodies specific for these surface molecules by flow

cytometric analysis (Figure 15). Thus, we could prove that the EF knock-in locus is functional *in vitro* as well as *in vivo* in our transgenic animals and in our housing conditions, very similar as published. (Torchia *et al.* 2007)

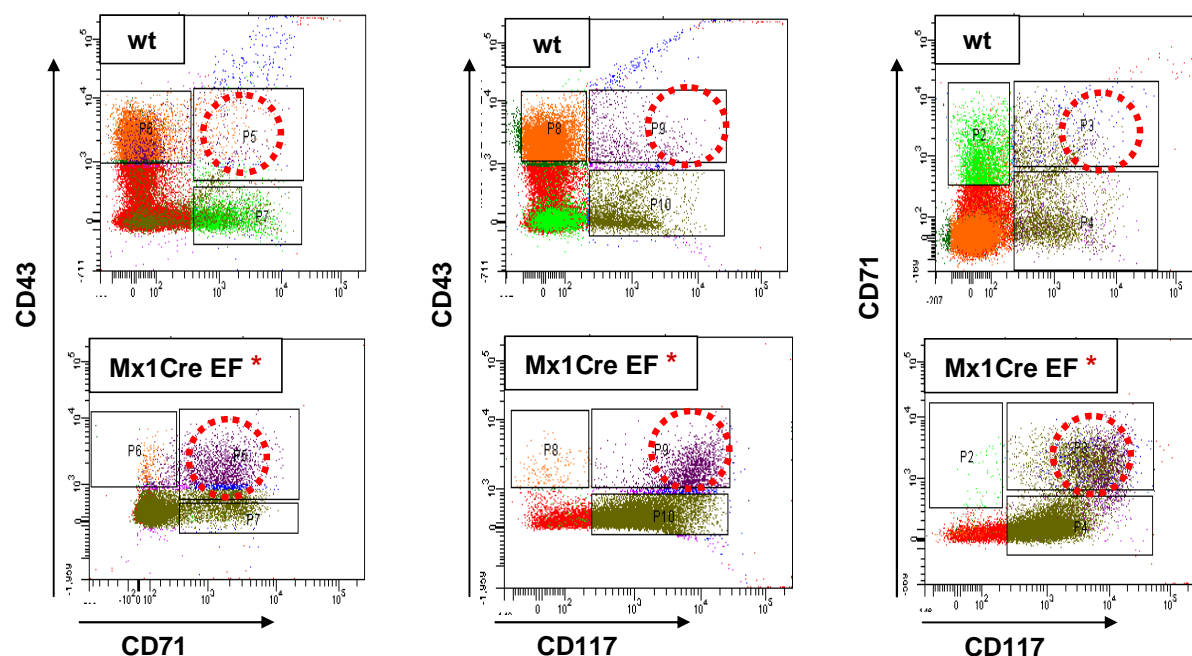


Figure 15: Flow cytometric analysis of Mx1Cre EF* mice. Splenocytes from wild type (wt) or Mx1Cre EF mice, 17 days after PolyIC injection (=Mx1Cre EF*), were stained with antibodies specific for CD71 (transferrine receptor essential for iron transport, expressed on immature erythroid cells), CD43 (highly expressed in myeloid and lymphoid precursors) and CD117 (expressed on haematopoietic stem cells and other haematopoietic progenitors). A CD43, CD71 and CD117 positive population could be identified only in Mx1Cre EF* but not in wild type mice.

3.1.3. Severe limb defects in Prx1Cre EF mice

It is currently hypothesised that ESFT originates from a cell with mesenchymal origin in which EWS/FLI-1 triggers development of ESFT (see 1.1.3.). Therefore, we conditionally expressed *EWS/FLI-1* in the mesenchymal lineage using the Prx1Cre line. *Prx1*, a paired-related homeobox gene, is expressed early in the limb bud mesenchyme from which skeletal cells arise. (Logan *et al.* 2002) We crossed the former mentioned EF mice to the Prx1Cre line. Double transgenic mice (hereafter called Prx1Cre EF) were not viable; they died a few hours after birth probably caused by an inability to consume milk (open facial cleft and abnormal limbs) and due to suffocation. Since Prx1Cre was also active in the sternum anlage, malformation of the sternum resulted in an open rib cage (Figure 17B). Thus, we

relied on analysis of embryos at different developmental stages. Prx1Cre EF mice had severe shortening of the limbs which could be seen from stage E 15.5 on and the phenotype got more pronounced the older the embryos were (Figure 16).

Skeletal analysis with Alcian Blue/Alizarin Red staining revealed an absence of calcification in the mutant limbs (Figure 17C). We could detect only cartilaginous elements in the place where the long bones should develop. Moreover, the head skeleton was also affected. Parietal, occipital and temporal bones were missing (Figure 17A). The facial bones and the axial skeleton were normally developed which is consistent with the expression pattern of Prx1Cre. (Logan *et al.* 2002) In addition, Prx1Cre EF mice displayed polydactyly being more severe in the forelimb than the hindlimb, which correlates with Cre activity (Figure 17C). (Logan *et al.* 2002)

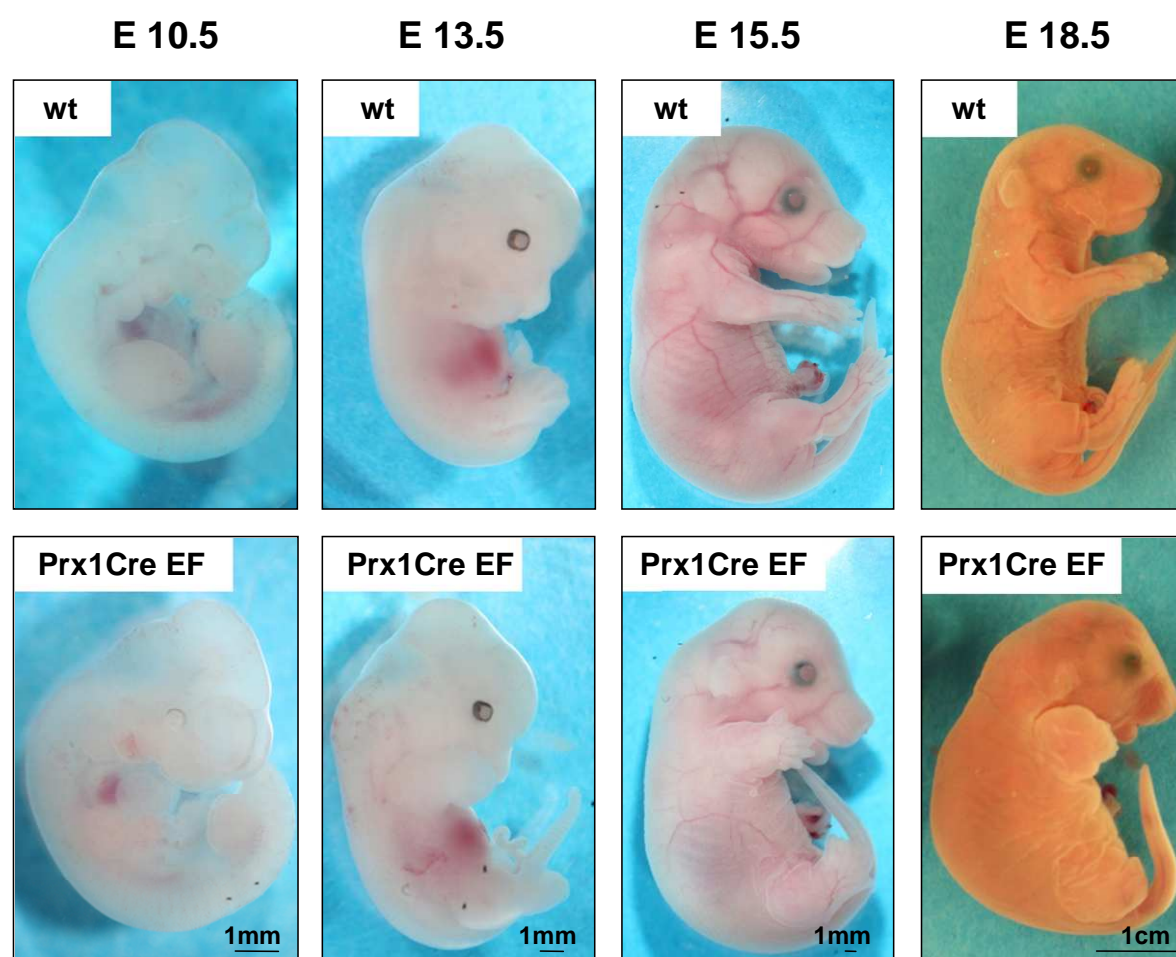
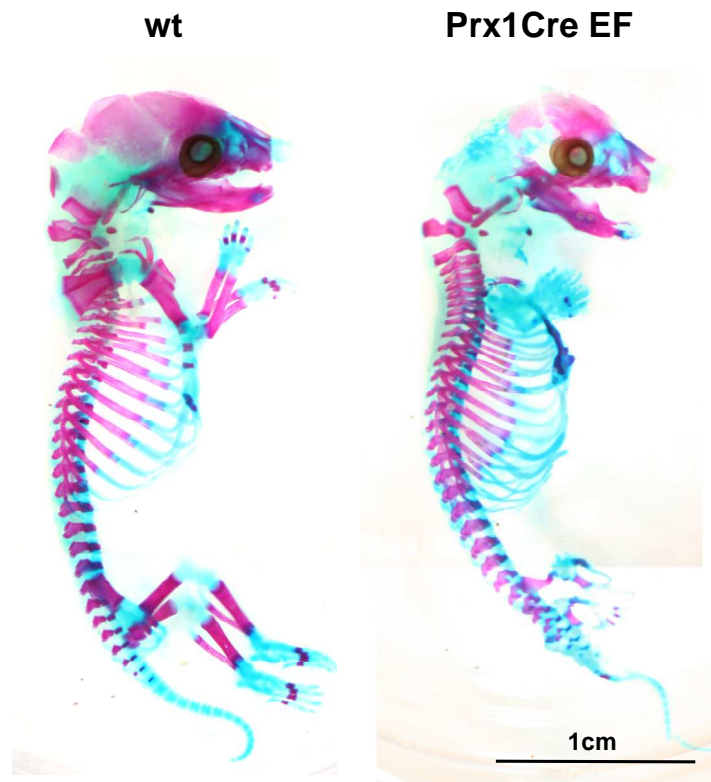
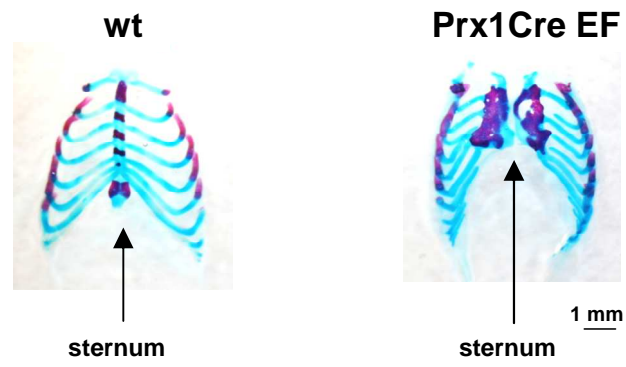


Figure 16: Skeletal defects in Prx1Cre EF mice. Developmental abnormalities in Prx1Cre EF mice were clearly visible from E 15.5 stage embryos on. Limbs from mutant mice were shorter when compared to wild type (wt) extremities. Representative examples are shown (n = 4 litters per embryonic day).

A



B



C

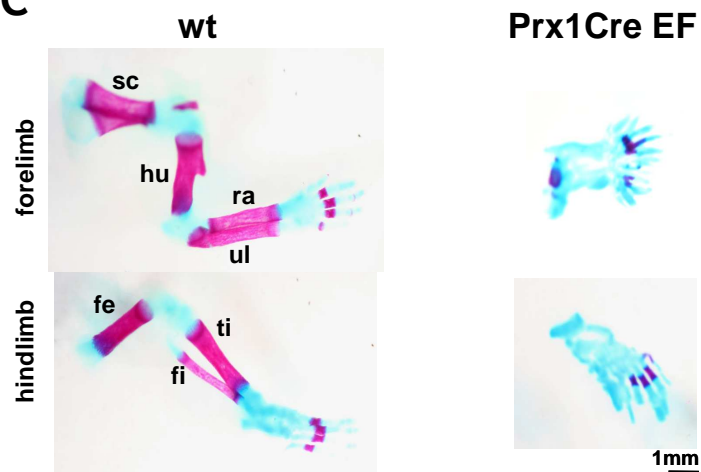


Figure 17: Skeletal analysis of Prx1Cre EF mice. Representative example of skeletal preparations of E 17.5 wild type (wt) and Prx1Cre EF embryos (n = 13). Blue staining marks cartilage elements whereas pink colour indicates calcified bone. Prx1Cre EF embryos had defects in development of parietal, occipital and temporal bones (A), the sternum (B) and most prominent in limb development (C). sc = scapula, hu = humerus, ra = radius, ul = ulna, fe = femur, ti = tibia, fi = fibula

Analysis of genomic DNA demonstrated efficient deletion of the STOP-cassette in limbs of Prx1Cre EF mice but no significant recombination could be observed in control tissue of Prx1Cre EF or wild type mice (Figure 18A). EWS/FLI-1 RNA and protein could only be detected in limbs of Prx1Cre EF mice (Figure 18B-C).

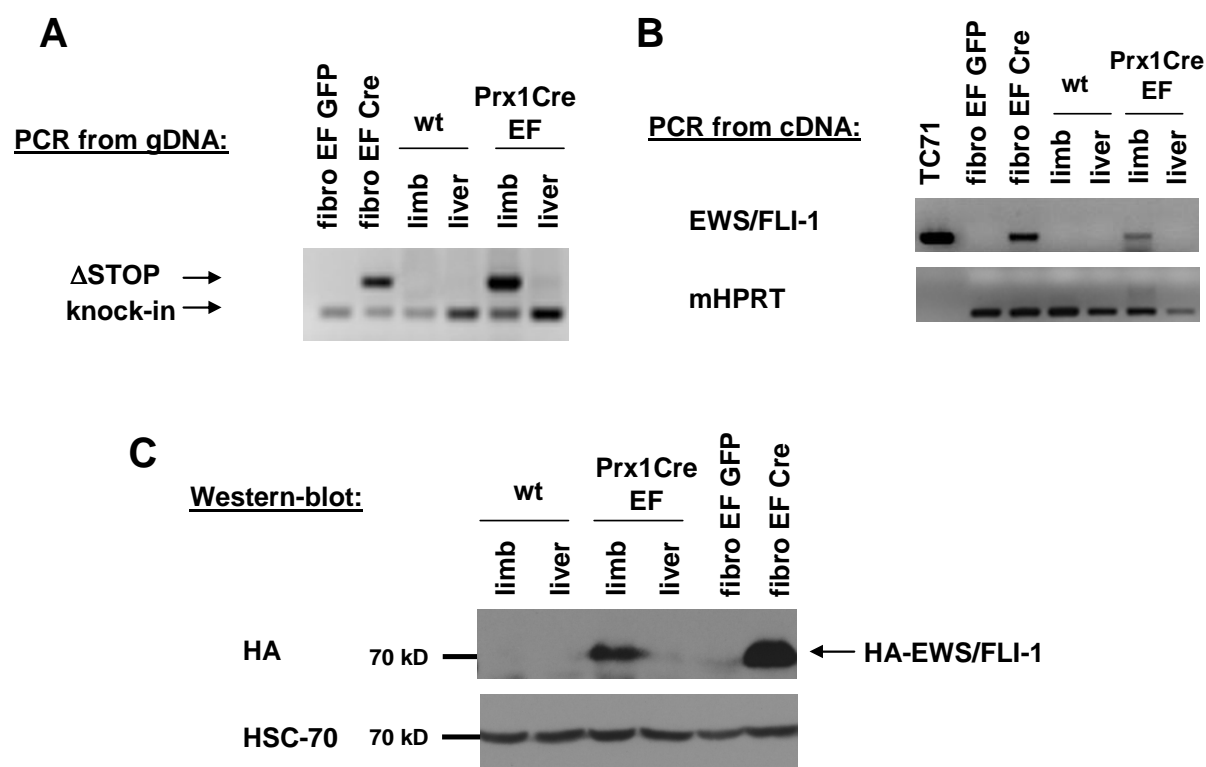


Figure 18: Expression of EWS/FLI-1 in the developing limb of Prx1Cre EF mice. A Genomic DNA (gDNA) of wild type (wt) and Prx1Cre mice (E 17.5) was analysed for deletion of STOP-cassette (Δ STOP) with a PCR strategy. STOP-cassette deletion was demonstrated in fibroblasts isolated from EF mice expressing the Cre recombinase and in limbs of Prx1Cre mice. B EWS/FLI-1 RNA was detected from reverse transcribed cDNA with specific primers in controls (TC71 and fibroblasts isolated from EF mice expressing Cre recombinase) and in limbs of Prx1Cre mice. mHPRT was used to ensure proper cDNA transcription. The human TC71 cell line had no HPRT band since the primers were specific for the mouse homologue and did not recognise the human counterpart. TC71: ESFT cell line used as a positive control for EWS/FLI-1 expression C Presence of EWS/FLI-1 protein in

Prx1Cre limbs was verified with Western blot analysis using an antibody specific for the HA-tag. HSC-70 was used as a loading control. fibro GFP or Cre: fibroblasts isolated from EF mice lentivirally transduced with a construct containing GFP or the Cre recombinase.

Histological analysis of E 18.5 limbs revealed that there was no hypertrophic region or mature chondrocytes present in Prx1Cre EF extremities (Figure 19A). The limbs of wild type mice were structured normally with the epiphysis at the end, diaphysis in the middle of the bone and an intact medullary cavity. All these structures were lacking in Prx1Cre EF limbs and only a condensed cartilaginous element was left. In addition, the periosteum displayed abnormal zones.

To determine the identity of these densely packed cells, we performed *in situ* hybridisation analysis with markers specific for distinct differentiation stages of chondrocytes and osteoblasts (see 1.1.5.). *Col2a1*, a marker for all chondrocyte stages was expressed in the epiphysis of wild type bone and also in the residual elements in Prx1Cre EF limbs (Figure 19B). But when it comes to markers for more differentiated chondrocytes like *Ihh* and *Col10a1*, they were completely lacking in limbs of Prx1Cre EF mice (Figure 19C-D). *Ihh* is secreted by prehypertrophic chondrocytes and *Col10a1* is expressed in hypertrophic chondrocytes. Both zones were nicely stained with the respective marker in wild type bones (Figure 19C-D). Concerning the differentiation of osteoblasts, *Runx2* is essential for precursor cells to enter the osteoblastic lineage and is itself induced by *Ihh*. Due to the lack of *Ihh* we also could not detect *Runx2* in Prx1Cre EF limbs (Figure 19E). Thus, markers for more mature osteoblasts were also absent (Figure 19F-H). *Osx* is expressed in committed osteo-progenitors whereas *Col1a1* and *Osc* are markers for mature osteoblast (see 1.1.5.). In bones of wild type mice all of these osteoblast markers were nicely expressed (Figure 19E-H).

In summary, expression of EWS/FLI-1 in developing limb buds resulted in a block of chondrocyte maturation and absence of mature osteoblasts, resulting in a severe malformation of the limbs.

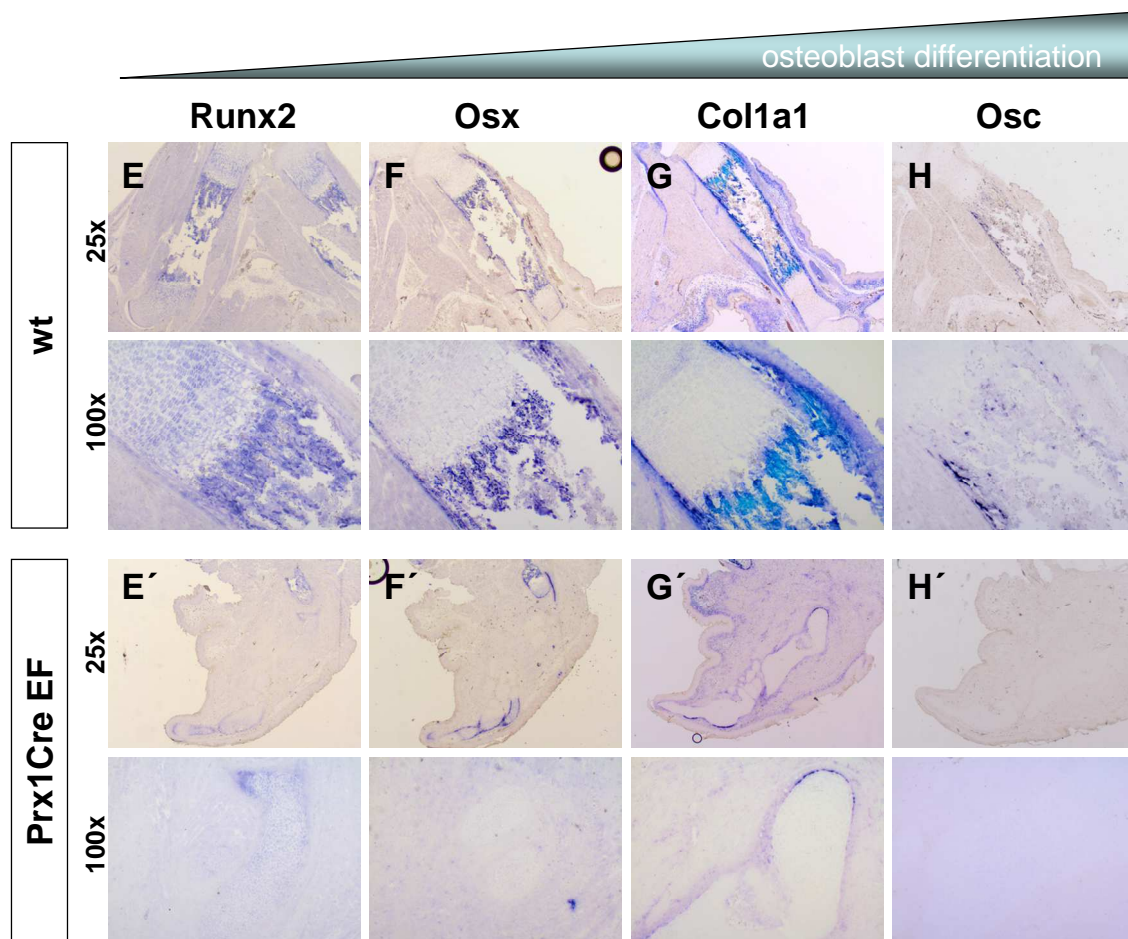
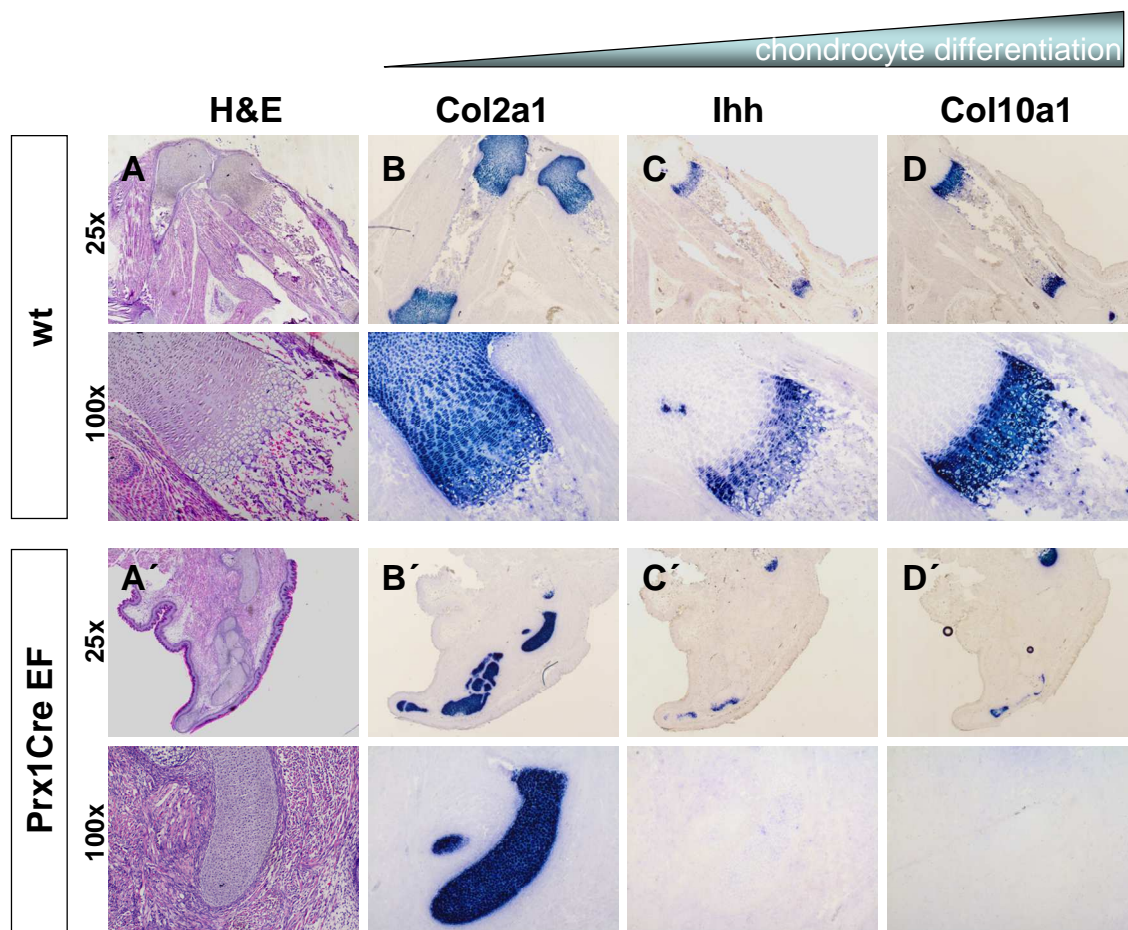


Figure 19: Lack of mature chondrocyte and osteoblast markers in Prx1Cre EF mice. Haematoxylin and eosin staining (H&E, A) on sectioned limbs of wild type and Prx1Cre EF mice (18.5) and non-radioactive *in situ* hybridisation using markers specific for different maturation stages of chondrocytes and osteoblasts. Col2a1 (B), Ihh (C) and Col10a1 (D) were expressed from chondrocytes at different maturation stages and Runx2 (E), Osx (F), Col1a1 (G) and Osc (H) were present in different osteoblast stages of wild type (wt) bone. In Prx1Cre limbs only Col2a1 was present.

	offspring	EWS/FLI-1 expression	phenotype
784 Runx2Cre EF	viable	no	none
1634 Runx2Cre EF	viable	no	none
777 Runx2Cre EF	embryonic lethal	n.d.	n.d.
784 Runx2Cre EF INK4A/ARF ^{-/-}	viable	no	no shift in tumour spectrum compared to INK4A/ARF ^{-/-} control mice
1634 Runx2Cre EF INK4A/ARF ^{-/-}	viable	no	no shift in tumour spectrum compared to INK4A/ARF ^{-/-} control mice
Mx1Cre EF	viable	yes	myeloid/erythroid leukemia
Prx1Cre EF	die shortly after birth	yes (limb specific)	limb shortening (no mature chondrocytes and osteoblasts)

Table 2: Overview of mouse colonies generated during this study. n.d.= not determined

3.2. JAK/STAT signalling in ESFT

Although the JAK/STAT signalling cascade is often de-regulated in cancer, not much is known about this pathway in ESFT. Several publications demonstrated that *JAK1* is up-regulated and *STAT3* is activated to variable degrees in ESFT patient samples but the cytokine signalling pathway involvement remains enigmatic. (Lai *et al.* 2006; Baird *et al.* 2005) Thus, the role of the JAK/STAT pathway in ESFT was investigated, in particular with respect to upstream cytokine receptors which can lead to *STAT1* or *STAT3* activation.

3.2.1. JAK/STAT activity in ESFT cells

Three ESFT cell lines (SK-N-MC; STA-ET-7.2; TC71) with a differential profile of p53 mutation, *EWS/FLI-1* fusion type and endogenous *EWS* expression (see 2.2.1.) were analysed for activation of the JAK/STAT signalling pathway. Cells were grown in monolayer culture in standard cell culture dishes. Alternatively, cells were also grown as spheroids in bacterial plates since formation of these multicellular structures resembled the situation in primary tumours more closely than monolayer culture. DNA binding and hence activity of *STAT* proteins was examined with electrophoretic mobility shift assays (EMSA). Neither in plain monolayer culture nor in spheroid cultures, activation of *STAT1*, *STAT3* or *STAT5* could be observed (Figure 20).

It was previously shown that *STAT3* is constitutively activated in colon cancer but is lost in cell culture and can be restored in xenografts. (Corvinus *et al.* 2005) Therefore ESFT cell lines were subcutaneously injected into immunocompromised mice (SCID) where they formed tumours within two to three weeks on average. When xenograft samples (n=18) were analysed for DNA binding ability of *STAT* proteins, activation of *STAT1* and *STAT3* could be detected with antibodies specific for the corresponding protein in EMSA (Figure 21A). In contrast, specific *STAT5* activation could not be observed in xenograft samples (Figure 21B).

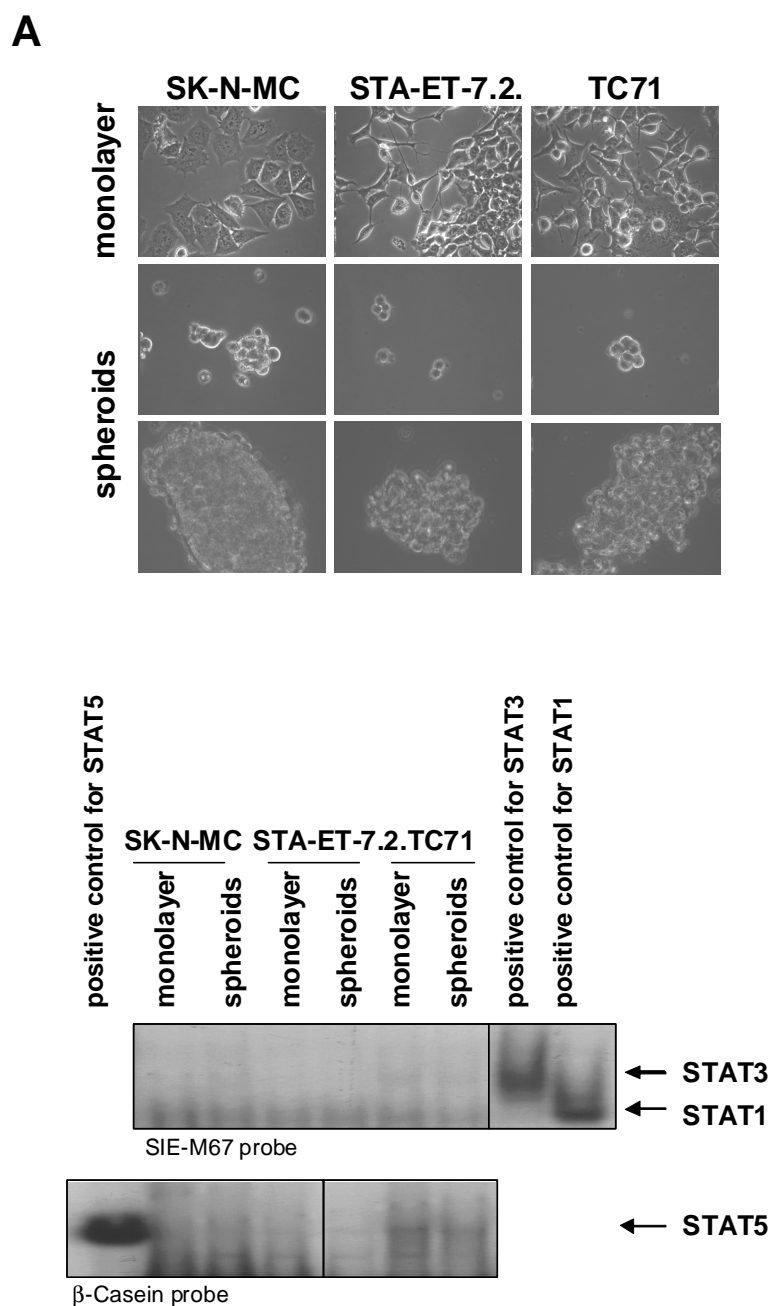


Figure 20: Analysis of JAK/STAT activity in ESFT cell lines. **A** Phase contrast micrograph of three different ESFT cell lines, grown in monolayer culture in standard cell culture dishes or as spheroids in bacterial plates. **B** Electrophoretic mobility shift assay (EMSA) with radioactively labelled oligonucleotides specific for either STAT1 and STAT3 (SIE-M67) or STAT5 (β -casein) demonstrated absence of specific activity in the three analysed cell lines whether grown as monolayer or spheroids. Positive control for STAT1: NIH3T3 cells stimulated with 10 ng/ml IFN- γ for 30 minutes; positive control for STAT3: 293T cells, transfected with STAT3 and stimulated with 20 ng/ml IL-6 for 30 minutes; positive control for STAT5: 293T cells, transfected with STAT5A and erythropoietin receptor, stimulated with 50 U/ml erythropoietin for 30 minutes. (STAT3 and STAT5 controls were a kind gift of Dr. Richard Moriggl and Dr. Jan-Wilhelm Kornfeld)

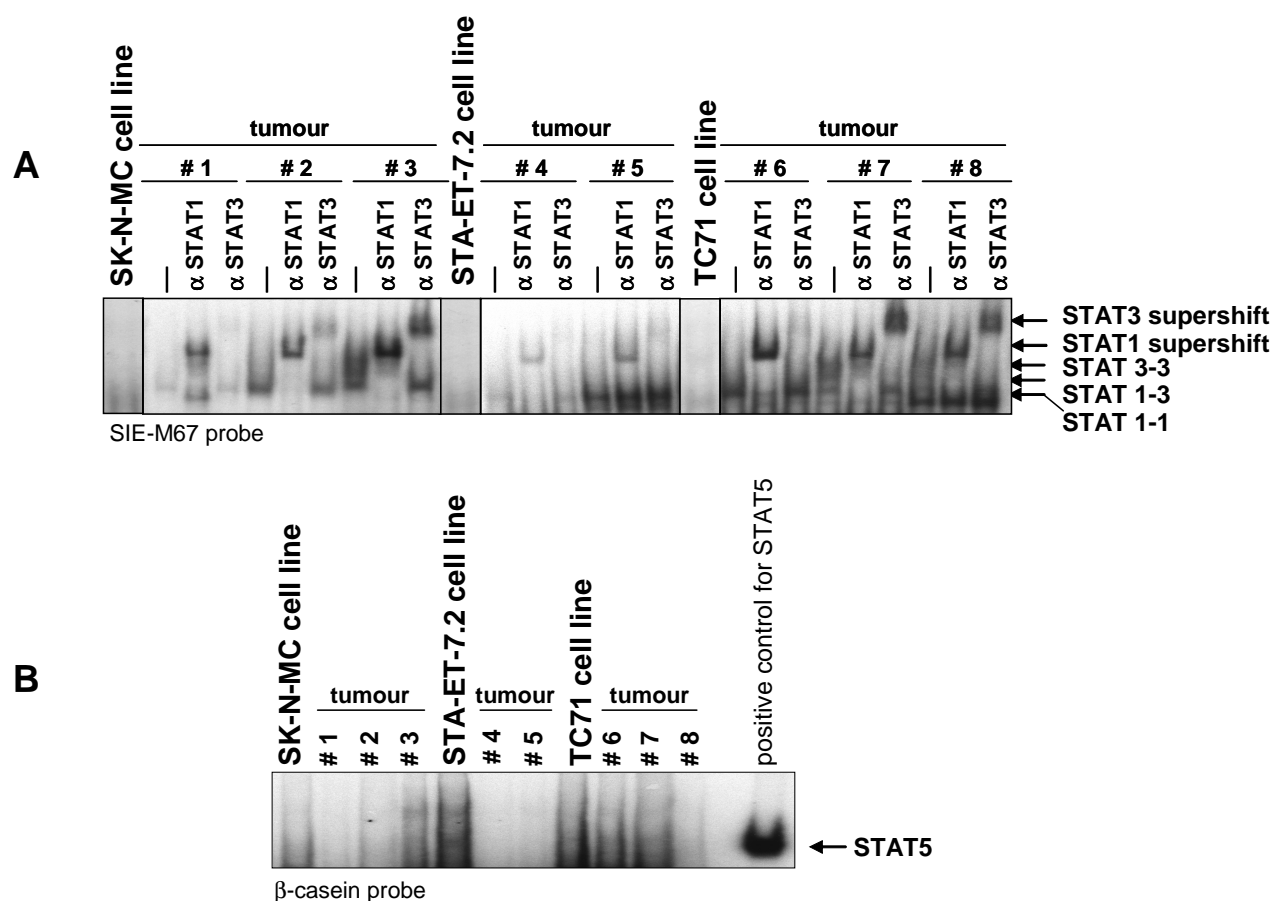


Figure 21: Analysis of JAK/STAT activity in ESFT cell line xenografts. Subcutaneous injection of ESFT cell lines into immunocompromised mice (SCID) resulted in tumour formation and xenografts were analysed for activity of STAT proteins. **A** EMSA was performed with radioactively labelled oligonucleotides specific for STAT1 and STAT3 (SIE-M67) and supershift with antibodies recognising either STAT1 or STAT3. The three analysed cell lines did not show STAT1 or STAT3 activation whereas upon xenograft injection, both STAT proteins were activated in tumour cell extracts. **B** Absence of specific STAT5 activation in extracts of cell lines and xenografts was demonstrated by EMSA using radioactively labelled oligonucleotides specific for STAT5 (β -casein). Positive control for STAT5: 293T cells, transfected with STAT5A and erythropoietin receptor, stimulated with 50 U/ml erythropoietin for 30 minutes (gift of Dr. Richard Moriggl and Dr. Jan-Wilhelm Kornfeld)

In consideration of these results, we concentrated on analysis of STAT1 and STAT3 and excluded STAT5 for further experiments.

Since the three cell lines used in this study were similar in their behaviour in regard to the analysed aspects, only one representative example is shown in up-coming figures.

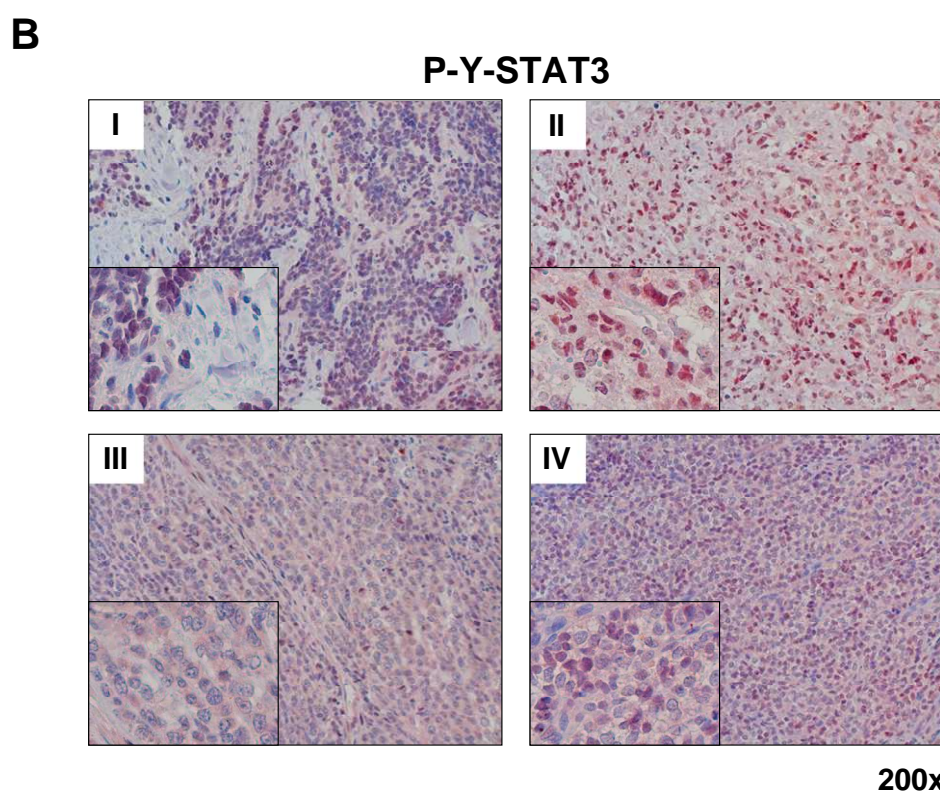
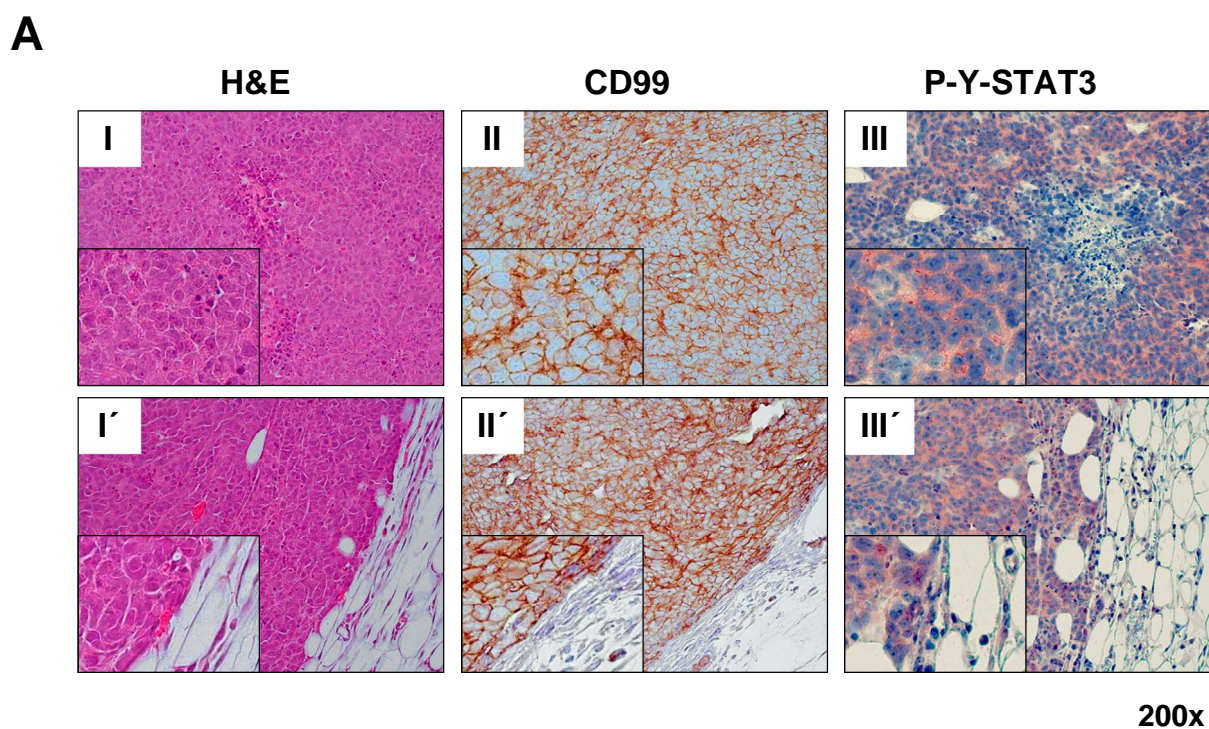


Figure 22: Histological analysis of ESFT cell line xenografts and ESFT tumour samples. A Sections of ESFT cell line xenografts were immunohistochemically stained with haematoxylin and eosin (H&E; I and I'), for CD99 (II and II') and for activated STAT3 (P-Y-STAT3; III and III'). H&E staining revealed that the tumours had a homogenous structure (I and I'). CD99, a cell surface marker used to identify ESFT, was expressed on the plasma membrane of tumour cells but not in adjacent cell types (II'). Most of the tyrosine phosphorylated STAT3 could be detected in the cytoplasm of ESFT xenografts and only weak staining was present in surrounding cells (III'). SK-N-MC xenograft samples are shown

as a representative example. **B** Immunohistochemical staining for activated STAT3 on sections of Ewing's tumour samples. A tissue microarray with 45 patients was stained with an antibody specific for P-Y-STAT3. Four examples representing the heterogeneity of staining pattern are shown: I - intermediate staining in nucleus and cytoplasm (normal bone structures were P-Y-STAT3 negative); II - strong staining only in the nucleus; III - weak staining only in the cytoplasm; IV - intermediate staining in nucleus and cytoplasm.

Five xenograft tumours were analysed for immunohistological features and one representative example is depicted in Figure 22A. H&E staining showed a homogenous structure in the xenograft tumours. CD99, a surface molecule used in diagnosis of ESFT, was only expressed in the tumour area but not in the surrounding tissue (Figure 22A-II'). Moreover, profound phosphorylation of STAT3 was present in the xenograft (Figure 22A-III and -III') and also in samples from ESFT patients (Figure 22B). Overall, 73% of the 45 patient samples analysed on a tissue micro array (in collaboration with Dr. Christopher Poremba, Research Park Trier, Center of Histopathology, Cytology, and Molecular Diagnostics, Trier, Germany) stained positively for phosphorylated STAT3. The staining pattern was very heterogeneous and varied from weakly positive to an intense staining (Figure 22B-III and -II, respectively). The cellular localisation was also not uniform, with most of the samples having a P-Y-STAT3 staining in both nucleus and cytoplasm (Figure 22B-I and -IV), but also only nuclear (Figure 22B-II) or only cytoplasmic localisation (Figure 22B-III) of P-Y-STAT3 staining was present. The status of STAT1 would also have been interesting but the immunohistology for P-Y-STAT1 unfortunately never worked properly.

3.2.2. Cytokines activating STAT1/STAT3

Absence of basal levels of JAK/STAT activation in cell culture and strong activation in xenograft tumours and patient samples suggested that signalling molecules present in the microenvironment of tumours, but not in cell culture, led to activation of this pathway. Thus, we tested a selection of cytokines, known to activate STAT1 and/or STAT3, on ESFT cell lines.

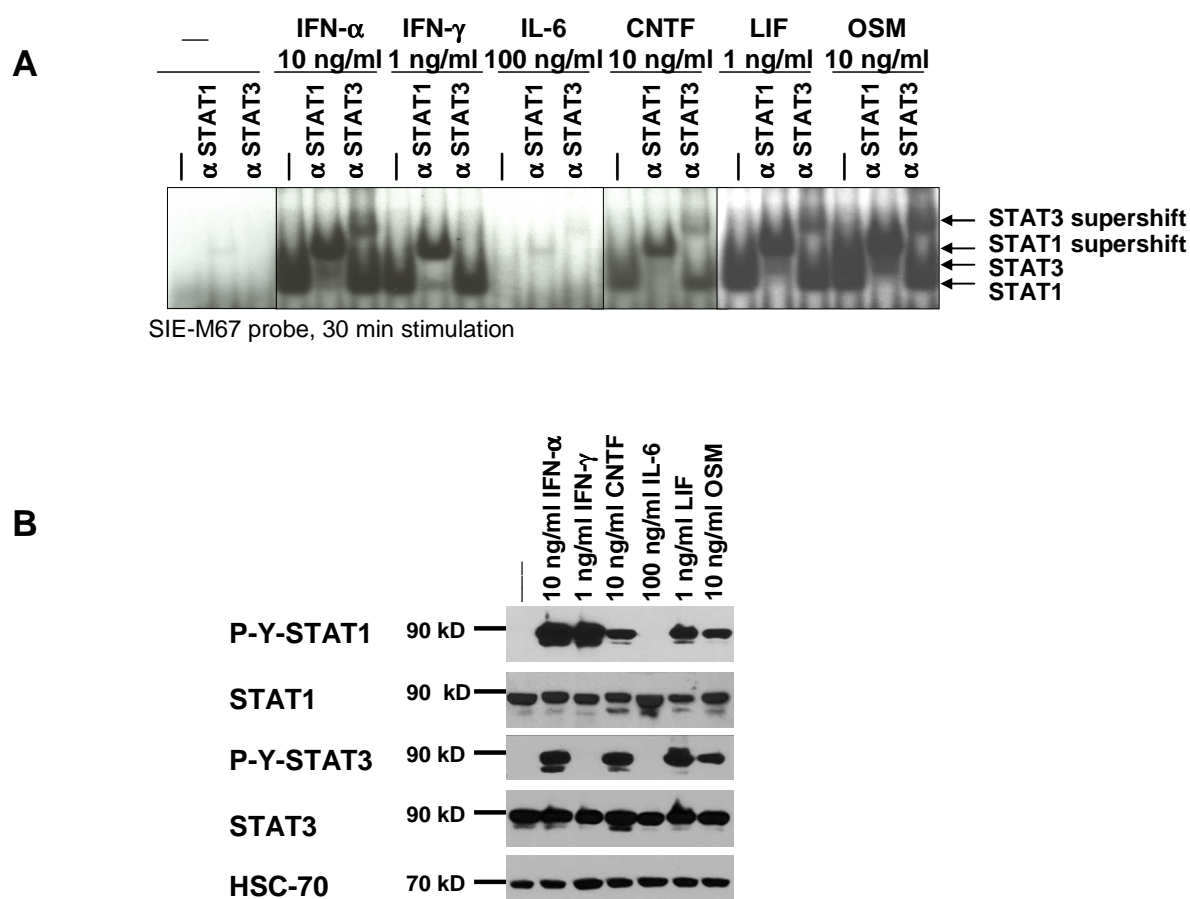


Figure 23: Response of ESFT cell lines to STAT1/STAT3 activating cytokines. ESFT cells were stimulated for 30 minutes with indicated concentrations of various cytokines or left untreated. The results from SK-N-MC are shown as a representative since the same picture was seen in TC71 and STA-ET-7.2. **A** EMSA was performed with radioactively labelled oligonucleotides specific for STAT1 and STAT3 (SIE-M67) and supershift with antibodies recognising either STAT1 or STAT3 was used to distinguish the STAT proteins present. DNA binding ability of STAT1 and STAT3 could be demonstrated upon IFN- α , CNTF, LIF and OSM stimulation whereas IFN- γ administration activated only STAT1. IL-6 stimulation led only to a weak STAT1 and STAT3 DNA binding. **B** Tyrosine phosphorylation and total levels of STAT1 and STAT3 were analysed with Western blot analysis. IFN- α , CNTF, LIF and OSM stimulation led to phosphorylation of STAT1 and STAT3, IFN- γ administration resulted in STAT1 phosphorylation and no phosphorylation of STAT1 or STAT3 was detected after IL-6 stimulation. HSC-70 was used as a loading control. IFN = interferon, IL-6 = interleukin-6, CNTF = ciliary neurotrophic factor, LIF = leukaemia inhibitory factor, OSM = oncostatin M

ESFT cells were incubated with indicated cytokines for 30 minutes at different concentrations. The potency of activating STAT1 and STAT3 varied greatly (data not shown) and only one concentration of each cytokine was chosen for the following experiments so that activation levels were quite equal. Interferon (IFN)-

α , ciliary neurotrophic factor (CNTF), leukaemia inhibitory factor (LIF) and oncostatin M (OSM) led to a profound activation of STAT1 and STAT3 as shown by the DNA binding ability to a STAT1 and STAT3 responsive element, whereas IFN- γ activated only STAT1 (Figure 23A). Surprisingly, ESFT cells were weakly responsive to the wide-range cytokine interleukin-6 (IL-6), only high levels of IL-6 (at least 100 ng/ml) could activate STAT3 as well as STAT1 to some extent.

Moreover, the data from the DNA binding assay could be verified with Western blot analysis using antibodies specific for the tyrosine phosphorylated forms of STAT1 or STAT3 (Figure 23B). Phosphorylation of STAT1 could be detected in IFN- α , IFN- γ , CNTF, LIF and OSM stimulated cells and STAT3 was phosphorylated upon stimulation with IFN- α , CNTF, LIF and OSM. Although a weak DNA binding ability of STAT1 and STAT3 could be detected in IL-6 stimulated cells (Figure 23A), significant tyrosine phosphorylation of the STAT proteins could not be observed in Western blot analysis (Figure 23B).

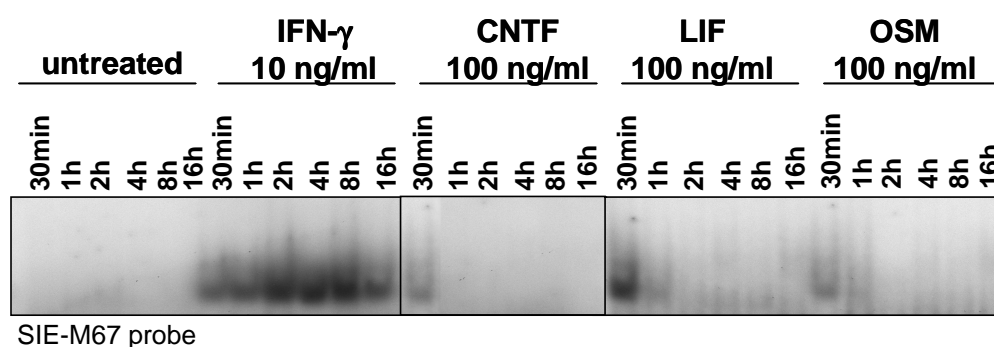


Figure 24: Duration of STAT activity in stimulated ESFT cell lines. ESFT cells were stimulated for indicated time periods with 10 ng/ml or 100 ng/ml of various cytokines or left untreated. EMSA was performed with radioactively labelled oligonucleotides specific for STAT1 and STAT3 (SIE-M67). Only IFN- γ caused prolonged STAT1 activity over time whereas gp130 cytokines led to a shotgun activation of STAT1/STAT3. Data from SK-N-MC are shown as a representative example; the same results were obtained for TC71 and STA-ET-7.2.

Furthermore, we investigated the duration of the JAK/STAT signal in cytokine stimulated cells. Therefore, we stimulated ESFT cells for different time periods with the cytokines most potently activating STAT1 and STAT3. We used an approximately ten fold higher concentration as needed to see DNA binding to circumvent limitation of the cytokine during the experiment. EMSA revealed that

gp130 cytokines (CNTF, LIF and OSM) activated STAT1 and STAT3 transiently whereas IFN- γ led to a sustained activation (Figure 24).

To better understand the mechanisms of JAK/STAT signalling we also investigated the corresponding receptors on the surface of ESFT cells. Gp130 is part of every gp130 cytokine receptor complex and therefore indispensable for activation of STAT1 and STAT3 in response to IL-6, CNTF, LIF or OSM. As expected, gp130 was nicely expressed in ESFT cells (Figure 25). Also LIF receptor (LIFR) and OSM receptor (OSMR) were highly expressed but no significant IL-6 receptor α (IL-6R) could be found on the ESFT cells analysed. Surprisingly, CNTF receptor α chain (CNTFR) could also not be detected, although the cells were clearly responsive to CNTF. This suggests signalling through an alternative complex, consisting of gp130, LIFR and the soluble IL-6R, which might be present but cannot be detected with flow cytometric analysis. (Schuster *et al.* 2003)

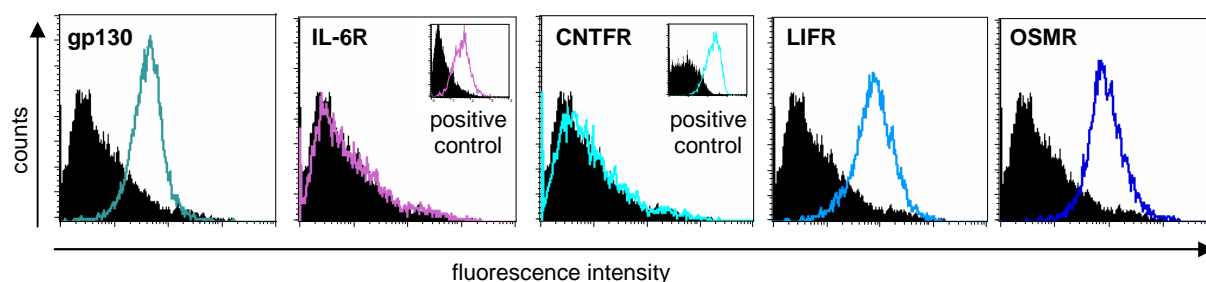


Figure 25: Cytokine receptor surface expression in ESFT cells. Flow cytometric analysis of non-permeabilised ESFT cell lines stained with antibodies specific for the receptors of the gp130 cytokine receptor family demonstrated prominent surface expression of gp130, LIFR and OSMR whereas IL-6R and CNTFR could not be detected. Black filled histograms represent the negative control without first antibody and the coloured line shows the level of the indicated receptor present on the surface of ESFT cells. Functionality of antibodies was tested with control cells. 293T cells expressed IL-6R and SH cells, a neuroblastoma cell line, expressed CNTFR on the cell surface. The results from SK-N-MC are shown as a representative; the same receptors were present in TC71 and STA-ET-7.2. Gp130 = glycoprotein 130, IL-6R = IL-6 receptor α , CNTFR = CNTF receptor α chain, LIFR = LIF receptor, OSMT = OSM receptor.

In regard to the biological functions of the tested cytokines, known to enhance or reduce cellular expansion, we investigated the effect on ESFT cell proliferation. A profound reduction in cell number was observed when cells were stimulated with

IFN- γ (Figure 26). IFN- α stimulation demonstrated a mild inhibition of proliferation. However, proliferation in response to gp130-cytokines was not altered dramatically; LIF stimulation was able to enhance cell growth to some extent but only at high concentrations (Figure 26 and data not shown).

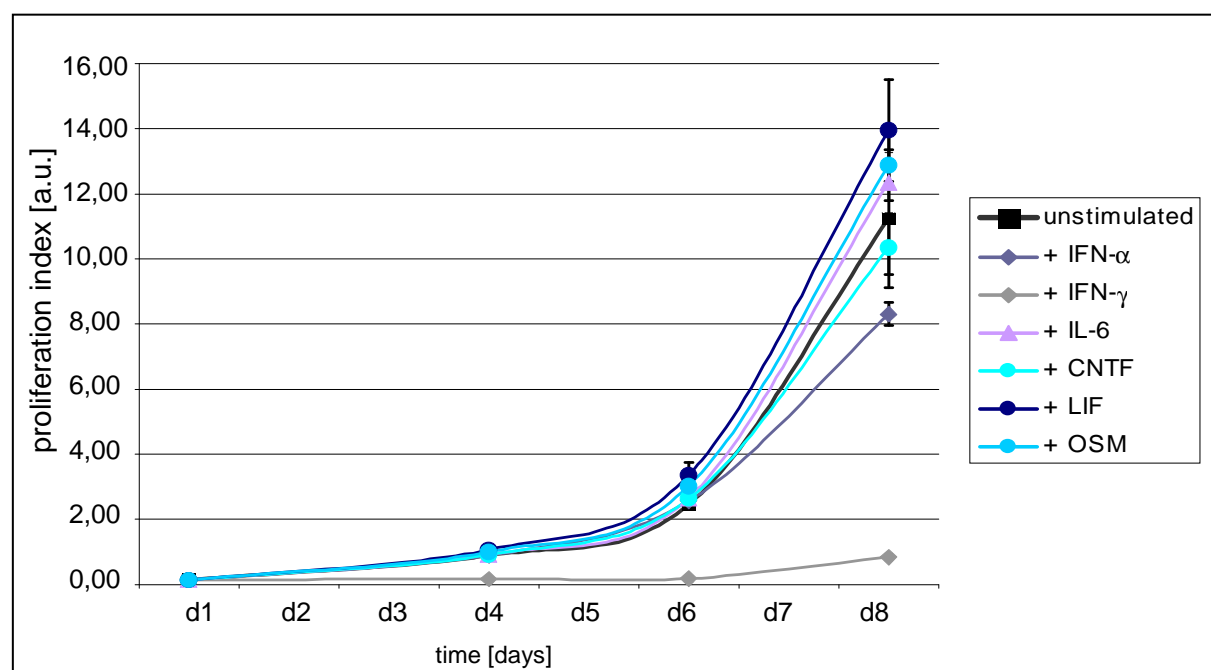


Figure 26: Proliferation in response to cytokines. ESFT cell lines were stimulated with 10 ng/ml cytokine and proliferation was monitored over a period of 8 days. Cell numbers were determined by incorporation of crystal violet and measurement of the extracted dye at 560 nm. IFN- γ led to a massive reduction in cell number, IFN- α reduced proliferation only modestly and administration of gp130 cytokines did not much alter proliferation in comparison to the untreated control. Results from SK-N-MC are shown as a representative but analysis was also performed with TC71 and STA-ET-7.2 having the same outcome.

Since STAT proteins are transcription factors regulating transcription of target genes we wanted to know which target genes are changed in cytokine stimulated ESFT cells. Analysis of JAK/STAT specific target genes with an OligoGEArrayTM demonstrated that STAT1 targets were clearly up-regulated in INF- γ stimulated cells (Figure 27). Some STAT1 targets, like *CDKN1A* or *IRF1* were also expressed at a higher level in response to CNTF, LIF or OSM. *CXCL9* and *SOCS1* were up-regulated after CNTF administration whereas LIF and OSM stimulation led in addition to an induction of *INDO*. Unexpectedly, STAT3 induced genes (*BCL2L1*, *MMP3*, *MYC*) did

not change their expression significantly. The level of the STAT3 target gene *CRP* was even lower after cytokine stimulation.

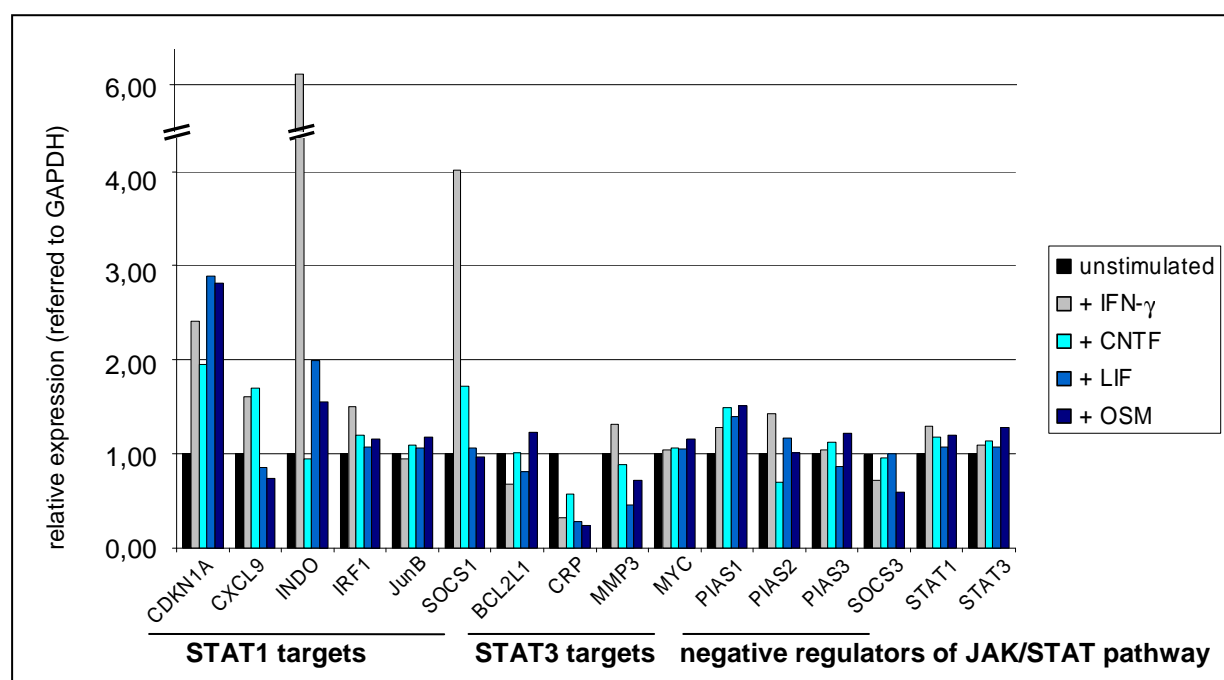


Figure 27: Analysis of JAK/STAT specific target genes. ESFT cell lines were stimulated with indicated cytokines for 4 hours and analysed for JAK/STAT relevant genes with an OligoGEArray™. The left part of the graph shows selected STAT1 target genes, the middle depicts a selection of STAT3 relevant targets and the right side presents genes that negatively regulate the JAK/STAT pathway. Stimulation with IFN- γ up-regulated almost all indicated STAT1 target genes while gp130 cytokines led to expression of some STAT1 targets, but no STAT3 target was significantly up-regulated. Data from SK-N-MC are shown as a representative though analysis was also performed with TC71, showing the same result.

3.2.3. Dominant negative forms of STAT1/STAT3 in ESFT cell lines

To answer the question if STAT1 and/or STAT3 were essential for ESFT tumour formation, we introduced mutant forms of STAT1 and STAT3 acting in a dominant negative way into ESFT cell lines. We used STAT mutants where the critical tyrosine residue was changed to phenylalanine so that it cannot be phosphorylated anymore (STAT1 Y701F and STAT3 Y705F later abbreviated as S1YF and S3YF, Figure 28B). These mutant forms of STATs bind to the receptor and block recruitment of wild type STAT proteins, inhibiting phosphorylation of wild type STATs and hence signal transduction. (Kaptein *et al.* 1996) The second mutant form we used was a

truncation of the carboxy-terminal part (STAT1 $\Delta 677$ and STAT3 $\Delta 683$ later abbreviated as S1 Δ and S3 Δ , Figure 28C). Since the transactivation domain is located in this region, the modified STAT proteins could not regulate gene expression anymore.

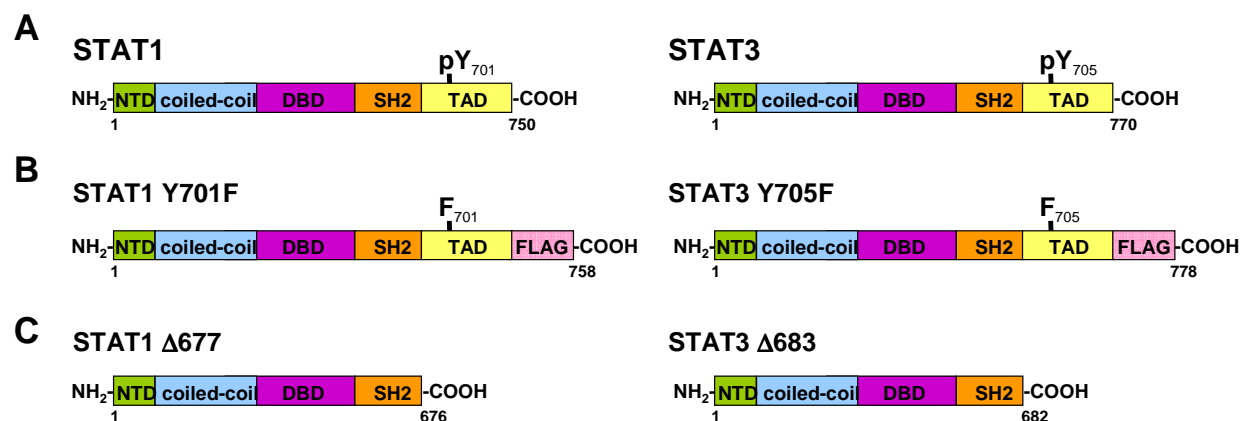


Figure 28. Dominant negative forms of STAT1 and STAT3. A Unmodified structure of STAT1 and STAT3. B Modified forms of STAT1 and STAT3 with a point mutation of the essential tyrosine necessary for STAT activity. A FLAG tag was introduced to distinguish the mutant from the endogenous STAT protein. C Mutant forms of STAT1 and STAT3 lacking the carboxy-terminal part, harbouring the transactivation domain. The mutated constructs were cloned into pMSCV, a vector based on the murine stem cell virus. The gene of interest was followed by an internal ribosomal entry site (IRES) and the green fluorescent protein (GFP), facilitating sorting of infected cells. NTD = N-terminal domain, DBD = DNA binding domain, SH2 = src homology 2, TAD = transactivation domain, pY = tyrosine phosphorylation site

SK-N-MC and TC71 cell lines were retrovirally transduced with dominant negative constructs of STAT1 or STAT3 and sorted for GFP (in collaboration with Dr. Matthias Mayerhofer, General Hospital Vienna, Austria and Gabi Stengl, Institute of Molecular Pathology, Vienna, Austria). Since both cell lines used in these experiments were similar in their behaviour in regard to the analysed aspects, only one representative example is shown in up-coming figures.

Expression of mutant STAT proteins was verified with Western blot analysis (Figure 29A). Cells transduced with the empty vector (GFP) were used as a control. The S1 Δ mutant could not be detected with a specific antibody recognising the amino-terminal part of STAT1 (Figure 29A) even though GFP expression could be verified with flow cytometry (Figure 29B). Thus, this mutant was excluded for further

experiments. Expression of S1YF and S3YF proteins could be demonstrated with an antibody detecting the FLAG-tag of these mutants and S3 Δ could be nicely visualised with an antibody specific for the STAT3 amino-terminus (Figure 29A). In extracts from S3YF transduced cells, the STAT3 antibody recognised a band that migrated similarly to the S3 Δ protein, but the same band appeared when the membrane was incubated with a FLAG specific antibody. Since the FLAG-tag is only present in the S3YF mutant form but not in S3 Δ , a contamination could be excluded (Figure 29A).

We wanted to analyse if there were differences in growth of xenografts expressing the STAT mutants, so we tested as a pre-experiment whether the established cell lines varied in their growth behaviour *in vitro*. A proliferation assay based on incorporation of crystal violet (see 2.2.6.) revealed that the cell lines expressing mutant forms of STAT1 or STAT3 did not differ much in their proliferation behaviour (Figure 29C). These data were in line with the observed absence of STAT1 and STAT3 activity in cell culture (Figure 23).

Next, we subcutaneously injected the established cell lines into immunocompromised mice and examined the resulting tumours. The dominant negative STAT forms were still expressed in the xenografts, but to a slightly lower level (Figure 30A). Tumour growth was not much altered when looking at the different mutants but all the manipulated cell lines grew a little slower in xenografted tumours than control cells (Figure 30B). Moreover, histological analysis with H&E, TUNEL and Ki67 staining (in collaboration with DI Michaela Schleder) did not reveal any striking differences (Figure 31).

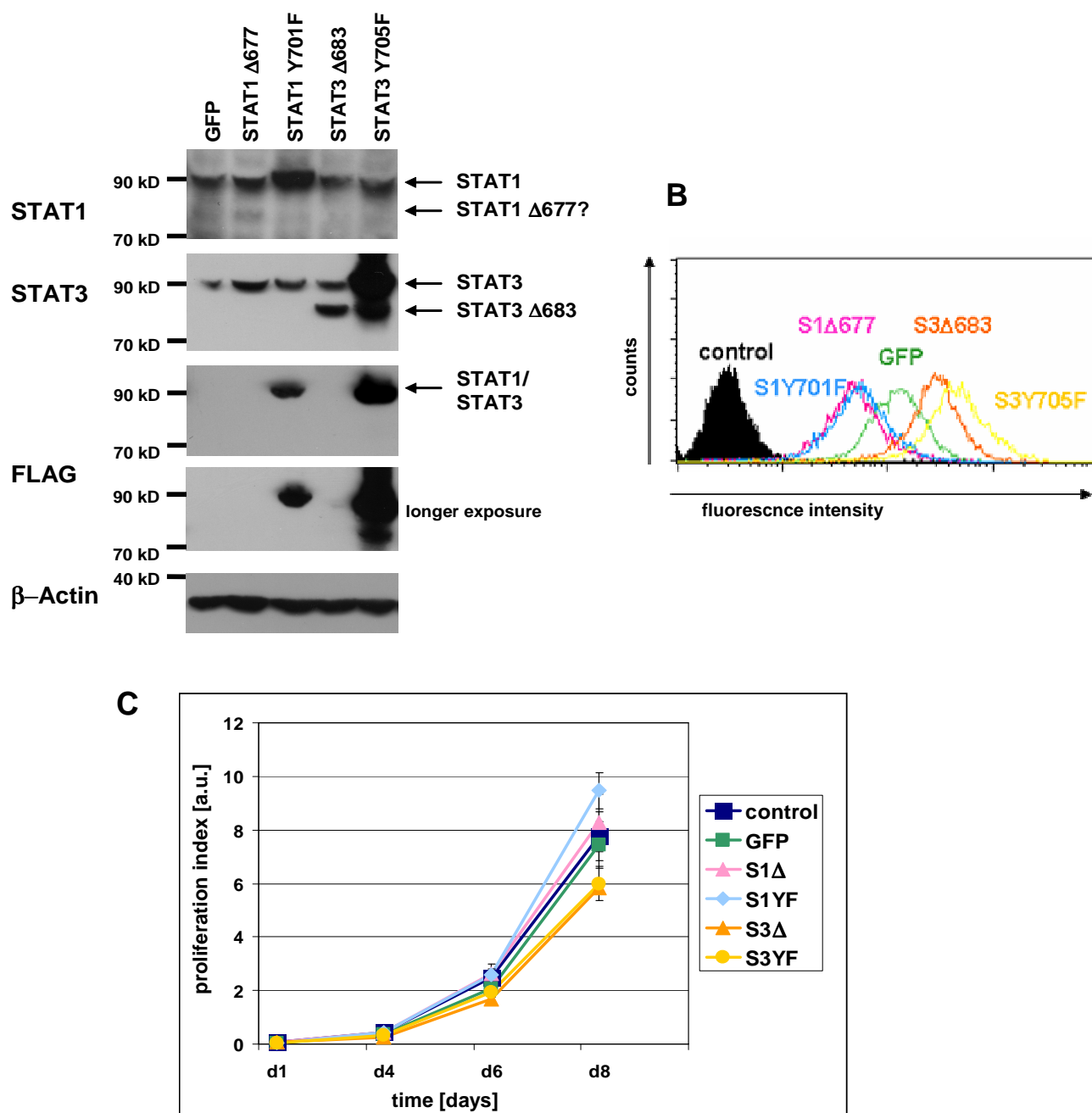
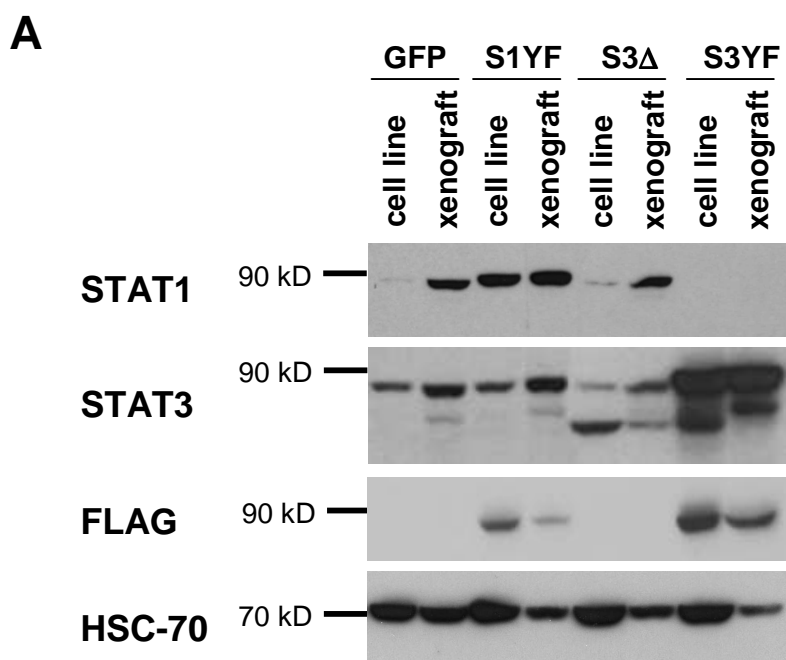


Figure 29: Expression of dominant-negative STATs in ESFT cell lines. A Western blot analysis of cells transduced with different mutant forms of STAT1, STAT3 or empty vector (GFP) with antibodies specific for STAT1, STAT3 or the FLAG-tag. β -Actin was used as a loading control. S1YF, S3 Δ and S3YF were nicely expressed whereas S1 Δ could not be detected. B Flow cytometric analysis for expression of GFP in cell lines transduced with mutant STATs indicated presence of the construct in all cell lines. Untransduced ESFT cells were used as a control. C Analysis for proliferation of cell lines expressing different mutant forms of STAT1 and STAT3 revealed quite similar growth curves. Data from SK-N-MC cell lines are shown as a representative; analysis of TC71 cell lines had the same results.



B

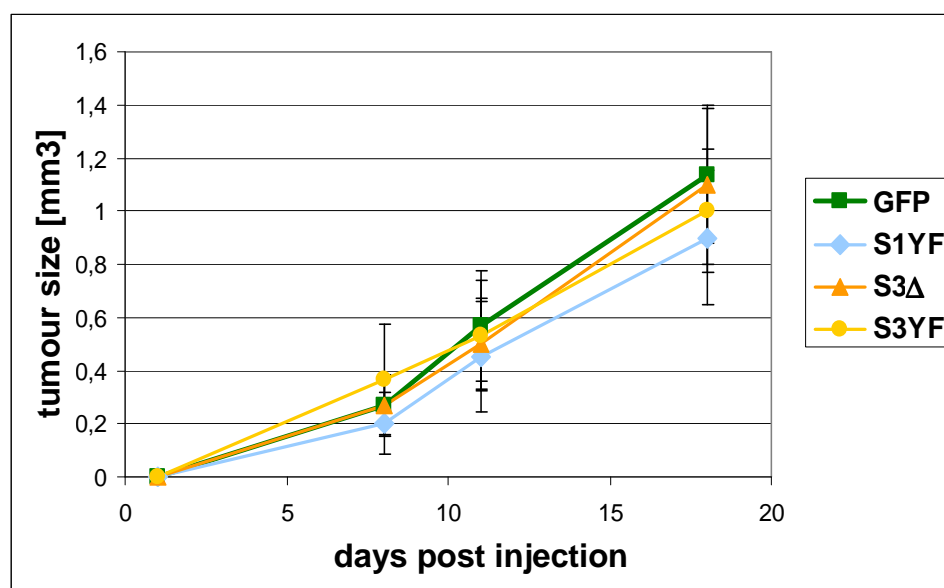


Figure 30: Analysis of ESFT cell line xenografts expressing dominant-negative forms of STAT proteins. **A** Western blot analysis of different mutant forms of STAT1 or STAT3 with antibodies specific for STAT1, STAT3 or the FLAG-tag in cell lines and xenograft samples. HSC-70 was used as a loading control. Mutant STAT proteins were expressed in the cell lines as well as in the xenograft tumours. **B** ESFT cell lines expressing dominant-negative forms of STAT1 or STAT3 were subcutaneously injected into SCID mice and tumour growth was monitored but was not much altered. Data from SK-N-MC are shown as a representative since analysis of TC71 demonstrated the same results.

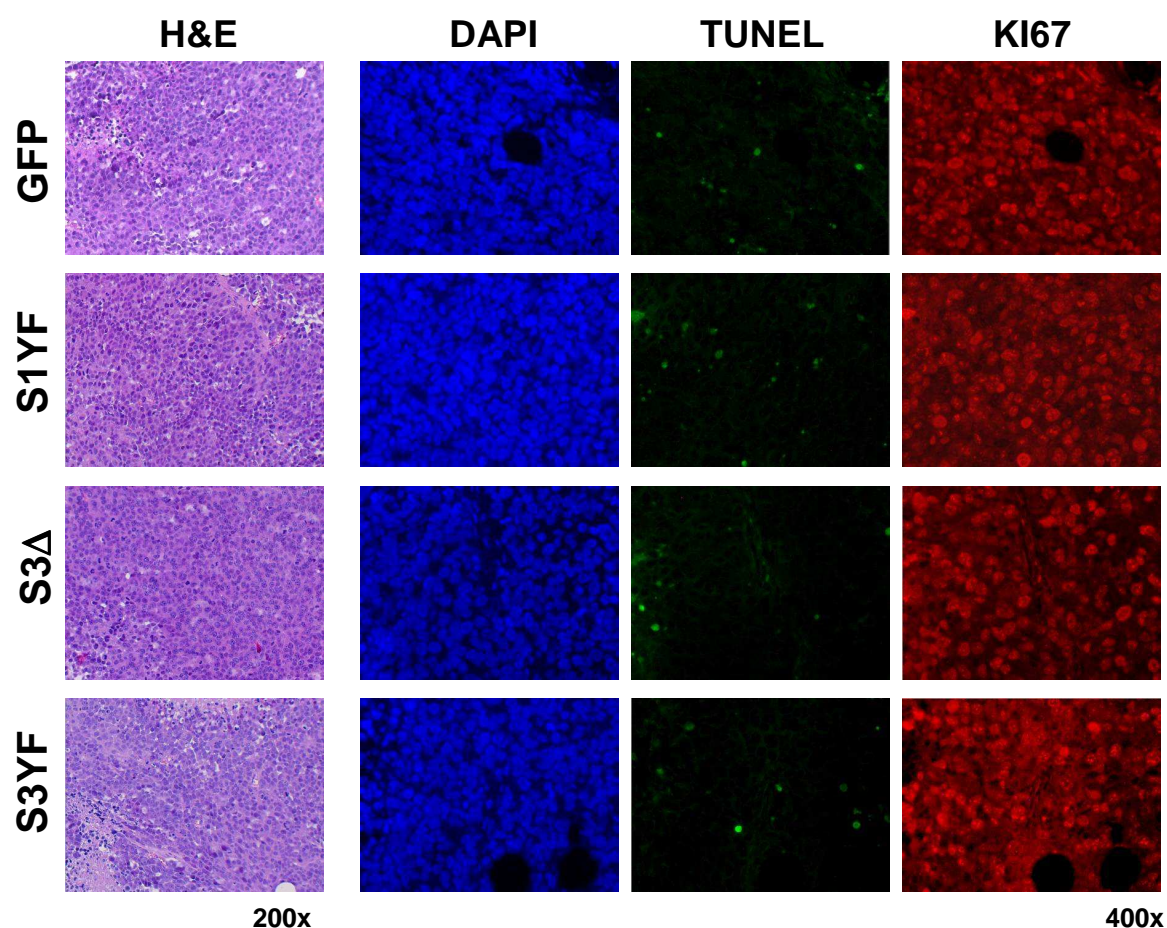


Figure 31: Analysis of ESFT cell line xenografts expressing dominant-negative forms of STAT proteins for markers of apoptosis and proliferation. Haematoxylin and eosin (H&E) staining showed a comparable structure of tumours expressing different mutant STAT proteins. Terminal deoxynucleotidyl transferase dUTP nick end labeling (TUNEL) detects DNA fragmentation, one sign of cell death, and only few cells stained positive in control (GFP) cells as well as in cells expressing dominant-negative STATs. KI67, associated with cellular proliferation, was present in most cells of the control (GFP) and comparable in cells expressing different STAT mutants. DAPI staining was used to visualise nuclei. Representative regions of SK-N-MC xenografts are shown; TC71 xenografts were also analysed, with the same result.

STAT activity should be diminished when cells expressing the dominant-negative forms are stimulated with STAT1 and/or STAT3 activating cytokines. Thus, we analysed the DNA binding of STAT1 and STAT3 in extracts of the established cell lines expressing the mutant STAT forms (Figure 32A). IFN- γ activated STAT1 to a lesser extent in the cell line expressing *S1YF* as in the control cell line (GFP). After stimulation with LIF, DNA binding ability of STAT3 and STAT1 was absent in cells containing the *S3YF* mutant. *S3 Δ* expressing cells did not show a reduction in

complexes that specifically bind to the STAT1/STAT3 consensus sequence, which was not surprising as only the transactivation domain was lacking in this mutant form but the domains for oligomerisation and DNA binding were still present.

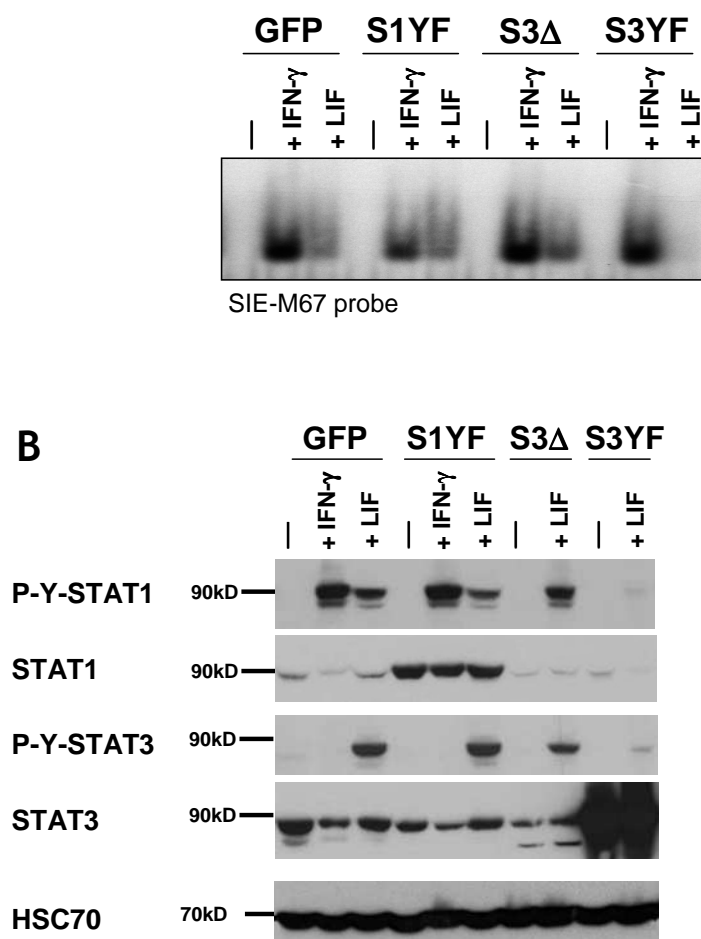


Figure 32: Activation of STATs in ESFT cell lines expressing dominant-negative forms of STAT proteins. SK-N-MC cells were stimulated for 30 minutes with 10 ng/ml cytokine or left untreated. **A** Equal amounts of total protein were analysed by EMSA with radioactively labelled oligonucleotides specific for STAT1 and STAT3 (SIE-M67). STAT1 complexes were reduced in IFN- γ stimulated S1YF cells and STAT1/STAT3 complexes were absent in LIF stimulated S3YF expressing cells. **B** Western blot analysis for tyrosine phosphorylation and total levels of STAT1 and STAT3 proteins revealed diminished phosphorylation of STAT1 and STAT3 in LIF stimulated S3YF expressing cells and a lower ratio of phosphorylated STAT1 compared to total STAT1 in IFN- γ stimulated cells expressing the S1YF mutant. The S3 Δ mutant led to a mildly reduced tyrosine phosphorylation of endogenous STAT3 upon LIF stimulation.

Additionally, we tested the mutants for tyrosine phosphorylation upon cytokine stimulation (Figure 32B). After stimulation with IFN- γ , cells expressing S1YF showed

quite the same amount of phosphorylated STAT1 than control cells expressing only *GFP*. However, when comparing P-Y-STAT1 and total STAT1 levels, there was a reduction in activated STAT1 in relation to the whole amount of STAT1 protein in *S1YF* expressing cells. The *S3Δ* mutant did result in a mild reduction of endogenous STAT3 phosphorylation upon LIF administration. Notably, the mutant protein migrating faster than the full length STAT3 was not tyrosine phosphorylated in response to LIF. Upon LIF stimulation, cells expressing the *S3YF* mutant did only show low levels of STAT1 and STAT3 phosphorylation, confirming the results from EMSA.

So, by two different methods at least the tyrosine mutated STATs were shown to diminish STAT activity but a biological relevance for ESFT cell growth in xenografts could not be observed.

Follow-up studies on the role of JAK/STAT signalling in ESFT are currently performed by Mag. Marc Wiedner. He compared SK-N-MC, an ESFT cell line also used in this work, and human MPCs, most likely the cellular origin of ESFT. From the analysed gp130 cytokines, MPCs were only responsive to OSM. Moreover, a second wave of STAT activation was seen in both cell types at about four to eight hours after initial cytokine administration. Interestingly, MPCs re-activated both STAT1 and STAT3 whereas in ESFT cells only STAT3 was activated a second time. A closer look on STAT target genes revealed that *c-fos* was induced upon OSM stimulation in MPCs and SK-N-MC. However, up-regulation of the STAT3 target gene was more pronounced in the analysed ESFT cell line (Marc Wiedner, unpublished). *C-fos* is a component of the AP-1 complex which regulates many steps of tumourigenesis, for instance proliferation, apoptosis, angiogenesis and metastasis. (Jochum *et al.* 2001) Hence, *c-fos* induction by OSM via JAK/STAT might provide insight how STAT3 activation could contribute to ESFT development.

4. Discussion

4.1. Establishment of a conditional EWS/FLI-1 knock-in mouse model

Although progress in the field of surgery and chemotherapy could increase survival rates, still less than 60% of ESFT patients survive long-term. (Khoury 2005) Novel treatment regimens are therefore needed, going along with the requirement of animals models for pre-clinical drug testing. Several groups already tried to establish a suitable mouse model but so far no mouse recapitulating the human phenotype could be created. (Codrington *et al.* 2005; Torchia *et al.* 2007)

Recent advances in the quest for the cellular origin of ESFT uncover a multi-potent mesenchymal progenitor as the starting point for this disease. (Kauer *et al.* 2009; Lin *et al.* 2008; Riggi *et al.* 2005; Tirode *et al.* 2007) It seems that only MPCs, which are able to differentiate along the osteogenic, chondrogenic and adipogenic lineage, have the adequate cellular background to allow expression of *EWS/FLI-1*. (Riggi *et al.* 2005) Moreover, differentiation of this cell type is blocked by *EWS/FLI-1* and tumour formation in xenograft models is facilitated. (Lin *et al.* 2008; Riggi *et al.* 2005; Torchia *et al.* 2003) In ESFT cells *EWS/FLI-1* suppression permits the tumour cells to differentiate into mesenchymal lineages but also impairs tumour growth. (Ouchida *et al.* 1995; Takigami *et al.* 2011; Tirode *et al.* 2007) These studies indicate that *EWS/FLI-1* contributes to the ESFT morphology by maintaining the tumour cells in an undifferentiated state resulting in uncontrolled proliferation and eventually tumour growth.

Based on the assumption that ESFT arise in a mesenchymal progenitor, we established conditional *EWS/FLI-1* knock-in mouse models where expression of the fusion protein is controlled by the presence/absence of the Cre recombinase in a particular target cell.

In the course of this study we used two different promoters for directing Cre expression into different stages of bone precursor cells, namely *Runx2* and *Prx1*. *Runx2* is expressed early in the mesenchymal lineage at the stage of skeletal precursor cells (Figure 6) and it is an essential transcription factor necessary for differentiation into the osteoblastic lineage. (Komori 2000) Expression in the embryo starts at around E 11.5. (Otto *et al.* 1997) *Prx1* is a homeobox gene which is expressed in mesenchymal cells (Figure 6) of the early limb bud mesenchyme from E 9.5 on. (Logan *et al.* 2002) Not only that *Runx2* has a later timing in embryonic development, expression is initiated in a cell type that is more mature compared to the primitive mesenchymal cell in which *Prx1* is present. These differences had a drastic effect on the outcome of *EWS/FLI-1* expression.

Researchers already showed that dependent at which stage of mesenchymal cell maturation manipulation of the same gene can have different effects. Deletion of *Dicer* in committed osteo-progenitors has a deleterious effect whereas lack of the same gene in mature osteoblasts gives a viable mouse and only a mild effect. (Gaur *et al.* 2010) But already minor differences in the onset of gene deletion in the same cell type can have opposing outcomes. For example, inactivation of *Ptch1* in *Prx1Cre* expressing cells results in a loss of digits in the forelimb but to a gain of digits in the hindlimb. (Butterfield *et al.* 2009) This discrepancy is due to a one day later activation of Cre. (Logan *et al.* 2002) Hence, perfect timing of gene manipulation in the process of bone development is essential since skeletal formation is a complex and sensitive system.

In *Runx2Cre* (784 and 1634 transgenic line) EF mice no *EWS/FLI-1* transcript was detectable whereas it was prominently expressed in the bones of *Prx1Cre* EF mice. Rearranged cells were only barely detectable and most of the cells in the adult bone of *Runx2Cre* EF mice had an unchanged *EF* allele with the *STOP*-cassette still present.

It is possible that *Cre* and hence *EWS/FLI-1* expression was toxic and rearranged cells had growth/survival defects. Several studies have reported that the Cre recombinase alone can lead to apoptosis in certain cell types. (Naiche and Papaioannou 2007; Jeannotte *et al.* 2011) However, analysis of *Cre* expression in bones of *Runx2Cre* and *Runx2Cre* EF mice revealed that the *Cre recombinase*

transcript was present when the *EWS/FLI-1* construct was not. Thus, we could exclude that Runx2Cre on its own was toxic to the cells in our transgenic mice. Additionally, Runx2Cre mice were already used successfully in other studies. (Rauch *et al.* 2010)

EWS/FLI-1 is known to have a growth inhibitory effect in primary cells and that loss of the *INK4A/ARF* locus or inhibition of p53 enables the cells to express *EWS/FLI-1*. (Deneen and Denny 2001; Lessnick *et al.* 2002) Moreover, human paediatric MPCs, whose gene expression profile resembles that of ESFT more closely than that of their adult counterparts, have lower p16^{INK4A}/p14^{ARF} levels than adult MPCs. (Riggi *et al.* 2010) Therefore, we assumed that the lethal effect *EWS/FLI-1* might have had on *Runx2Cre* expressing cells could be relieved by deleting p16^{INK4A}/p19^{ARF}. We crossed Runx2Cre EF mice to an *INK4A/ARF* deficient background, thereby eliminating two important regulators of Rb and p53 checkpoint control. However, impairment of RB/p16^{INK4A} and p53/p19^{ARF} pathways in osteoblast precursors did not create an environment permissive for *EWS/FLI-1*, in contrast to *in vitro* studies. (Deneen and Denny 2001; Lessnick *et al.* 2002) *EWS/FLI-1* was not detectable in these mice, suggesting that the toxic effect during embryonal development could not be abrogated. So, other mechanism apart from growth arrest could have been responsible for the absence of *Cre* and *EWS/FLI-1* expression.

Although we could detect at least some rearrangement of the *EF* allele, *Cre* expression was completely absent in bones of Runx2Cre EF and Runx2Cre EF *INK4A/ARF*^{-/-} mice. At some point Runx2Cre must have been active otherwise we would not have been able to detect any deletion of the *STOP*-cassette. A possible explanation would be silencing of *Runx2* by *EWS/FLI-1*, which we did not expect prior to the start of our experiments. Indeed, presence of the fusion protein in ESFT cells results in low levels of *Runx2* and vice versa *Runx2* is induced upon *EWS/FLI-1* silencing. (Tirode *et al.* 2007) One could assume that *EWS/FLI-1* down-regulates *Runx2* at the transcriptional level which would explain the lack of *Cre* expression from the *Runx2* promoter seen in Runx2Cre EF mice. But caution is advised when interpreting that *EWS/FLI-1* directly regulates *Runx2* since there is no evidence that *Runx2* is a target gene of *EWS/FLI-1* and down-regulation of *Runx2* might be just the consequence of *EWS/FLI-1* hindering the osteoblast differentiation programme. It was recently published that *EWS/FLI-1* is able to bind

Runx2 thereby regulating its activity and inhibiting differentiation of mesenchymal cells along the osteoblastic lineage. (Li *et al.* 2010) The *Runx2* promoter harbours runx consensus binding sites to which the protein can bind and auto-regulate itself. (Stock and Otto 2005) Therefore, it is conceivable that EWS/FLI-1 binds to Runx2 and shuts down expression from the *Runx2* promoter. This negative feedback loop would result in loss of *Cre* expression but would also lead to a block in osteoblast differentiation due to absent Runx2 protein. However, there are two *Runx2* promoters and the transgenic Runx2Cre lines we used contain the bone specific P1 promoter. (Rauch *et al.* 2010; Stock and Otto 2005) Normal bone development could be accomplished by the other Runx2 isoform expressed from the P2 promoter since it was shown that the isoforms can substitute each other to some extent. (Stock and Otto 2005) Mice that are specifically deficient in the Runx2 isoform expressed from the P1 promoter show a certain degree of compensation. They display abnormal bone development, although the phenotype is not as severe as in the complete knock-out where calcified bones are almost completely lacking. (Zhang *et al.* 2009) Nonetheless, we did not observe overt differences in size or bone development in Runx2Cre EF compared to wild type mice. But this hypothesis might at least explain why we could observe rearrangement of the *EF* allele in some rare cells but no *Cre* expression at all. The selective pressure might have been so strong that most of these rearranged cells died and were replaced by non-rearranged cells to ensure proper bone development.

Runx2 is expressed from the skeletal precursor stage on (Figure 6) but cells earlier in this lineage, the mesenchymal cells, do not express it yet. During the maturation process these primitive mesenchymal cells that still have a non-rearranged *EF* allele must inevitably express *Runx2* to initiate the osteoblast differentiation programme. Hence, *Cre* and *EWS/FLI-1* would also be expressed and initiate the negative feedback loop discussed above, resulting in a blockage of differentiation along the osteoblastic lineage. Silencing of the exogenous *Runx2* promoter by e.g. methylation in mesenchymal cells would circumvent this differentiation arrest since the endogenous *Runx2* promoter would not have been affected. These cells would have a selective advantage and would replace the rearranged cells to guarantee normal bone development. In Prx1Cre EF mice expression of *EWS/FLI-1* was directed to the early mesenchymal cell (Figure 6), so there was no earlier cell

type in the limb bud that could have compensated for the arrested *EWS/FLI-1* expressing cells. Hence, we could detect the phenotype of a differentiation block that lead to disturbed limb development.

Skeletal malformation in Prx1Cre EF mice was due to a lack of calcification in bones of the skull, the limbs and the rib cage. The absence of mature chondrocytes and osteoblasts would explain the lack of calcified bone. As already mentioned earlier, there is *in vitro* evidence that *EWS/FLI-1* blocks differentiation of several cell types. (Eliazar *et al.* 2003; Li *et al.* 2010; Torchia *et al.* 2003) This ability of *EWS/FLI-1* could account for the defective chondrocyte maturation seen in Prx1Cre EF mice.

The phenotype of absent bone mineralisation in Prx1Cre EF mice partly resembled the *β-catenin* knock-out, where *β-catenin* deficiency impairs differentiation of osteoblasts. (Hill *et al.* 2005) However, the phenotype observed in Prx1Cre EF mice is more severe, since already pre-hypertrophic chondrocytes are missing while they are still present in the *β-catenin* knock-out. *EWS/FLI1* was shown to reduce expression of the Wnt inhibitor *DKK-1* and to impede *β-catenin/TCF*-dependent transcription by binding to the transcription factor Lef1. (Navarro *et al.* 2010) This inhibition of the Wnt pathway by *EWS/FLI-1* might explain in part the differentiation block seen in Prx1Cre EF mice.

Loss of *IHH* causes shortened limbs and disturbs chondrocyte differentiation, the same defects presented in Prx1Cre EF mice. (St-Jacques *et al.* 1999) The proposed involvement of Hedgehog signalling in ESFT as mentioned later might explain the similarity of phenotypes.

Reduced TGF- β RII signalling could also account for the phenotype we detected in Prx1Cre EF mice. *EWS/FLI-1* directly represses *TGF- β RII* and it is suggested that TGF- β RII acts to limit chondrogenesis thereby maintaining the interzone in endochondral bone formation. (Hahm *et al.* 1999; Seo and Serra 2007) It was further demonstrated that deletion of *TGF- β RII* in *Prx1Cre* expressing cells results in limb shortening and a failure of chondrocyte differentiation. (Seo and Serra 2007) So, part of the Prx1Cre EF phenotype might be explained with repression of *TGF- β RII* by *EWS/FLI-1* resulting in a disturbed chondrocyte development.

Altogether, perturbed chondrocyte development can be observed in mouse models where components of the Wnt, Hedgehog and TGF- β pathway are deleted but none

of the phenotypes is as severe as the effects we examined in our mouse model. The differentiation block at the stage of chondroblasts in Prx1Cre EF mice was possibly due to a dysfunction of a combination of these pathways but this has still to be elucidated. Additionally, more work particularly on younger embryos needs to be performed, which is currently done at the Ludwig Boltzmann Institute for Cancer Research with a successor of this project.

Additionally, Prx1Cre EF mice displayed polydactyly reminiscent of the *GLI3* knock-out mouse. (Hui and Joyner 1993) Polydactyly is also present in a hypermorphic *GLI3* mutant mouse and in the hindlimbs of mice with conditional deletion of *Ptch1* in *Prx1* expressing cells. (Butterfield *et al.* 2009; Wang *et al.* 2007) As determined by *GLI1* expression, Hedgehog signalling is enhanced in limbs deficient in *Ptch1*, the negative regulator of this pathway. (Butterfield *et al.* 2009) EWS/FLI-1 was shown to directly regulate *GLI1* and to increase its expression. (Beauchamp *et al.* 2009; Zwerner *et al.* 2008) This might explain at least in part the similarity of phenotypes in these mice although the Hedgehog pathway was so far not analysed in detail in our mice. We concentrated our analysis on the developmental defects causing the limb shortening.

During the work for this thesis a new EWS/FLI-1 transgenic mouse which was crossed with the Prx1Cre line was published. (Lin *et al.* 2008) The design of the construct that is present in these mice has some similarity to the one employed in EF mice (Figure 3C and B). Both constructs harbour a *loxP* cassette that silences the rearranged *EWS/FLI-1* gene and only upon Cre activity the fusion gene is expressed. (Lin *et al.* 2008; Torchia *et al.* 2007) The construct in EF mice contains several *STOP* signals between the two *loxP* sites whereas a *GFP*-cassette is located at this site in the other construct. In EF mice the EWS/FLI-1 construct is under control of the ubiquitous *Rosa26* promoter while transgene expression in the other mouse model is driven by a β -actin promoter. Moreover, the EWS/FLI-1 construct in EF mice resides in the endogenous *Rosa26* locus which is widely used for the generation of transgenic mice and does not encode for protein. (Torchia *et al.* 2007) In contrast, there are several copy numbers of the EWS/FLI-1 construct present in the other mouse model and the genomic localisation of the constructs was not determined. (Lin *et al.* 2008) Loss or enhancement of gene expression of

unknown targets caused by the random introduction of the EWS/FLI-1 construct might have influenced the observed phenotype.

Three transgenic lines were established by this group: the first one has shorter limbs, another one shows a mild polydactyly and a third line has severe limb defects but is not viable. The short limb phenotype in the first transgenic line is not as prominent as in our Prx1Cre EF mice and also the polydactyly of the second line is not as severe. None of the lines develops tumours *per se* but the first EWS/FLI-1 transgenic line in combination with conditional deleted *p53* leads to formation of poorly differentiated sarcomas. *p53* deficiency in mesenchymal progenitors alone results already in formation of predominantly osteosarcomas and additional presence of EWS/FLI-1 then shifts the tumour spectrum and reduces the median tumour latency. (Lin *et al.* 2008) The phenotype of our Prx1Cre EF mice was more severe compared to the two viable EWS/FLI-1 transgenic lines. (Lin *et al.* 2008) Therefore we focused our analysis on the developmental aspects present in Prx1Cre EF mice which might contribute to the understanding of ESFT pathogenesis.

In addition to the so far discussed 784 and 1634 transgenic Runx2Cre EF mice, we analysed another transgenic Runx2Cre line. However, we could not obtain double transgenic offspring from crosses with mice harbouring the *EF* allele and the 777 line of Runx2Cre. Fetal survival in 777Runx2Cre EF mice was compromised at E 13.5. *Cre recombinase* in the 777 line was expressed at higher levels compared to the 784 and 1634 line and Cre activity was shown in bone, cartilage and also in the haematopoietic system (Dr. Jan Tuckermann, personal communication). High levels of *EWS/FLI-1* and expression in the haematopoietic system might have led to the early fatal effect. In line, EWS/FLI-1 was already demonstrated to have a drastic impact on haematopoiesis. (Torchia *et al.* 2007)

We have shown that mesenchymal progenitors (expressing *Prx1*) but not skeletal precursors (being more committed to the osteoblast lineage and expressing *Runx2*) offer a suitable background for *EWS/FLI-1* expression *in vivo*. Furthermore, the

absence of mature chondrocytes in our transgenic mouse model would support the finding that the presence of *EWS/FLI-1* results in a differentiation block. (Eliazer *et al.* 2003; Li *et al.* 2010; Torchia *et al.* 2003) The severe developmental defects we observed in Prx1Cre EF mice and the fact that they die shortly after birth due to an open rib cage causing suffocation could be circumvented by utilisation of an inducible Prx1Cre transgenic line (Dr. Malcolm Logan, unpublished). Cre activation and hence *EWS/FLI-1* expression can then be temporally controlled and started only after birth at different time points. These mice could be prone to develop tumours since tumour formation was already shown to be facilitated by *EWS/FLI-1* expression in mesenchymal progenitor cells. (Lin *et al.* 2008; Riggi *et al.* 2005) Therefore, we imported inducible Prx1Cre-ERT2 mice and generated compound mice with EF and *INK4A/ARF* deletion. Analysis of these mice is currently ongoing at the Ludwig Boltzmann Institute for Cancer Research in close collaboration with the CCRI and Prof. Erben to obtain a sarcoma mouse model resembling the phenotype of ESFT.

4.2. JAK/STAT signalling in ESFT

Among other signalling pathways, the JAK/STAT pathway is often de-regulated in human cancers but not much is known about its function in ESFT. Only JAK1 and STAT3 activation were shown to be elevated in ESFT patient samples. (Baird *et al.* 2005; Lai *et al.* 2006) On this informative basis and the fact that this pathway was not well studied we were interested in the role of the JAK/STAT pathway in ESFT.

We analysed three different ESFT cell lines and could demonstrate that JAK/STAT signalling is active in ESFT cell line xenografts but absent in monolayer and spheroid culture. Additionally, most of the tumours on a ESFT tissue micro array also displayed tyrosine phosphorylation of STAT3, pointing to the relevance for Ewing's tumours. Hence, we could exclude the possibility that cells produce an autocrine factor activating STAT1 and STAT3 proteins. Rather cytokines released by the microenvironment were suggested to stimulate this pathway. Similar results were already obtained for colon cancer cells, where STAT3 is constitutively activated in colon cancer cells but is lost in cell culture. However, activation can be restored in xenografts by extracellular stimuli. (Corvinus *et al.* 2005)

The question then was which cytokines were able to activate STAT proteins in the xenograft tumours. ESFT cell lines were responsive to INF- α , IFN- γ and gp130 cytokines like CNTF, LIF and OSM. Surprisingly, these cells were unresponsive to the well-known inflammatory cytokine IL-6 which was due to a lack of IL-6 receptor alpha chain expression, as measured by flow cytometric analysis. High cytokine receptor surface expression could be demonstrated for gp130, LIFR and OSMR. CNTFR was not present on ESFT cell lines but cells were clearly responsive to the cytokine CNTF which would argue for an alternative usage of gp130 cytokine receptor combinations. In the absence of CNTFR, signalling through gp130 and LIFR upon CNTF administration can be sustained by engagement of soluble IL-6R (sIL-6R). (Schuster *et al.* 2003) It is feasible that sIL-6R was present in our cell cultures but we did not analyse this in detail. sIL-6R is either produced by alternative mRNA splicing or proteolytic cleavage of the membrane bound IL-6R and can be measured by analysis of mRNA or by an enzyme-linked immunosorbent assay. (Chalaris *et al.* 2011)

Proliferation in response to the analysed cytokines was not changed dramatically. Only interferons led to a reduction in cell number whereby IFN- γ , which only activated STAT1, was very potent and IFN- α was less effective, which could be due to dual activation of STAT1 and STAT3.

Analysis of JAK/STAT specific target genes in gp130 stimulated cells revealed that some STAT1 induced genes (*CDKN1A*, *IRF1*) were up-regulated as also seen in IFN- γ treated cells. Expression of STAT3 target genes was not increased in CNTF, LIF or OSM stimulated ESFT cells although we demonstrated DNA binding of STAT3 complexes. We used a commercially available OligoGEArrayTM with a defined but limited set of STAT target genes (classical targets of tyrosine phosphorylated STAT proteins) which could explain that we have missed target genes induced by gp130 cytokines. Clearly, we could detect tyrosine phosphorylation and DNA binding ability of STAT1 and STAT3 upon gp130 cytokine stimulation. An alternative possibility would be that the absence of STAT3 target gene activation could be due to functions of phosphorylated STAT proteins in the cytoplasm. (Sehgal *et al.* 2008) Based on the DNA binding ability, STAT1 had a more profound activation than STAT3. It is conceivable that this overbalance of STAT1 could have resulted in sequestration of STAT3 and consequently suppression of STAT3 target gene activation but the opposite case was reported. In response to IFN- α , activated STAT3 is able to sequester activated STAT1 thereby hindering STAT1 homodimer formation and hence STAT1-dependent target gene activation. (Ho and Ivashkiv 2006) However, the biological role of this STAT1/STAT3 heterodimers is not clear yet. (Regis *et al.* 2008)

Examination of the duration of STAT protein activation in ESFT cells revealed that STAT1 and STAT3 complexes were active over a period of at least 16 hours in IFN- γ stimulated cells whereas stimulation with CNTF, LIF and OSM led to a transient activation. DNA binding ability of STAT1 and STAT3 was prominent at 30 minutes, but highly diminished at 60 minutes. PIAS proteins negatively regulate the JAK/STAT pathway by binding activated STAT dimers and inhibiting STAT-mediated gene transcription. (Klampfer 2006) It is possible that the *PIAS* expression per se was already high in ESFT cells compared to other cell lines that initiate target gene transcription in response to activated STATs. Indeed, we found significant *PIAS1* and *PIAS3* expression on the array, which could account for inhibition of STAT1 and STAT3 DNA binding complexes in ESFT cells. The increased expression of *PIAS* was

even more pronounced in the gp130 stimulated cells which could account for the short STAT activation.

Since STAT1 and STAT3 were activated in ESFT xenografts we asked whether these STAT proteins were essential for tumour formation. We established ESFT cell lines with dominant-negative forms of STAT1 and STAT3, analysed them *in vitro* and subjected these cells to xenotransplantation.

The mutant forms *S1YF*, *S3Δ* and *S3YF* were nicely expressed, but *S1Δ* was not detected appropriately on the protein level, which could be a result of misfolding resulting in an unstable protein. This mutant form of *STAT1* was cloned based on the reported and widely used *S3Δ* mutant, where the protein is truncated after the SH2 domain lacking the transactivation domain. (Oh and Eaves 2002)

In vitro growth of the cell lines expressing mutant forms of *STAT1* and *STAT3* was not much altered. Since STATs were not activated in ESFT cells in cell culture we did not anticipate a change in their proliferation capacity.

Unfortunately, we could also not observe a difference in tumour growth although strong activation of STAT1 and STAT3 was noticed in xenografts arguing for a too weak expression of the dominant negative acting STAT variants or counter selection of ESFT cells expressing low levels of STAT variants. However, we could detect significant expression in endpoint xenograft samples and hence excluded these theories. STAT3 in particular was reported to have immunomodulatory function in tumours and it could be possible that an immunocompromised mouse model will not show effects upon blocked STAT activity. Alternatively, the long term ESFT cell lines we have used for our studies of blocking STAT activity might have had too many other genetic alterations which could bypass any functional role of STAT protein activation.

The critical tyrosine residue was missing in all of the mutants, impeding full activation of STAT proteins. Moreover, the *S1YF* and *S3YF* mutants block recruitment of wild type STAT proteins to the receptors. (Kaptein *et al.* 1996) Therefore, a reduced DNA binding was expected in the established cell lines. EMSA revealed that *S1YF* and *S3YF* expressing cells displayed a reduction in STAT DNA binding ability when stimulated with INF- γ and LIF, respectively. DNA binding of the other mutants retained pretty much the same. Moreover, Western blot analysis for tyrosine phosphorylated STAT proteins showed the same inhibition of STAT activity

in *S1YF* and *S3YF* expressing cells. Additionally, the *S3Δ* mutant was demonstrated to diminish endogenous STAT3 phosphorylation to some extent. Hence, the dominant negative forms of STAT1 and STAT3 were shown to impair STAT activity in ESFT cells. Although the mutant forms of STAT proteins were already reported to have biological relevance in many different cell lines their effect in ESFT cells remains illusive. (Corvinus *et al.* 2005; Kortylewski *et al.* 2004; Oh and Eaves 2002; Walter *et al.* 1997)

In this study we used mutant forms of STAT proteins that block recruitment of wild type STAT proteins to the receptors thereby inhibiting phosphorylation of wild type STATs (Kaptein *et al.* 1996) or a mutant with a truncation of the transactivation domain that could not induce gene transcription and concentrated our analysis on the classical role of the JAK/STAT pathway. But what about the role of unphosphorylated STAT proteins or cytoplasmic functions of phosphorylated STATs? The latter process could at least explain why we detected pronounced STAT1 and STAT3 activity in response to gp130 cytokines but no induction of classical target genes. To answer the question if these “non-classical” functions were involved in ESFT tumourigenesis total STAT protein levels should have been reduced which can be achieved by employment of the RNAi technology.

In summary, with our work we could give some insight to the JAK/STAT pathway, a signalling pathway that is often de-regulated in cancer, but further analysis is needed to understand the biological function and consequences of STAT activation in ESFT cancer cells which is an ongoing project at the Ludwig Boltzmann Institute for Cancer Research.

5. References

- Aaronson, D. S. and Horvath, C. M. (2002) A road map for those who don't know JAK-STAT. *Science* 296(5573):1653-5
- Alberts, B., Bray, D., Lewis, J., Raff, M., Roberts, K. and Watson, J. (1994) *Molecular Biology of the Cell*. Garland Publishing
- Andersson, M. K., Stahlberg, A., Arvidsson, Y., Olofsson, A., Semb, H., Stenman, G., Nilsson, O. and Aman, P. (2008) The multifunctional FUS, EWS and TAF15 proto-oncoproteins show cell type-specific expression patterns and involvement in cell spreading and stress response. *BMC Cell Biol* 9(37):1-17
- Arvand, A. and Denny, C. T. (2001) Biology of EWS/ETS fusions in Ewing's family tumors. *Oncogene* 20(40):5747-54
- Baird, K., Davis, S., Antonescu, C. R., Harper, U. L., Walker, R. L., Chen, Y., Glatfelter, A. A., Duray, P. H. and Meltzer, P. S. (2005) Gene expression profiling of human sarcomas: insights into sarcoma biology. *Cancer Res* 65(20):9226-35
- Beauchamp, E., Bulut, G., Abaan, O., Chen, K., Merchant, A., Matsui, W., Endo, Y., Rubin, J. S., Toretsky, J. and Uren, A. (2009) GLI1 is a direct transcriptional target of EWS-FLI1 oncoprotein. *J Biol Chem* 284(14):9074-82
- Beauchamp, E. M., Ringer, L., Bulut, G., Sajwan, K. P., Hall, M. D., Lee, Y. C., Peaceman, D., Ozdemirli, M., Rodriguez, O., Macdonald, T. J., Albanese, C., Toretsky, J. A. and Uren, A. (2011) Arsenic trioxide inhibits human cancer cell growth and tumor development in mice by blocking Hedgehog/GLI pathway. *J Clin Invest* 121(1):148-60
- Bertolotti, A., Melot, T., Acker, J., Vigneron, M., Delattre, O. and Tora, L. (1998) EWS, but not EWS-FLI-1, is associated with both TFIID and RNA polymerase II: interactions between two members of the TET family, EWS and hTAFII68, and subunits of TFIID and RNA polymerase II complexes. *Mol Cell Biol* 18(3):1489-97
- Biedler, J. L., Helson, L. and Spengler, B. A. (1973) Morphology and growth, tumorigenicity, and cytogenetics of human neuroblastoma cells in continuous culture. *Cancer Res* 33(11):2643-52

- Braun, B. S., Frieden, R., Lessnick, S. L., May, W. A. and Denny, C. T. (1995) Identification of target genes for the Ewing's sarcoma EWS/FLI fusion protein by representational difference analysis. *Mol Cell Biol* 15(8):4623-30
- Bromberg, J. (2002) Stat proteins and oncogenesis. *J Clin Invest* 109(9):1139-42
- Burchill, S. A. (2003) Ewing's sarcoma: diagnostic, prognostic, and therapeutic implications of molecular abnormalities. *J Clin Pathol* 56(2):96-102
- Butterfield, N. C., Metzis, V., McGlinn, E., Bruce, S. J., Wainwright, B. J. and Wicking, C. (2009) Patched 1 is a crucial determinant of asymmetry and digit number in the vertebrate limb. *Development* 136(20):3515-24
- Castillero-Trejo, Y., Eliazer, S., Xiang, L., Richardson, J. A. and Ilaria, R. L., Jr. (2005) Expression of the EWS/FLI-1 oncogene in murine primary bone-derived cells Results in EWS/FLI-1-dependent, ewing sarcoma-like tumors. *Cancer Res* 65(19):8698-705
- Cavazzana, A. O., Miser, J. S., Jefferson, J. and Triche, T. J. (1987) Experimental evidence for a neural origin of Ewing's sarcoma of bone. *Am J Pathol* 127(3):507-18
- Chalaris, A., C. Garbers, B. Rabe, S. Rose-John and J. Scheller (2011) The soluble Interleukin 6 receptor: Generation and role in inflammation and cancer. *Eur J Cell Biol* 90(6-7):484-94
- Chansky, H. A., Hu, M., Hickstein, D. D. and Yang, L. (2001) Oncogenic TLS/ERG and EWS/Fli-1 fusion proteins inhibit RNA splicing mediated by YB-1 protein. *Cancer Res* 61(9):3586-90
- Cheon, H., Yang, J. and Stark, G. R. (2011) The functions of signal transducers and activators of transcriptions 1 and 3 as cytokine-inducible proteins. *J Interferon Cytokine Res* 31(1):33-40
- Cho, J., Shen, H., Yu, H., Li, H., Cheng, T., Lee, S. B. and Lee, B. C. (2011) Ewing's sarcoma gene EWS regulates hematopoietic stem cell senescence. *Blood* 117(4):1156-66
- Codrington, R., Pannell, R., Forster, A., Drynan, L. F., Daser, A., Lobato, N., Metzler, M. and Rabbitts, T. H. (2005) The Ews-ERG fusion protein can initiate neoplasia from lineage-committed haematopoietic cells. *PLoS Biol* 3(8):e242
- Corvinus, F. M., Orth, C., Moriggl, R., Tsareva, S. A., Wagner, S., Pfitzner, E. B., Baus, D., Kaufmann, R., Huber, L. A., Zatloukal, K., Beug, H., Ohlschlager, P., Schutz, A., Halbhuber, K. J. and Friedrich, K. (2005) Persistent STAT3

- activation in colon cancer is associated with enhanced cell proliferation and tumor growth. *Neoplasia* 7(6):545-55
- Dauphinot, L., De Oliveira, C., Melot, T., Sevenet, N., Thomas, V., Weissman, B. E. and Delattre, O. (2001) Analysis of the expression of cell cycle regulators in Ewing cell lines: EWS-FLI-1 modulates p57KIP2 and c-Myc expression. *Oncogene* 20(25):3258-65
- Day, T. F. and Yang, Y. (2008) Wnt and hedgehog signaling pathways in bone development. *J Bone Joint Surg Am* 90:19-24
- de Alava, E., Antonescu, C. R., Panizo, A., Leung, D., Meyers, P. A., Huvos, A. G., Pardo-Mindan, F. J., Healey, J. H. and Ladanyi, M. (2000) Prognostic impact of P53 status in Ewing sarcoma. *Cancer* 89(4):783-92
- Decker, T. and Kovarik, P. (2000) Serine phosphorylation of STATs. *Oncogene* 19(21):2628-37
- Deneen, B. and Denny, C. T. (2001) Loss of p16 pathways stabilizes EWS/FLI1 expression and complements EWS/FLI1 mediated transformation. *Oncogene* 20(46):6731-41
- Eliazer, S., Spencer, J., Ye, D., Olson, E. and Ilaria, R. L., Jr. (2003) Alteration of mesodermal cell differentiation by EWS/FLI-1, the oncogene implicated in Ewing's sarcoma. *Mol Cell Biol* 23(2):482-92
- Endo, Y., Beauchamp, E., Woods, D., Taylor, W. G., Toretsky, J. A., Uren, A. and Rubin, J. S. (2008) Wnt-3a and Dickkopf-1 stimulate neurite outgrowth in Ewing tumor cells via a Frizzled3- and c-Jun N-terminal kinase-dependent mechanism. *Mol Cell Biol* 28(7):2368-79
- Erkizan, H. V., Uversky, V. N. and Toretsky, J. A. (2009) Oncogenic partnerships: EWS-FLI1 protein interactions initiate key pathways of Ewing's sarcoma. *Clin Cancer Res* 16(16):4077-83
- Ewing, J. (1972) Diffuse endothelioma of bone. *CA Cancer J Clin* 22(2):95-8
- Friedbichler, K., Kerényi, M. A., Kovacic, B., Li, G., Hoelbl, A., Yahiaoui, S., Sexl, V., Mullner, E. W., Fajmann, S., Cerny-Reiterer, S., Valent, P., Beug, H., Gouilleux, F., Bunting, K. D. and Moriggl, R. (2010) Stat5a serine 725 and 779 phosphorylation is a prerequisite for hematopoietic transformation. *Blood* 116(9):1548-58

- Friedbichler, K., Hoelbl, A., Li, G., Bunting, K.D., Sexl, V., Gouilleux, F., Moriggl, R. (2011) Serine phosphorylation of the Stat5a C-terminus is a driving force for transformation. *Front Biosci.* 17:3043-3056
- Fukuma, M., Okita, H., Hata, J. and Umezawa, A. (2003) Upregulation of Id2, an oncogenic helix-loop-helix protein, is mediated by the chimeric EWS/ets protein in Ewing sarcoma. *Oncogene* 22(1):1-9
- Fulda, S. and Debatin, K. M. (2002) IFN γ sensitizes for apoptosis by upregulating caspase-8 expression through the Stat1 pathway. *Oncogene* 21(15):2295-308
- Garcia-Aragoncillo, E., Carrillo, J., Lalli, E., Agra, N., Gomez-Lopez, G., Pestana, A. and Alonso, J. (2008) DAX1, a direct target of EWS/FLI1 oncoprotein, is a principal regulator of cell-cycle progression in Ewing's tumor cells. *Oncogene* 27(46):6034-43
- Gaur, T., Hussain, S., Mudhasani, R., Parulkar, I., Colby, J. L., Frederick, D., Kream, B. E., van Wijnen, A. J., Stein, J. L., Stein, G. S., Jones, S. N. and Lian, J. B. (2010) Dicer inactivation in osteoprogenitor cells compromises fetal survival and bone formation, while excision in differentiated osteoblasts increases bone mass in the adult mouse. *Dev Biol* 340(1):10-21
- Ghoreschi, K., Laurence, A. and O'Shea, J. J. (2009) Janus kinases in immune cell signalling. *Immunol Rev* 228(1):273-87
- Hahm, K. B. (1999) Repression of the gene encoding the TGF-beta type II receptor is a major target of the EWS-FLI1 oncoprotein. *Nat Genet* 23(4):481
- Haldar, M., Hancock, J. D., Coffin, C. M., Lessnick, S. L. and Capecchi, M. R. (2007) A conditional mouse model of synovial sarcoma: insights into a myogenic origin. *Cancer Cell* 11(4):375-88
- Hamelin, R., Zucman, J., Melot, T., Delattre, O. and Thomas, G. (1994) p53 mutations in human tumors with chimeric EWS/FLI-1 genes. *Int J Cancer* 57(3):336-40
- Hanahan, D. and Weinberg, R. A. (2000) The hallmarks of cancer. *Cell* 100(1):57-70
- Hartmann, C. (2007) Skeletal development--Wnts are in control. *Mol Cells* 24(2):177-84
- Heinrich, P. C., Behrmann, I., Haan, S., Hermanns, H. M., Muller-Newen, G. and Schaper, F. (2003) Principles of interleukin (IL)-6-type cytokine signalling and its regulation. *Biochem J* 374(Pt 1):1-20

- Hill, T. P., Spater, D., Taketo, M. M., Birchmeier, W. and Hartmann, C. (2005) Canonical Wnt/beta-catenin signaling prevents osteoblasts from differentiating into chondrocytes. *Dev Cell* 8(5):727-38
- Ho, H. H. and Ivashkiv, L. B. (2006) Role of STAT3 in type I interferon responses. Negative regulation of STAT1-dependent inflammatory gene activation. *J Biol Chem* 281(20):14111-8
- Huang, H. Y., Illei, P. B., Zhao, Z., Mazumdar, M., Huvos, A. G., Healey, J. H., Wexler, L. H., Gorlick, R., Meyers, P. and Ladanyi, M. (2005) Ewing sarcomas with p53 mutation or p16/p14ARF homozygous deletion: a highly lethal subset associated with poor chemoresponse. *J Clin Oncol* 23(3):548-58
- Hughes, D. P. (2009) Novel agents in development for pediatric sarcomas. *Curr Opin Oncol* 21(4):332-7
- Hui, C. C. and Joyner, A. L. (1993) A mouse model of greig cephalopolysyndactyly syndrome: the extra-toesJ mutation contains an intragenic deletion of the Gli3 gene. *Nat Genet* 3(3):241-6
- Hu-Lieskovan, S., Heidel, J. D., Bartlett, D. W., Davis, M. E. and Triche, T. J. (2005a) Sequence-specific knockdown of EWS-FLI1 by targeted, nonviral delivery of small interfering RNA inhibits tumor growth in a murine model of metastatic Ewing's sarcoma. *Cancer Res* 65(19):8984-92
- Hu-Lieskovan, S., Zhang, J., Wu, L., Shimada, H., Schofield, D. E. and Triche, T. J. (2005b) EWS-FLI1 fusion protein up-regulates critical genes in neural crest development and is responsible for the observed phenotype of Ewing's family of tumors. *Cancer Res* 65(11):4633-44
- Jeannotte, L., Aubin, J., Bourque, S., Lemieux, M., Montaron, S. and Provencher St-Pierre, A. (2011) Unsuspected effects of a lung-specific cre deleter mouse line. *Genesis* 49(3):152-9
- Jochum, W., Passegue, E. and Wagner, E. F. (2001) AP-1 in mouse development and tumorigenesis. *Oncogene* 20(19):2401-12
- Kaptein, A., Paillard, V. and Saunders, M. (1996) Dominant negative stat3 mutant inhibits interleukin-6-induced Jak-STAT signal transduction. *J Biol Chem* 271(11):5961-4
- Kauer, M., Ban, J., Kofler, R., Walker, B., Davis, S., Meltzer, P. and Kovar, H. (2009) A molecular function map of Ewing's sarcoma. *PLoS One* 4(4):e5415

- Kawaguchi, K. and Koike, M. (1986) Neuron-specific enolase and Leu-7 immunoreactive small round-cell neoplasm. The relationship to Ewing's sarcoma in bone and soft tissue. *Am J Clin Pathol* 86(1):79-83
- Keller, C., Arenkiel, B. R., Coffin, C. M., El-Bardeesy, N., DePinho, R. A. and Capecchi, M. R. (2004) Alveolar rhabdomyosarcomas in conditional Pax3:Fkhr mice: cooperativity of Ink4a/ARF and Trp53 loss of function. *Genes Dev* 18(21):2614-26
- Khoury, J. D. (2005) Ewing sarcoma family of tumors. *Adv Anat Pathol* 12(4):212-20
- Klampfer, L. (2006) Signal transducers and activators of transcription (STATs): Novel targets of chemopreventive and chemotherapeutic drugs. *Curr Cancer Drug Targets* 6(2):107-21
- Knoop, L. L. and Baker, S. J. (2000) The splicing factor U1C represses EWS/FLI-mediated transactivation. *J Biol Chem* 275(32):24865-71
- Kolb, E. A., Gorlick, R., Houghton, P. J., Morton, C. L., Lock, R., Carol, H., Reynolds, C. P., Maris, J. M., Keir, S. T., Billups, C. A. and Smith, M. A. (2008) Initial testing (stage 1) of a monoclonal antibody (SCH 717454) against the IGF-1 receptor by the pediatric preclinical testing program. *Pediatr Blood Cancer* 50(6):1190-7
- Komori, T. (2000) A fundamental transcription factor for bone and cartilage. *Biochem Biophys Res Commun* 276(3):813-6
- Komuro, H., Hayashi, Y., Kawamura, M., Hayashi, K., Kaneko, Y., Kamoshita, S., Hanada, R., Yamamoto, K., Hongo, T., Yamada, M. and Tsuchida, Y. (1993) Mutations of the p53 gene are involved in Ewing's sarcomas but not in neuroblastomas. *Cancer Res* 53(21):5284-8
- Kortylewski, M., Komyod, W., Kauffmann, M. E., Bosserhoff, A., Heinrich, P. C. and Behrmann, I. (2004) Interferon-gamma-mediated growth regulation of melanoma cells: involvement of STAT1-dependent and STAT1-independent signals. *J Invest Dermatol* 122(2):414-22
- Kovar, H. (2005) Context matters: the hen or egg problem in Ewing's sarcoma. *Semin Cancer Biol* 15(3):189-96
- Kovar, H., Aryee, D. N., Jug, G., Henockl, C., Schemper, M., Delattre, O., Thomas, G. and Gardner, H. (1996) EWS/FLI-1 antagonists induce growth inhibition of Ewing tumor cells in vitro. *Cell Growth Differ* 7(4):429-37

- Kovar, H., Auinger, A., Jug, G., Aryee, D., Zoubek, A., Salzer-Kuntschik, M. and Gadner, H. (1993) Narrow spectrum of infrequent p53 mutations and absence of MDM2 amplification in Ewing tumours. *Oncogene* 8(10):2683-90
- Kovar, H., Jug, G., Aryee, D. N., Zoubek, A., Ambros, P., Gruber, B., Windhager, R. and Gadner, H. (1997) Among genes involved in the RB dependent cell cycle regulatory cascade, the p16 tumor suppressor gene is frequently lost in the Ewing family of tumors. *Oncogene* 15(18):2225-32
- Kovar, H., Jug, G., Hattinger, C., Spahn, L., Aryee, D. N., Ambros, P. F., Zoubek, A. and Gadner, H. (2001) The EWS protein is dispensable for Ewing tumor growth. *Cancer Res* 61(16):5992-7
- Kreppel, M., Aryee, D. N., Schaefer, K. L., Amann, G., Kofler, R., Poremba, C. and Kovar, H. (2006) Suppression of KCMF1 by constitutive high CD99 expression is involved in the migratory ability of Ewing's sarcoma cells. *Oncogene* 25(19):2795-800
- Kuhn, R., Schwenk, F., Aguet, M. and Rajewsky, K. (1995) Inducible gene targeting in mice. *Science* 269(5229):1427-9
- Lai, L. P. and Mitchell, J. (2005) Indian hedgehog: its roles and regulation in endochondral bone development. *J Cell Biochem* 96(6):1163-73
- Lai, R., Navid, F., Rodriguez-Galindo, C., Liu, T., Fuller, C. E., Ganti, R., Dien, J., Dalton, J., Billups, C. and Khoury, J. D. (2006) STAT3 is activated in a subset of the Ewing sarcoma family of tumours. *J Pathol* 208(5):624-32
- Lawlor, E. R., Scheel, C., Irving, J. and Sorensen, P. H. (2002) Anchorage-independent multi-cellular spheroids as an in vitro model of growth signaling in Ewing tumors. *Oncogene* 21(2):307-18
- Le Deley, M. C., Delattre, O., Schaefer, K. L., Burchill, S. A., Koehler, G., Hogendoorn, P. C., Lion, T., Poremba, C., Marandet, J., Ballet, S., Pierron, G., Brownhill, S. C., Nessler, M., Ranft, A., Dirksen, U., Oberlin, O., Lewis, I. J., Craft, A. W., Jurgens, H. and Kovar, H. (2010) Impact of EWS-ETS fusion type on disease progression in Ewing's sarcoma/peripheral primitive neuroectodermal tumor: prospective results from the cooperative Euro-E.W.I.N.G. 99 trial. *J Clin Oncol* 28(12):1982-8
- Lessnick, S. L., Dacwag, C. S. and Golub, T. R. (2002) The Ewing's sarcoma oncoprotein EWS/FLI induces a p53-dependent growth arrest in primary human fibroblasts. *Cancer Cell* 1(4):393-401

- Li, H., Watford, W., Li, C., Parmelee, A., Bryant, M. A., Deng, C., O'Shea, J. and Lee, S. B. (2007) Ewing sarcoma gene EWS is essential for meiosis and B lymphocyte development. *J Clin Invest* 117(5):1314-23
- Li, X., McGee-Lawrence, M. E., Decker, M. and Westendorf, J. J. (2010) The Ewing's sarcoma fusion protein, EWS-FLI, binds Runx2 and blocks osteoblast differentiation. *J Cell Biochem* 111(4):933-43
- Lin, P. P., Brody, R. I., Hamelin, A. C., Bradner, J. E., Healey, J. H. and Ladanyi, M. (1999) Differential transactivation by alternative EWS-FLI1 fusion proteins correlates with clinical heterogeneity in Ewing's sarcoma. *Cancer Res* 59(7):1428-32
- Lin, P. P., Pandey, M. K., Jin, F., Xiong, S., Deavers, M., Parant, J. M. and Lozano, G. (2008) EWS-FLI1 induces developmental abnormalities and accelerates sarcoma formation in a transgenic mouse model. *Cancer Res* 68(21):8968-75
- Lin, P. P., Wang, Y. and Lozano, G. (2011) Mesenchymal Stem Cells and the Origin of Ewing's Sarcoma. *Sarcoma* Article ID 276463, 8 pages
- Logan, M., Martin, J. F., Nagy, A., Lobe, C., Olson, E. N. and Tabin, C. J. (2002) Expression of Cre Recombinase in the developing mouse limb bud driven by a Prxl enhancer. *Genesis* 33(2):77-80
- Lopez-Guerrero, J. A., Pellin, A., Noguera, R., Carda, C. and Llombart-Bosch, A. (2001) Molecular analysis of the 9p21 locus and p53 genes in Ewing family tumors. *Lab Invest* 81(6):803-14
- Ludwig, J. A. (2008) Ewing sarcoma: historical perspectives, current state-of-the-art, and opportunities for targeted therapy in the future. *Curr Opin Oncol* 20(4):412-8
- Mackall, C. L., Meltzer, P. S. and Helman, L. J. (2002) Focus on sarcomas. *Cancer Cell* 2(3):175-8
- Masuya, M., Moussa, O., Abe, T., Deguchi, T., Higuchi, T., Ebihara, Y., Spyropoulos, D. D., Watson, D. K. and Ogawa, M. (2005) Dysregulation of granulocyte, erythrocyte, and NK cell lineages in Fli-1 gene-targeted mice. *Blood* 105(1):95-102
- Matsumoto, Y., Tanaka, K., Nakatani, F., Matsunobu, T., Matsuda, S. and Iwamoto, Y. (2001) Downregulation and forced expression of EWS-Fli1 fusion gene results in changes in the expression of G(1)regulatory genes. *Br J Cancer* 84(6):768-75

- May, W. A., Arvand, A., Thompson, A. D., Braun, B. S., Wright, M. and Denny, C. T. (1997) EWS/FLI1-induced manic fringe renders NIH 3T3 cells tumourigenic. *Nat Genet* 17(4):495-7
- May, W. A., Gishizky, M. L., Lessnick, S. L., Lunsford, L. B., Lewis, B. C., Delattre, O., Zucman, J., Thomas, G. and Denny, C. T. (1993a) Ewing sarcoma 11;22 translocation produces a chimeric transcription factor that requires the DNA-binding domain encoded by FLI1 for transformation. *Proc Natl Acad Sci U S A* 90(12):5752-6
- May, W. A., Lessnick, S. L., Braun, B. S., Klemsz, M., Lewis, B. C., Lunsford, L. B., Hromas, R. and Denny, C. T. (1993b) The Ewing's sarcoma EWS/FLI-1 fusion gene encodes a more potent transcriptional activator and is a more powerful transforming gene than FLI-1. *Mol Cell Biol* 13(12):7393-8
- Nagano, A., Ohno, T., Shimizu, K., Hara, A., Yamamoto, T., Kawai, G., Saitou, M., Takigami, I., Matsushashi, A., Yamada, K. and Takei, Y. (2010) EWS/Fli-1 chimeric fusion gene upregulates vascular endothelial growth factor-A. *Int J Cancer* 126(12):2790-8
- Naiche, L. A. and Papaioannou, V. E. (2007) Cre activity causes widespread apoptosis and lethal anemia during embryonic development. *Genesis* 45(12):768-75
- Navarro, D., Agra, N., Pestana, A., Alonso, J. and Gonzalez-Sancho, J. M. (2010) The EWS/FLI1 oncogenic protein inhibits expression of the Wnt inhibitor DICKKOPF-1 gene and antagonizes beta-catenin/TCF-mediated transcription. *Carcinogenesis* 31(3):394-401
- Oh, I. H. and Eaves, C. J. (2002) Overexpression of a dominant negative form of STAT3 selectively impairs hematopoietic stem cell activity. *Oncogene* 21(31):4778-87
- Oikawa, T. and Yamada, T. (2003) Molecular biology of the Ets family of transcription factors. *Gene* 303:11-34
- Olmos, D., Postel-Vinay, S., Molife, L. R., Okuno, S. H., Schuetze, S. M., Paccagnella, M. L., Batzel, G. N., Yin, D., Pritchard-Jones, K., Judson, I., Worden, F. P., Gualberto, A., Scurr, M., de Bono, J. S. and Haluska, P. (2010) Safety, pharmacokinetics, and preliminary activity of the anti-IGF-1R antibody figitumumab (CP-751,871) in patients with sarcoma and Ewing's sarcoma: a phase 1 expansion cohort study. *Lancet Oncol* 11(2):129-35

- Ordóñez, J. L., Osuna, D., Herrero, D., de Alava, E. and Madoz-Gurpide, J. (2009) Advances in Ewing's sarcoma research: where are we now and what lies ahead? *Cancer Res* 69(18):7140-50
- Ortmann, R. A., Cheng, T., Visconti, R., Frucht, D. M. and O'Shea, J. J. (2000) Janus kinases and signal transducers and activators of transcription: their roles in cytokine signaling, development and immunoregulation. *Arthritis Res* 2(1):16-32
- Otto, F., Thornell, A. P., Crompton, T., Denzel, A., Gilmour, K. C., Rosewell, I. R., Stamp, G. W., Beddington, R. S., Mundlos, S., Olsen, B. R., Selby P. B. and Owen M. J. (1997) Cbfa1, a candidate gene for cleidocranial dysplasia syndrome, is essential for osteoblast differentiation and bone development. *Cell* 89(5):765-71
- Ouchida, M., Ohno, T., Fujimura, Y., Rao, V. N. and Reddy, E. S. (1995) Loss of tumorigenicity of Ewing's sarcoma cells expressing antisense RNA to EWS-fusion transcripts. *Oncogene* 11(6):1049-54
- Park, Y. K., Chi, S. G., Kim, Y. W., Park, H. R. and Unni, K. K. (2001) P53 mutations in Ewing's sarcoma. *Oncol Rep* 8(3):533-7
- Perez-Losada, J., Sanchez-Martin, M., Rodriguez-Garcia, M. A., Perez-Mancera, P. A., Pintado, B., Flores, T., Battaner, E. and Sanchez-Garcia, I. (2000) Liposarcoma initiated by FUS/TLS-CHOP: the FUS/TLS domain plays a critical role in the pathogenesis of liposarcoma. *Oncogene* 19(52):6015-22
- Pilz, A., Kratky, W., Stockinger, S., Simma, O., Kalinke, U., Lingnau, K., von Gabain, A., Stoiber, D., Sexl, V., Kolbe, T., Rulicke, T., Muller, M. and Decker, T. (2009) Dendritic cells require STAT-1 phosphorylated at its transactivating domain for the induction of peptide-specific CTL. *J Immunol* 183(4):2286-93
- Platanias, L. C. (2005) Mechanisms of type-I- and type-II-interferon-mediated signalling. *Nat Rev Immunol* 5(5):375-86
- Prieur, A., Tirode, F., Cohen, P. and Delattre, O. (2004) EWS/FLI-1 silencing and gene profiling of Ewing cells reveal downstream oncogenic pathways and a crucial role for repression of insulin-like growth factor binding protein 3. *Mol Cell Biol* 24(16):7275-83
- Rauch, A., Seitz, S., Baschant, U., Schilling, A. F., Illing, A., Stride, B., Kirilov, M., Mandic, V., Takacz, A., Schmidt-Ullrich, R., Ostermay, S., Schinke, T.,

- Spanbroek, R., Zaiss, M. M., Angel, P. E., Lerner, U. H., David, J. P., Reichardt, H. M., Amling, M., Schutz, G. and Tuckermann, J. P. (2010) Glucocorticoids suppress bone formation by attenuating osteoblast differentiation via the monomeric glucocorticoid receptor. *Cell Metab* 11(6):517-31
- Regis, G., Pensa, S., Boselli, D., Novelli, F. and Poli, V. (2008) Ups and downs: the STAT1:STAT3 seesaw of Interferon and gp130 receptor signalling. *Semin Cell Dev Biol* 19(4):351-9
- Richter, G. H., Plehm, S., Fasan, A., Rossler, S., Unland, R., Bennani-Baiti, I. M., Hotfilder, M., Lowel, D., von Luetlichau, I., Mossbrugger, I., Quintanilla-Martinez, L., Kovar, H., Staeger, M. S., Muller-Tidow, C. and Burdach, S. (2009) EZH2 is a mediator of EWS/FLI1 driven tumor growth and metastasis blocking endothelial and neuro-ectodermal differentiation. *Proc Natl Acad Sci U S A* 106(13):5324-9
- Riggi, N., Cironi, L., Provero, P., Suva, M. L., Kaloulis, K., Garcia-Echeverria, C., Hoffmann, F., Trumpp, A. and Stamenkovic, I. (2005) Development of Ewing's sarcoma from primary bone marrow-derived mesenchymal progenitor cells. *Cancer Res* 65(24):11459-68
- Riggi, N., Suva, M. L., De Vito, C., Provero, P., Stehle, J. C., Baumer, K., Cironi, L., Janiszewska, M., Petricevic, T., Suva, D., Tercier, S., Joseph, J. M., Guillou, L. and Stamenkovic, I. (2010) EWS-FLI-1 modulates miRNA145 and SOX2 expression to initiate mesenchymal stem cell reprogramming toward Ewing sarcoma cancer stem cells. *Genes Dev* 24(9):916-32
- Riggi, N., Suva, M. L., Suva, D., Cironi, L., Provero, P., Tercier, S., Joseph, J. M., Stehle, J. C., Baumer, K., Kindler, V. and Stamenkovic, I. (2008) EWS-FLI-1 expression triggers a Ewing's sarcoma initiation program in primary human mesenchymal stem cells. *Cancer Res* 68(7):2176-85
- Rocchi, A., Manara, M. C., Sciandra, M., Zambelli, D., Nardi, F., Nicoletti, G., Garofalo, C., Meschini, S., Astolfi, A., Colombo, M. P., Lessnick, S. L., Picci, P. and Scotlandi, K. (2010) CD99 inhibits neural differentiation of human Ewing sarcoma cells and thereby contributes to oncogenesis. *J Clin Invest* 120(3):668-80
- Rorie, C. J., Thomas, V. D., Chen, P., Pierce, H. H., O'Bryan, J. P. and Weissman, B. E. (2004) The Ews/Fli-1 fusion gene switches the differentiation program of

- neuroblastomas to Ewing sarcoma/peripheral primitive neuroectodermal tumors. *Cancer Res* 64(4):1266-77
- Schuster, B., Kovaleva, M., Sun, Y., Regenhard, P., Matthews, V., Grotzinger, J., Rose-John, S. and Kallen, K. J. (2003) Signaling of human ciliary neurotrophic factor (CNTF) revisited. The interleukin-6 receptor can serve as an alpha-receptor for CTNF. *J Biol Chem* 278(11):9528-35
- Scotlandi, K., Baldini, N., Cerisano, V., Manara, M. C., Benini, S., Serra, M., Lollini, P. L., Nanni, P., Nicoletti, G., Bernard, G., Bernard, A. and Picci, P. (2000) CD99 engagement: an effective therapeutic strategy for Ewing tumors. *Cancer Res* 60(18):5134-42
- Scotlandi, K., Benini, S., Nanni, P., Lollini, P. L., Nicoletti, G., Landuzzi, L., Serra, M., Manara, M. C., Picci, P. and Baldini, N. (1998) Blockage of insulin-like growth factor-I receptor inhibits the growth of Ewing's sarcoma in athymic mice. *Cancer Res* 58(18):4127-31
- Scotlandi, K., Benini, S., Sarti, M., Serra, M., Lollini, P. L., Maurici, D., Picci, P., Manara, M. C. and Baldini, N. (1996) Insulin-like growth factor I receptor-mediated circuit in Ewing's sarcoma/peripheral neuroectodermal tumor: a possible therapeutic target. *Cancer Res* 56(20):4570-4
- Sehgal, P. B. (2008) Paradigm shifts in the cell biology of STAT signalling. *Semin Cell Dev Biol* 19(4):329-40
- Seo, H. S. and Serra, R. (2007) Deletion of Tgfbr2 in Prx1-cre expressing mesenchyme results in defects in development of the long bones and joints. *Dev Biol* 310(2):304-16
- Serrano, M., Lee, H., Chin, L., Cordon-Cardo, C., Beach, D. and DePinho, R. A. (1996) Role of the INK4a locus in tumor suppression and cell mortality. *Cell* 85(1):27-37
- Siligan, C., Ban, J., Bachmaier, R., Spahn, L., Kreppel, M., Schaefer, K. L., Poremba, C., Aryee, D. N. and Kovar, H. (2005) EWS-FLI1 target genes recovered from Ewing's sarcoma chromatin. *Oncogene* 24(15):2512-24
- Smith, R., Owen, L. A., Trem, D. J., Wong, J. S., Whangbo, J. S., Golub, T. R. and Lessnick, S. L. (2006) Expression profiling of EWS/FLI identifies NKX2.2 as a critical target gene in Ewing's sarcoma. *Cancer Cell* 9(5):405-16
- Spyropoulos, D. D., Pharr, P. N., Lavenburg, K. R., Jackers, P., Papas, T. S., Ogawa, M. and Watson, D. K. (2000) Hemorrhage, impaired hematopoiesis,

- and lethality in mouse embryos carrying a targeted disruption of the Fli1 transcription factor. *Mol Cell Biol* 20(15):5643-52
- St-Jacques, B., Hammerschmidt, M. and McMahon, A. P. (1999) Indian hedgehog signaling regulates proliferation and differentiation of chondrocytes and is essential for bone formation. *Genes Dev* 13(16):2072-86
- Stock, M. and Otto, F. (2005) Control of RUNX2 isoform expression: the role of promoters and enhancers. *J Cell Biochem* 95(3):506-17
- Subbiah, V. and Anderson, P. (2011) Targeted Therapy of Ewing's Sarcoma. *Sarcoma* Article ID 686985
- Suva, M. L., Riggi, N., Stehle, J. C., Baumer, K., Tercier, S., Joseph, J. M., Suva, D., Clement, V., Provero, P., Cironi, L., Osterheld, M. C., Guillou, L. and Stamenkovic, I. (2009) Identification of cancer stem cells in Ewing's sarcoma. *Cancer Res* 69(5):1776-81
- Szuhai, K., Ijszenga, M., de Jong, D., Karseladze, A., Tanke, H. J. and Hogendoorn, P. C. (2009) The NFATc2 gene is involved in a novel cloned translocation in a Ewing sarcoma variant that couples its function in immunology to oncology. *Clin Cancer Res* 15(7):2259-68
- Takigami, I., Ohno, T., Kitade, Y., Hara, A., Nagano, A., Kawai, G., Saitou, M., Matsushashi, A., Yamada, K. and Shimizu, K. (2011) Synthetic siRNA targeting the breakpoint of EWS/Fli-1 inhibits growth of Ewing sarcoma xenografts in a mouse model. *Int J Cancer* 128(1):216-26
- Teitell, M. A., Thompson, A. D., Sorensen, P. H., Shimada, H., Triche, T. J. and Denny, C. T. (1999) EWS/ETS fusion genes induce epithelial and neuroectodermal differentiation in NIH 3T3 fibroblasts. *Lab Invest* 79(12):1535-43
- Tirado, O. M., Mateo-Lozano, S., Villar, J., Dettin, L. E., Llorca, A., Gallego, S., Ban, J., Kovar, H. and Notario, V. (2006) Caveolin-1 (CAV1) is a target of EWS/FLI-1 and a key determinant of the oncogenic phenotype and tumorigenicity of Ewing's sarcoma cells. *Cancer Res* 66(20):9937-47
- Tirode, F., Laud-Duval, K., Prieur, A., Delorme, B., Charbord, P. and Delattre, O. (2007) Mesenchymal stem cell features of Ewing tumors. *Cancer Cell* 11(5):421-9

- Torchia, E. C., Boyd, K., Rehg, J. E., Qu, C. and Baker, S. J. (2007) EWS/FLI-1 induces rapid onset of myeloid/erythroid leukemia in mice. *Mol Cell Biol* 27(22):7918-34
- Torchia, E. C., Jaishankar, S. and Baker, S. J. (2003) Ewing tumor fusion proteins block the differentiation of pluripotent marrow stromal cells. *Cancer Res* 63(13):3464-8
- Toretsky, J. A., Connell, Y., Neckers, L. and Bhat, N. K. (1997) Inhibition of EWS-FLI-1 fusion protein with antisense oligodeoxynucleotides. *J Neurooncol* 31(1-2):9-16
- Toub, N., Bertrand, J. R., Tamaddon, A., Elhames, H., Hillaireau, H., Maksimenko, A., Maccario, J., Malvy, C., Fattal, E. and Couvreur, P. (2006) Efficacy of siRNA nanocapsules targeted against the EWS-Fli1 oncogene in Ewing sarcoma. *Pharm Res* 23(5):892-900
- Triche, T. J. (1987) Morphologic tumor markers. *Semin Oncol* 14(2):139-72
- Truong, A. H. and Ben-David, Y. (2000) The role of Fli-1 in normal cell function and malignant transformation. *Oncogene* 19(55):6482-9
- Uren, A., Wolf, V., Sun, Y. F., Azari, A., Rubin, J. S. and Toretsky, J. A. (2004) Wnt/Frizzled signaling in Ewing sarcoma. *Pediatr Blood Cancer* 43(3):243-9
- van Doorninck, J. A., Ji, L., Schaub, B., Shimada, H., Wing, M. R., Krailo, M. D., Lessnick, S. L., Marina, N., Triche, T. J., Sposto, R., Womer, R. B. and Lawlor, E. R. (2010) Current treatment protocols have eliminated the prognostic advantage of type 1 fusions in Ewing sarcoma: a report from the Children's Oncology Group. *J Clin Oncol* 28(12):1989-94
- van Valen, F., Winkelmann, W. and Jurgens, H. (1992) Expression of functional Y1 receptors for neuropeptide Y in human Ewing's sarcoma cell lines. *J Cancer Res Clin Oncol* 118(7):529-36
- Walter, M. J., Look, D. C., Tidwell, R. M., Roswit, W. T. and Holtzman, M. J. (1997) Targeted inhibition of interferon-gamma-dependent intercellular adhesion molecule-1 (ICAM-1) expression using dominant-negative Stat1. *J Biol Chem* 272(45):28582-9
- Wang, C., Pan, Y. and Wang, B. (2007) A hypermorphic mouse Gli3 allele results in a polydactylous limb phenotype. *Dev Dyn* 236(3):769-76

- Whang-Peng, J., Triche, T. J., Knutsen, T., Miser, J., Douglass, E. C. and Israel, M. A. (1984) Chromosome translocation in peripheral neuroepithelioma. *N Engl J Med* 311(9):584-5
- Yu, H. and Jove, R. (2004) The STATs of cancer--new molecular targets come of age. *Nat Rev Cancer* 4(2):97-105
- Zenali, M. J., Zhang, P. L., Bendel, A. E. and Brown, R. E. (2009) Morphoproteomic confirmation of constitutively activated mTOR, ERK, and NF-kappaB pathways in Ewing family of tumors. *Ann Clin Lab Sci* 39(2):160-6
- Zhang, J., S. Hu, D. E. Schofield, P. H. Sorensen and T. J. Triche (2004) Selective usage of D-Type cyclins by Ewing's tumors and rhabdomyosarcomas. *Cancer Res* 64(17): 6026-34
- Zhang, S., Xiao, Z., Luo, J., He, N., Mahlios, J., Quarles, L. D. (2009) Dose-dependent effects of Runx2 on bone development. *J Bone Miner Res* 24(11):1889-904
- Zhou, Z., Bolontrade, M. F., Reddy, K., Duan, X., Guan, H., Yu, L., Hicklin, D. J. and Kleinerman, E. S. (2007) Suppression of Ewing's sarcoma tumor growth, tumor vessel formation, and vasculogenesis following anti vascular endothelial growth factor receptor-2 therapy. *Clin Cancer Res* 13(16):4867-73
- Zwerner, J. P., Joo, J., Warner, K. L., Christensen, L., Hu-Lieskovan, S., Triche, T. J. and May, W. A. (2008) The EWS/FLI1 oncogenic transcription factor deregulates GLI1. *Oncogene* 27(23):3282-91

6. Abbreviations

A	ampere
AEC	3-amino-9-ethylcarbazole
ALK	anaplastic lymphoma kinase
APC	adenomatous polyposis coli
APS	ammoniumpersulfate
ATP	adenosintriphosphat
BCL2L1	B-cell lymphoma 2 like 1
Bp	base pairs
BSA	bovine serum albumin
CAV1	caveolin-1
CD	cluster of differentiation, cell surface molecule to identify haematopoietic cell lineages
cDNA	complementary desoxyribonucleic acid
cKit	transmembrane tyrosine kinase receptor, CD117
CNTF	ciliary neurotrophic factor
CNTFR	ciliary neurotrophic factor receptor a chain
Col1	collagen1
Col10	collagen10
Col2	collagen2
CRP	c-reactive protein
CSC	cancer stem cell
CXCL9	chemokine (C-X-C motif) ligand 9
DAX1	dosage-sensitive sex reversal
DBD	DNA binding domain
ddH ₂ O	double distilled water
DEPC	diethylpyrocarbonate
dH ₂ O	distilled water
DKK-1	dickkopf-1
DMEM	Dulbecco's Modified Eagle Medium
DMSO	dimethylsulfoxide
DNA	desoxyribonucleic acid

DNase	deoxyribonuclease
dNTP	deoxyribonucleotide triphosphate
Dsh	dishevelled
DTT	dithiothreitol
E	embryonic day
ECL	enhanced chemiluminescence
EDTA	ethylenediaminetetraacetic acid
EMSA	electrophoretic mobility shift assay
ERG	ets related gene
ESFT	Ewing's sarcoma family of tumours
ETS	e-twenty six
EWS	Ewing's sarcoma breakpoint region 1
EZH2	enhancer of zeste homolog 2
FACS	fluorescence activated cell sorting
FCS	fetal calf serume
FISH	fluorescence <i>in situ</i> hybridisation
FITC	fluorescein-5-isothiocyanat
FLI1	Friend leukaemia virus integration site 1
Fz	frizzled
GAS	γ -activated sequence
gDNA	genomic desoxyribonucleic acid
GFP	green fluorescent protein
gp130	glycoprotein 130
Gsk3	glycogen synthase kinase 3
H&E	haematoxylin n and eosin staining
HA	hemagglutinin
HRP	horseradish peroxidase
ID2	inhibitor of DNA binding 2
IFN	interferon
IGF	insulin-like growth factor
IGF-1	insulin-like growth factor-1
IGF-1R	insulin-like growth factor-1 receptor
IGFBP3	insulin-like growth factor binding protein 3
Ihh	Indian Hedgehog

IL	interleukin
IL-6R	interleukin-6 receptor a
INDO	indoleamine-pyrrole 2,3-dioxygenase
IRES	internal ribosomal entry site
IRF	interferon regulated factor
ISGF3	interferon-stimulated gene factor 3
ISRE	interferon stimulated response element
JAK	Janus kinase
kB	kilobases
kD	kilodalton
l	litre
LB	lysogeny broth
Lef	lymphoid enhancer factor
LIF	leukaemia inhibitory factor
LIFR	leukaemia inhibitory factor receptor
loxP	Cre recombinase recognition site
LRP	lipoprotein receptor-related protein
m	meter
m	milli (10^{-3})
M	molar (mol/l)
MAPK	mitogen activated protein kinase
MEF	mouse embryonic fibroblasts
MEM	Minimum Essential Medium
miRNA	micro ribonucleic acid
MK-STYX	mitogen-activated protein kinase phospho- serine/threonine/tyrosine-binding protein
MMP	matrix metalloprotease
MOPS	morpholino propane sulfonic acid
MPC	mesenchymal progenitor cell
mRNA	messenger RNA
MSC	mesenchymal stem cell
mTOR	mammalian target of rapamycin
Mx1	myxovirus resistance 1
n	nano (10^{-9})

n	number
NKX2.2	homeobox protein NK2.2
NP-40	nonidet P-40
NTD	n-terminal domain
NTRK1	neurotrophic tyrosine kinase
OD	optical density
Osc	osteocalcin
OSM	oncostatin M
OSMR	oncostatin M receptor
Osx	osterix
p	pico (10^{-12})
p16 ^{INK4a}	cyclin-dependent kinase inhibitor 2A, inhibitor of CDK4 kinase
p19 ^{ARF}	alternate open reading frame
p21	waf1, cyclin-dependent kinase inhibitor 1A
p57	kip2, cyclin-dependent kinase inhibitor 1C
PAA	polyacrylamid
PBS	phosphate buffered saline
PCR	polymerase chain reaction
PE	phycoerythrin
PIAS	protein inhibitor of activated signal transducer and activator of transcription
PI3K	phosphatidylinositol 3-kinase
pMSCV	vector based on the murine stem cell virus
PMSF	phenylmethylsulfonylfluorid
PNET	primitive neuroectodermal tumour
PolyIC	polyinosinic and polycytydilic acid
Prx1	paired related homeobox gene-1
Prx1Cre EF mice	mice expressing EWS/FLI-1 in Prx1 positive cells
Ptch1	patched1
PTHrP	parathyroid hormone related peptide
PTP1B	protein tyrosine phosphatase 1B
RNA	ribonucleic acid
rpm	rotations per minute

RPMI	Roswell Park Memorial Institute medium
runx	runt-related transcription factor
Runx	runt-related transcription factor
Runx2Cre EF mice	mice expressing EWS/FLI-1 in Runx2 positive cells
SCID	severe combined immunodeficiency
SDS	sodiumdodecylsulfate
SH2	src homology 2
SHP	src homology domain containing protein tyrosine phosphatase
SIE-M67	serum inducible element from the c-fos promotor mutated at position 67
siRNA	small interfering ribonucleic acid
Smo	smoothened
SOCS	suppressor of cytokine signalling
SOX	SRY-like HMG-box gene
STAT	signal transducer and activator of transcription
S1 Δ	mutant form of STAT1 lacking the transactivation domain
S1YF	mutant form of STAT1 where tyrosine 701 is changed to phenylalanine
S3 Δ	mutant form of STAT3 lacking the transactivation domain
S3YF	mutant form of STAT3 where tyrosine 705 is changed to phenylalanine
TAD	transactivation domain
Taq	Thermus aquaticus
Tcf	T-cell factor
TEMED	N,N,N',N'-tetramethylethylenediamine
TET	TLS/FUS, EWS, TAFII68
TFIID	transcription factor IID
TGF- β	tumour growth factor beta
TGF- β RII	tumour growth factor beta receptor type II
TLS/FUS	translocated in liposarcoma/fused in sarcoma
Tris	tris(hydroxymethyl)-aminomethan
U	enzymatic unit
UTR	untranslated region

V	volt
VEGF	vascular endothelial growth factor
VEGFR-2	vascular endothelial growth factor receptor-2
W	watt
Wnt	wingless, int-1
wt	wild type
μ	micro (10^{-6})

Curriculum Vitae

MAG. BARBARA SAX

Wienerstrasse 20/2/8
2514 Traiskirchen
email: b.zankl@aon.at
0676/7771981

PERSONAL DETAILS

Date of birth: 29th October 1981

Place of birth: Vienna

Nationality: Austria

LANGUAGES

German: Native language

English: Fluent

Latin: Basic knowledge

EDUCATION

JANUARY 2006 - NOVEMBER 2009	PhD thesis "Establishment of a Ewing's Sarcoma Mouse Model JAK/STAT Signalling in Ewing's Sarcoma" Ludwig Boltzmann Institute for Cancer Research, group of Univ.-Doz. DI. Dr. Richard Moriggl	Vienna
OCTOBER 2005	Graduated with master (Mag.rer.nat.) at the University of Vienna, passed with distinction	Vienna
JUNE 2004 - MARCH 2005	Diploma thesis "Characterisation of PP2A and its substrates <i>in vivo</i> " Medical University Vienna, Institute of Medical Biochemistry, Department of Molecular Biology, laboratory of Ao. Univ.-Prof. Dr. Egon Ogris,	Vienna
2000-2005	Studies of Molecular Biology, University of Vienna	Vienna

JUNE 2000	Highschool graduation with good results	St. Pölten
1992-2000	Highschool "Gymnasium der Englischen Fräulein"	St. Pölten

ADDITIONAL EDUCATION

Business Administration for scientists
 Practical lab in Business Administration for scientists
 Basics of economics
 Overview over the Austrian Law
 Marketing
 Basics of Patent Law
 EDV in molecular biology

AWARDS

2005	Honour of the city Traiskirchen for passing university studies with distinction
2004	"Top-Stipend" from the Lower Austrian provincial government for excellent study results
2003	Scholarship from the University Vienna
2003	Scholarship from "Windhag" scholarship foundation for Lower Austria
2002	Scholarship from the Scientific Faculty, University Vienna

WORK EXPERIENCE

NOVEMBER 2003	Practical work at the IMP Vienna , laboratory Dr. Jan- Michael Peters "Localisation of condensing I and II in different phases of the cell cycle"	Vienna
AUGUST/ SEPTEMBER 2003	Practical work at Boehringer Ingelheim Austria, Department for Cancer Research, laboratory Dr. Guido Böhmelt "Recombinant expression and characterisation of the	Vienna

phosphatidylinositol phosphatase Sac1”

- MAY 2003 Practical work at the Medical University Vienna, Institute of Medical Biochemistry, Department of Molecular Biology, laboratory Ao. Univ.-Prof. Dr. Egon Ogris Vienna
“Ubiquitination of PP2A in yeast and downregulation of hCAP-D3 and the B α -subunit of PP2A in HeLa-cells with RNAi-technology”
- NOVEMBER 2002 Practical work at the University Vienna, Institute of Biochemistry and Cellular Biology, laboratory O. Univ.-Prof. Dr. Gerhard Wiche Vienna
“Characterisation and localisation of PKC δ in Plectin knock-out and wild type cells”
- SEPTEMBER 2002 Practical work at the University of Agricultural Science, laboratory Ao. Univ.-Prof. DI Dr. Marie-Theres Hauser Vienna
“Effect of toxins and sugar concentration on root growth of *Arabidopsis thaliana* and mapping of a T-DNA insertion”
- AUGUST 2002 Practical work at the General Hospital (AKH), Institute for Cancer Research, laboratory Ao. Univ.-Prof.Dr. Brigitte Marian Vienna
“Effect of antioxidants on colon carcinoma cell lines”
- JULY 2001 Practical work at the University of Agricultural Science (BOKU), laboratory Ao. Univ.-Prof. DI Dr. Marie-Theres Hauser Vienna
“Cultivation of *Arabidopsis thaliana* and mapping of a root development gene”

TALKS AND POSTER PRESENTATIONS

- APRIL 2009 Poster presentation at the 100th annual meeting of the AACR Denver, USA
“JAK/STAT signaling in Ewing’s sarcoma”
Barbara Sax, Wolfgang Mikulits, Gerhard Müller-Newen, Christopher Poremba, Heinrich Kovar, Richard Moriggl
- OCTOBER 2007 Talk at the Children’s Cancer Research Institute Vienna

“Unexplored Avenues in Ewing Tumor Research2:
Generation of a Transgenic Mouse Model and JAK/STAT
Signaling”

OCTOBER 2006 Talk at the Children’s Cancer Research Institute Vienna
“Unexplored Avenues in Ewing Tumor Research:
Generation of a Transgenic Mouse Model and JAK/STAT
Signaling”

CONGRESSES

APRIL 2009 100th annual meeting AACR Denver,
USA

APRIL 2007 5th International Aachen Symposium on Cytokine Signalling Aachen,
Germany

AUGUST 2006 Cytokines 2006 - 6th Joint Meeting of the International Vienna
Cytokine Society, International Society for Interferon and
Cytokine Research & the European Cytokine Society